January 2013

Structure and Function of Pinniped Vibrissae

Christin Taylor Murphy
University of South Florida, ctmurphy@mail.usf.edu

Structure and Function of Pinniped Vibrissae

by

Christin T. Murphy

A dissertation submitted in partial fulfillment
of the requirements for the degree of
Doctor of Philosophy
College of Marine Science
University of South Florida

Major Professor: David Mann, Ph.D.
Colleen Reichmuth, Ph.D.
Gordon Bauer, Ph.D.
Jose Torres, Ph.D.
Mya Breitbart, Ph.D.

Date of Approval:
June 26, 2013

Keywords: Whiskers, Vibrotactile, Sensitivity, Laser Vibrometer, Tagging

DEDICATION

This dissertation is dedicated to my family and to the many teachers I have had along this path. Thank you for the love, support, and inspiration.

ACKNOWLEDGMENTS

Thank you to my advisor David Mann for the amazing opportunity to undertake this graduate work. Thank you to Gordon Bauer, Heidi Harley, Jose Torres, and Mya Breitbart for your brilliant teaching and mentorship. Thank you to the amazing team at the UCSC Pinniped Cognition and Sensory Systems Laboratory. Thank you to Colleen Reichmuth for accepting me into the lab family, to Asila Ghoul for extensive input and assistance with animal training, and to Sarah, Brendan, Andrew, Rebecca, Janine, Megan, Roxanne, and Sonny for help with data collection. Thank you to Carolyn, Jenna, and Michelle for help with training (both me and the animals) and to Guy, Kane, Peter, and Jillian for your insight. And of course, thank you to Sprouts!! Thank you to the Bio-Thermal-Fluids Lab at UVA for collaborating with me on the flume experiments. Thank you to Joseph Humphrey for making this cooperative research possible, to Benton Calhoun for guidance and support, and Craig Eberhardt for tolerating our marathon data collection sessions. Thank you to Danielle and the Mann Lab team. Thank you to the Marine Mammal Center for help with sample collection. Thank you to Kenneth Mann and Ryan Izant for collaboration on the CT scan research. Thank you to True Blue Films and Discovery Communications for high speed video footage. Thank you to Matthias Elliott, Jesse Stagg and Jenn Cossaboon for graphic design. Thank you to the NSF and the Lake Fellowship for funding my graduate work. Thank you to Erin Symonds and to Chris Reeves for your unwavering support. Thank you to my father for teaching me hard work and dedication. Thank you to my mother for being the greatest champion of my education and for being there every step of the way.

TABLE OF CONTENTS

LIST OF TABLES

LIST OF FIGURES

ABSTRACT

The vibrissal system of pinnipeds relies on sturdy, specialized vibrissae and supporting neural architecture apparently designed for the reception of waterborne disturbances. Although it is known that pinnipeds can use their vibrissae for fine-scale tactile discrimination and hydrodynamic detection, many aspects of vibrissal function remain poorly understood. The present work examined the adaptive significance of vibrissal structure, the sensitivity of the vibrissal system, and the signals received by this system. All of these points were considered with respect to their function in hydrodynamic reception. Four methods of study: laser vibrometry, computed tomography (CT) scanning, psychophysical testing and animal-borne tagging were used to investigate the functioning of this sensory system.

Laser vibrometer recordings were used to investigate the effect of vibrissal surface structure and orientation on flow-induced vibrations in excised vibrissae. Vibrations were recorded from the shaft of excised vibrissae exposed to laminar water flow in a flume tank. Samples from three pinniped species were tested: the harbor seal (*Phoca vitulina*), northern elephant seal (*Mirounga angustirostris*) and California sea lion (*Zalophus californianus*). The vibrissae of the seals had an undulated surface structure, while the vibrissae of the sea lion had a smooth surface. No significant difference between species, and therefore surface structure, was observed. However, when vibrissae were tested at three angles of orientation to the water flow, a strong effect of orientation on vibration frequency and velocity was observed across species. CT

scanning data revealed that the vibrissae of all the species tested had flattened cross-sectional profiles. This cross-sectional flattening could account for the observed orientation effects. Furthermore, this morphological characteristic may represent an adaptation for improved functioning in the aquatic environment by reducing self-induced-noise from swimming and potentially enhancing detection of signals from other planes.

Psychophysical testing was conducted with a trained harbor seal in order to investigate the sensitivity of the vibrissal system of this species. A behavioral procedure was used to measure absolute detection thresholds for sinusoidal stimuli delivered to the vibrissae by a vibrating plate. Thresholds were measured at 9 discrete frequencies from 10 to 1000 Hz. The seal's performance in this stimulus detection task showed that the vibrissal array was sensitive to directly coupled vibrations across the range of frequencies tested, with best sensitivity of 0.09 mm/s at 80 Hz. The velocity thresholds as a function of frequency showed a characteristic U-shaped curve with a gradual low-frequency roll-off below 80 Hz and a steeper high-frequency roll-off above 250 Hz. The thresholds measured for the harbor seal in this study were about 100 times more sensitive than previous in-air measures of vibrissal sensitivity for this species. The results were similar to those reported by others for the detection of waterborne vibrations, but show an extended range of frequency sensitivity.

Animal-borne tagging methods were used to investigate the signals received by the vibrissae and better understand the relevant signal components involved in hydrodynamic detection. A novel tagging system, wLogger, was developed to record vibrations directly from a vibrissa by means of an accelerometer coupled to the vibrissal shaft. Laboratory testing using excised whiskers in a water flume confirmed that the tag

is capable of recording vibrational signals without hampering the natural movement of the vibrissa. In addition, the tag successfully measured vibrations from the vibrissae of a harbor seal during active swimming and hydrodynamic detection. Live animal testing, along with the supplemental recordings from excised vibrissae, revealed that interaction with hydrodynamic disturbances disrupted the vibrational signal received by the whisker. When exposed to a hydrodynamic signal, whisker vibrations increased in bandwidth, spreading energy across a wider range of frequencies. This finding suggests that modulation of the vibrational signal may play a key role in the detection of hydrodynamic stimuli by the seal.

The results of this dissertation research provide insight into the functioning of the vibrissal system in pinnipeds and establishes the groundwork for future pathways of investigation. By investigating the vibrissal system from the focal points of structure, sensitivity and received signals, a more comprehensive understanding of this refined sensory modality is emerging.

GENERAL INTRODUCTION

Vibrissae, otherwise known as sinus hairs, sensory hairs, tactile hairs, or whiskers, are keratinous structures of epidermal origin that are present in nearly all mammals (Hirons et al., 2001; Ling, 1977). Vibrissae are distinct from the pelage hairs, which cover the body, in that they are highly innervated and possess a blood sinus system with a dense connective tissue capsule (Reep, 2002; Reep, 2001). Furthermore, these specialized hairs are typically longer, stiffer, and found on restricted regions of the body. Vibrissae primarily occur on the head and limbs but are sometimes present on other areas of the body surface (Hanke, 2010; Reep, 2002; Huber, 1930).

Vibrissae occur to some extent in most marsupials and placental mammals, but are absent in the monotremes (Abbie, 1934; Huber, 1930; Pocock, 1914). Differences in degree of vibrissal development exist among species. Advanced development of the vibrissae is believed to be linked to lifestyles with greater emphasis on tactile information. For example, these structures are highly developed in many burrowing and active arboreal species. The atrophy of the vibrissae may correlate with limited reliance on tactile information or the advancement of other highly specialized senses. For example in primates, the vibrissae are progressively reduced going from lower to higher order species, possibly correlating with the advancement of the sensitivity of the hands (Pocock, 1914).

In marine mammals, degree of vibrissal specialization varies greatly between species. These structures are nearly absent in polar bears, as they are in most Ursidae

(Pocock, 1914; Huber, 1930). Cetaceans (whales, dolphins and porpoises) possess some form of vibrissae. These structures are larger and more developed in the mysticetes (baleen whales) than in the odontocetes (toothed whales). In the mysticetes, vibrissae are found on the chin, on nodules on the lower jaw, along the edge of the lower lip and around the blowhole (Ling, 1977). Most odontocete species have only a sparse arrangement of vibrissae in their adult stage and in some species, the vibrissal follicles atrophy before birth (Ling, 1977). The freshwater river-dwelling Platanistidae appear to be an exception among the odontocetes, having numerous well-developed vibrissae along their upper and lower jaws. The structures are thought to aid in foraging along turbid river bottoms and may compensate for reduced vision in these species (Ling, 1977). Sea otters have a dense array of facial vibrissae and the sirenians (manatees and dugongs) have specialized facial vibrissae as well as a complex array of postcranial vibrissae covering the surface of the body (Reep et al., 2002; Huber, 1930; Wilson et al. 1991).

Pinnipeds (seals, sea lions and walruses) have the largest and most highly developed vibrissae of all mammals (Ling, 1977; Ling, 1966). All members of this group, which include the phocids (true seals), otariids (sea lions and fur seals) and odobenids (walruses), possess specialized vibrissal arrays. Pinnipeds have up to three groupings of facial vibrissae: mystacial, supraorbital, and rhinal. It is currently unknown if the different vibrissal groups have specialized function apart from each other.

The mystacial vibrissae, which are located on the muzzle around lips, are the most distinct and numerous. These vibrissae are arranged in parallel rows and vary in number and size between species. Harbor seals (*Phoca vitulina*) have about 88 vibrissae on the mystacial pads and southern elephant seals (*Mirounga leonina*) possess a mean number

of 76 vibrissae (Ling, 1977; Dehnhardt, 2002). The bearded seal (*Erignathus barbatus*) has the maximum number of vibrissae among the phocid seals, 244, while the walrus (*Odobenus rosmarus*) has the most vibrissae of all pinnipeds, numbering up to 700 (Ling, 1977; Marshall et al., 2006).

Located above the eyes are the supraorbital (or supercilliary) vibrissae. Based on their appearance they have been colloquially referred to as "eyebrows" (Ling, 1977). These occur in small patches of approximately 2 to 7 on each side. The supraorbital vibrissae appear to be more developed in phocids than in otariids and odobenids (Pocock, 1914; Ling, 1966; Ling, 1977).

The rhinal (or nasal) vibrissae are located above the nose. Rhinal vibrissae are present in phocids but absent in the otariids and odobenids. They occur as a single or pair of vibrissae on each side of the face (Ling, 1977).

In all reported accounts, pinnipeds possess only these facial groupings of vibrissae. A possible exception to this may be the Hawaiian monk seal (*Monachus schauinslandi*), in which a pair of vibrissal-like hairs under the lower jaw has been observed but not formally documented (*personal observation*). The placement of these hairs is consistent with the classification of interramal vibrissae in terrestrial mammals (Pocock, 1914), but histological examination of the follicle would be required for confirmation.

Motor control

Pinnipeds exhibit motor control over their mystacial vibrissal array (Oliver, 1978). While motor control of individual vibrissae has not been reported in phocids or otraiids, these animals are able to move their mystacial array as a whole. The mystacial

vibrissae can lie back against the face or be protracted so that the bases of the hair shafts are positioned nearly perpendicular to the rostro-caudal axis of the body (Dehnhardt et al., 2001; Gläser et al., 2010). The odobenids are unique among the pinnipeds in that they have highly mobile vibrissae and motor control over individual regions of the vibrissal pad (Kastelein and Van Gaalen, 1988).

The extent to which the supraorbital vibrissae may be voluntarily controlled appears to vary between pinniped groups. Some phocids are able to raise the supraorbital vibrissae from a resting position nearly flat against the head to an alert position standing out from the face (Ling, 1966). Motor control of the supraorbital vibrissae in otariids and odobenids has not been reported. The rhinal vibrissae, when present, appear to be immobile.

Little is known about the fine motor control that pinnipeds have over the rotation and precise positioning of the vibrissae. It is known that pinnipeds do not “whisk”, as many rodents do. Rats and mice, among other species, display high amplitude, rhythmic movements of the vibrissae that can occur at rates of up to 25 Hz (Jin et. al., 2004). Whisking behavior has not been observed in any marine mammal. Although pinnipeds do not whisk, they do appear to utilize lateral head movements during object exploration. In tactile discrimination studies of the walrus, Kastelein and Van Gaalen (1988) observed head movements as well as movement of the vibrissal array, however individual vibrissal movement could not be resolved or investigated. Dehnhardt (1994) and Dehnhardt & Kaminski (1995) reported that California sea lions and harbor seals kept their vibrissal array erect and performed short lateral head movements during active tactile discrimination tasks, but did not move the vibrissae independently of the head. Dehnhardt

et al. (2001) also described slight lateral head movements in a harbor seal while searching for an underwater hydrodynamic trail. The absence of whisking behavior in marine mammals may possibly be an adaptation to the aquatic environment, compensating for the higher viscosity of water.

Anatomy and innervation

The base of each vibrissa is encased in a sub-dermal capsule composed of hard, dense collagenous tissue (Stephens et al.,1973). In pinnipeds, the vibrissal follicles are larger than in any other mammal, with the capsule extending up to 2 cm below the skin surface (Hyvärinen and Katajisto, 1984). The capsule houses the follicle sinus complex (FSC), the highly innervated sinus structure that surrounds the base of each vibrissa (Rice et al., 1986). When the sinuses are engorged with blood, the follicle becomes a rigid structure (Hyvärinen, 1989; Ling, 1966). Most of the facial musculature of pinnipeds appears to be associated with the base of the follicles, and erector pilli muscles have been reported in some pinniped species; this may be related to degree of mobility of the vibrissae (Hyvärinen et al., 2009; Ling, 1966; Marshall et al., 2006).

The FSCs of pinnipeds are characterized by a three-part blood sinus system, composed of an upper cavernous sinus, ring sinus and lower cavernous sinus (Ling, 1966; Marshall et al., 2006). The upper cavernous sinus is a unique feature of the pinniped vibrissal system. All terrestrial mammals possess a two-part sinus system (Rice et al., 1986). In pinnipeds, the upper cavernous sinus composes approximately 60% of the length of the follicle, lacks innervation and is hypothesized to have mainly a thermoregulatory function (Hyvärinen and Katajisto, 1984; Dehnhardt et al., 1998b; Marshall et al., 2006). Dehnhardt et al. (1998b) demonstrated that the mystacial vibrissae

of harbor seals do not experience a loss of sensitivity when exposed to cold water temperatures and no vasoconstriction occurs in the vibrissal region during cold exposure. This is in contrast to, for example, the touch receptors in the human hand which experience numbness under low temperature conditions (Dehnhardt et al., 1998b). The presence of the large upper cavernous sinus may allow the vibrissal system to function well in cold marine environments by thermally insulating the sensory elements below it.

Below the upper cavernous sinus is a large ring sinus area with an asymmetrical collar of connective tissue, called the ringwulst, encircling the hair shaft (Rice et al., 1986; Ling, 1977; Stephens et al., 1973). The function of the ringwulst is not understood. The ring sinus appears to be the primary sensory area of the FSC and the majority of nerve fibers terminate here, above the ringwulst (Hyvärinen and Katajisto, 1984).

The mystacial vibrissae are innervated by the infraorbital branch of the trigeminal nerve and the supraorbital vibrissae are innervated by the supraorbital branch (Ling, 1977). In contrast to terrestrial mammals, no superficial innervation occurs at the apical end of the follicle (Rice et al., 1986). Rather, the innervating elements, as well as the blood supply to the follicle, enter from the basal end of the capsule, below the lower cavernous sinus (Ginter et al., 2010; Stephens et al., 1973). The nerve branches that enter at the capsule base are termed the deep vibrissal nerve. These ascend, ramify, and terminate in mechanoreceptors in the lower cavernous sinus and ring sinus (Ling, 1966; Marshall et al., 2006). The branches contain both rapidly adapting (RA) and slowly adapting (SA) nerve fibers (Dykes, 1975) and terminate in three types of nerve endings: Merkel-Neurite complexes, laminated corpuscles and lanceolate endings (Stephens et al., 1973; Marshall et al., 2006).

The vibrissal system of pinnipeds is highly innervated, as is expressed by the number of myelinated axons serving each FSC. Bearded seals *(Erignathus barbatus)* possess the greatest innervation per FSC of any mammal recorded, at 811–1,650 myelinated axons per FSC (Marshall et al., 2006). The ringed seal (*Phoca hispida)* possesses a comparable degree of innervation, with 1,000 to 1,500 myelinated axons innervating a single vibrissa. These numbers are tenfold higher than those recorded for the rat and beaver (Hyvärinen and Katajisto, 1984). When compared to more closely related carnivore species, degree of vibrissal innervation appears to relate to degree of aquatic adaptation. The ringed seal possesses four times more myelinated axons per FSC than the semi-aquatic European otter (*Lutra lutra*) and ten times that of the terrestrial pole cat (*Mustela putorius*) (Hyvärinen, 2009). Considering this trend, adaptation to the aquatic environment may account for the high degree of innervation observed in pinniped vibrissae.

Neural pathways associated with vibrissal stimulation project onto the somatosensory area of the cerebral cortex. In pinnipeds, this has been studied only in the northern fur seal (*Callorhinus ursinus*) and was measured via microelectrode recordings of cortical activity (Ladygina at al., 1985; Ladygina at al., 1992). In this species, and likely in most pinnipeds, a very large portion of the head projection area of the somatosensory cortex is devoted to representation of the vibrissae (Ladygina at al., 1992). Independence between vibrissae is maintained in cortical organization. Small fields of cortical points respond to stimulation from only one vibrissa and are independent from excitation of the surrounding skin (Ladygina et al., 1992).

Morphology

Two types of vibrissal surface structures, undulated and smooth, exist among pinnipeds. The vibrissae of all phocids, with the exception of the bearded seal (*Erignathus barbatus)*, Ross seal *(Ommatophoca rossii)*, and monk seals (*Monachus spp.)*, have undulated surfaces (Hyvärinen & Katajisto, 1984; Ling, 1972). This undulated surface profile is characterized by repeating crests and troughs along the length of the vibrissal shaft and has also been described as wavy, beaded, or corrugated in appearance. Phocids are the only animal group known to possess undulated vibrissae. In contrast, the vibrissae of the otariids, odobenids, and all other mammals, have smooth surfaces (Dehnhardt and Kaminski, 1995; Ginter et al., 2010). The adaptive significance of these differences in surface structure is currently unknown.

While the vibrissae of terrestrial mammals are circular in cross-section, the vibrissae of all pinnipeds appear to be flattened in profile, to some extent (Ginter et al., 2010; Hyvärinen et al., 2009). It has been hypothesized that undulated vibrissae exhibit more extreme flattening, while the smooth vibrissae have an oval cross-section (Dehnhardt et al., 2004). There may be variability between species in the degree of cross-sectional flattening; however, this has not been studied in detail.

Sensitivity

In pinnipeds, the vibrissae are known to function in both tactile discrimination and the detection of water-borne disturbances from hydrodynamic stimuli (Dehnhardt and Kaminski, 1995; Dehnhardt et al., 1998a; Dehnhardt et al., 2001; Gläser et al., 2010). The vibrissal systems of pinniped species are highly sensitive, being capable of detecting water velocities as low as 245 μms^{-1} (Dehnhardt et al., 1998a) and having tactile

discrimination abilities comparable to that of a monkey's hand (with a Weber fraction as low as 0.08 for size of actively touched objects) (Dehnhardt & Kaminski, 1995).

Active touch studies on the Pacific walrus (*O. rosmarus*), demonstrated the ability to detect shapes down to 0.4 cm^2 in both a smooth and rough background (Kastelein & Van Gaalen, 1988; Kastelein et. al., 1990). Active touch experiments with a California sea lion (*Zalophus californianus*) demonstrated that this species has good discrimination abilities and is able to distinguish the shape of three-dimensional objects (Dehnhardt, 1990). Additional behavioral experiments with a California sea lion discriminating circular disks of differing diameters measured absolute size difference thresholds of 0.33 cm for disks of 1.12 cm and thresholds of 1.55 cm for disks of 8.74 cm. This results in Weber fractions of .29 and .22 (Dehnhardt, 1994). The same tests were conducted on two harbor seals, revealing equivalent sensitivity to the sea lion at the smaller disk size and superior sensitivity for the larger disk sizes, with Weber fractions as low as 0.08 (Dehnhardt & Kaminski, 1995). These values can be compared to Weber fractions obtained from tactile discrimination studies of the human hand and the hands of lower primates (which have average Weber fractions of 0.03 and 0.1 respectively) and suggest that pinniped vibrissal systems are comparably sensitive structures.

One fundamental approach used to understand the capabilities of a sensory system is to measure its sensitivity at a range of frequencies. The first study to investigate the vibrissal sensitivity of pinnipeds in this manner (Dykes, 1975) utilized direct recordings from the infraorbital nerve to investigate responses to mechanical stimulation of the vibrissae. Dykes (1975) measured neural responses in anesthetized grey seals (*Halichoerus grypus*) and harbor seals (*Phoca vitulina)* to deflection of individual

vibrissae that had been clipped and fixed to a mechanical transducer. These tests identified both rapidly adapting (RA) and slowly adapting (SA) nerve fibers and, based on response patterns, concluded that SA fibers encode stimulus intensity and RA fibers encode stimulus frequency.

Dykes (1975) also examined frequency sensitivity by contacting vibrissae with tuning forks of different resonances and recording the percentage of RA fibers that phase-locked to the stimulus frequency. Responses were recorded to forks with resonant frequencies from 128, 256, 512 and 1024 Hz. The percentage of responsive fibers decreased as stimulus frequency increased and only a small proportion of the fibers were responsive at the highest test frequency. This tentatively suggests a frequency of best sensitivity at or below 128 Hz. However, the inability of a fiber to phase lock to a frequency does not necessarily indicate inability to detect the stimulus.

Although the study did not directly measure response thresholds, Dykes (1975) concluded that a stimulus must be sufficiently large to induce a response from the vibrissae and that the system overall was likely to be sensitive only to direct stimulation. However, this conclusion is likely an underestimate of the vibrissal system's sensitivity and the methodology utilized by Dykes to identify phase locking of fibers does not necessarily indicate minimum detectable stimulus level.

Subsequent studies utilized less invasive psychophysical methods to investigate vibrissal sensitivity in seals. Renouf (1979) and Mills and Renouf (1986) used an in-air behavioral signal detection task to test sensitivity of the vibrissae of the harbor seal. Vibrissae were directly stimulated by contact with a metal rod vibrating at frequencies from 50 to 2500 Hz. These studies found greatest sensitivity to be at the higher end

(above 500 Hz) of the test frequency range. The first of these studies (Renouf, 1979) estimated the vibrissae to be relatively insensitive at frequencies below 500 Hz, measuring very high thresholds at low frequencies (approximately 21 μm at 250 Hz and 103 μm at 100 Hz). Dramatically better sensitivity was reported at the higher test frequencies, with thresholds of less than 1 μm at 750 and 1000 Hz. However, this study was criticized for lack of adequate measures to control for acoustic cues and potential response bias by the animal (Watkins and Wartzok, 1985). Mills and Renouf (1986) addressed these methodological concerns and found similar trends but slightly different sensitivity values. Poor sensitivity was reported at lower frequencies (100 to 500 Hz), with average thresholds of 30 μm displacement. Better sensitivity was measured at 750 Hz and above, with thresholds below 12 μm. The smallest vibration reliably detected by the seal was 2.12 μm at 1000 Hz. Mills and Renouf concluded that the vibrissal system of the harbor seal was relatively insensitive at frequencies below 500 Hz and hypothesized that seals may be specialized for high frequency sensitivity in order to detect fine texture differences during active touch.

These prior electrophysiological and psychophysical studies report contradictory ranges of frequency sensitivity for the same species. Unfortunately, direct comparison of the results is challenging due to differences in methodology and aims of the studies. Dykes tested the point at which a unit would fire one impulse for every cycle of the vibration stimulus, while Renouf (1979) and Mills and Renouf (1986) examined absolute thresholds. In addition, Dykes' electrophysiological recordings were from single infraorbital nerve fibers while the subsequent work utilized behavioral methods and stimulated whole whiskers.

While all of the early investigations of pinniped vibrissal sensitivity were conducted in air, more recently studies have begun to investigate this sensory system in water. Using plates with grooves of varying thickness, the texture difference thresholds of two adult harbor seals were determined underwater with behavioral methods (Dehnhardt et al., 1998b). The seals' could detect a minimum of 0.18 mm groove width difference against a standard with 2 mm groove width. The seals' performance was comparable to that of the human hand tested on the same experimental setup. When this task was repeated in cold water temperatures, the seals' sensitivity remained the same, now surpassing that of the human hand, which was subject to numbness under such thermal conditions. The maintenance of advanced functioning of the vibrissal system under environmental stress underscores the importance of this sensory modality to the ecology of these animals.

More recent studies have begun to focus on detectability of stimuli propagating through a fluid medium. This shift was motivated by interests in understanding how the sensitivity of the pinniped vibrissal system aids in the detection of biologically relevant underwater signals, such as hydrodynamic trails. While hydrodynamic signals are difficult to control and measure in typical testing environments, several methodologies have been developed to explore sensitivity to these signals.

Dehnhardt et al. (1998a) produced the first measure of the sensitivity of pinniped vibrissae to low amplitude water movements. This study employed a behavioral task to test the sensitivity of a trained harbor seal to low-frequency (10 – 100 Hz), underwater, vibrational signals produced by a dipole source (constant-volume oscillating sphere). The particle motion component in the near field of the stimulus was used to simulate

hydrodynamic signals. The seal's performance could then be used to infer its ability to sense biogenic signals such as would be contained in the water movements around a swimming fish. This study identified the frequency of maximum sensitivity to be 50 Hz and determined that water velocities as low as 245 μm/s and particle displacements of 0.8 μm could be detected. Based on comparison of the sensitivity curves of the harbor seal, calculated in terms of particle acceleration, velocity and displacement, these researchers hypothesized that below 50 Hz, the vibrissal system is responsive to acceleration, while above that level it is responsive to displacement. Preliminary studies were also conducted with a California sea lion, using the same paradigm to test thresholds at 20 and 30 Hz (Dehnhardt et al., 2004; Dehnhardt and Mauck, 2008). At these frequencies the sea lion showed greater sensitivity than the harbor seal, but the data are too limited to provide a comprehensive comparison between the species. The velocity threshold levels measured for the harbor seal and California sea lion in these psychophysical experiments are below those measured in the wake of a swimming fish and indicate that the vibrissal system of at least some pinnipeds has the capacity to detect naturally occurring hydrodynamic trails (Dehnhardt et al., 1998a).

In addition to the studies of hydrodynamic stimulus detection conducted by Dehnhardt and colleagues (1998a, 2004, 2008), performance trials with actively swimming pinnipeds allowed for demonstration of hydrodynamic detection abilities in a more natural context. Dehnhardt et al (2001) and Schulte-Pelkum et al. (2007) demonstrated harbor seals could accurately track biogenic and hydrodynamic trails. Experimental controls eliminated acoustic and visual cues, demonstrating that the animals utilized the vibrissal array to accomplish this task. The experiments imposed a

time delay condition, to allow for natural degradation of the hydrodynamic trail and simulate long distance detection. The subjects were able to perform accurately with increasing delays up to 20 seconds, which would have corresponded to the trail generator traveling 40 m away. These results indicated the potential for use of hydrodynamic signals in long-range prey detection. This contradicted a previous suggestion that hydrodynamic trail detection by pinnipeds was likely only possible over short ranges due to particle velocity attenuation with distance from the source (Levenson and Schusterman, 1999).

Gläser et al. (2010) demonstrated that a California sea lions was also able to effectively track hydrodynamic wakes. This study found that the sea lion followed linear trails with great accuracy but showed increased difficulty once curved trails were used or a delay condition imposed. Based on these findings the authors argued that sea lions have a lower ability to detect hydrodynamic trails. However, it is difficult to parse out individual subject differences and training confounds from true species differences, making an accurate comparison difficult.

Some creative approaches are emerging that enable detailed analyses of the components of hydrodynamic stimuli that are detectable to seals. Wieskotten et al. (2010b) utilized a modified wake tracking task to examine the effect of swimming mode on the trackability of hydrodynamic trails. Using an artificially generated wake to simulate burst and glide movements of a swimming object, the study demonstrated that the introduction of glide phases increased the difficulty of the trail following task for the animal. This raises interesting questions regarding the characteristics of complex biogenic trails and the saliency of their components to the vibrissal system. Wieskotten et

al. (2010a) also used a behavioral task to test the ability of a harbor seal to discriminate wakes generated by an artificial fin. This study demonstrated the ability of the seal to discriminate objects of different size or shape solely by their hydrodynamic signature. These works continue to highlight the specialized abilities of the vibrissal systems of pinnipeds as well as raise interesting questions about their functioning.

Investigations of the pinniped vibrissal system has spanned four decades, the findings of which underscore the importance of this sensory modality in the ecology of these species. Although it is known that pinnipeds can use their vibrissae to perform active touch and hydrodynamic detection tasks, many aspects of vibrissal function remain poorly understood. The present work examines the adaptive significance of vibrissal structure, the sensitivity of the vibrissal system, and the signals received by this system. All of these points are considered within the framework of hydrodynamic detection. Four methods of study: laser vibrometer recordings, computed tomography (CT) scanning methods, behavioral signal detection experiments and animal-borne tag measurements were used to investigate the functioning of this sensory system. Where possible, comparative measurements are made between pinniped species and when not, detailed measures are made on a representative species, the harbor seal (*Phoca vitulina*).

References

Abbie, A. (1934). The Brain-Stem and Cerebellum of Echidna aculeata. *Philosophical Transactions of the Royal Society B: Biological Sciences*, 224(509), 1-74.

Bleckmann, H. (1993) Role of the lateral line in fish behavior. In *Behavior of Teleost Fishes 2nd edition.* ed. T.J. Pitcher. pp. 201-246. London: Chapman and Hall.

Coombs, S., Hastings, M., & Finneran, J. (1996). Modeling and measuring lateral line excitation patterns to changing dipole source locations. *Journal of comparative physiology. A, Sensory, neural, and behavioral physiology*, 178(3), 359-71.

Dehnhardt, G. (1990) Preliminary results from psychophysical studies on the tactile sensitivity in marine mammals. In: Thomas JA, Kastelein RA (eds) Sensory abilities of cetaceans. Plenum Press, New York, pp. 435-446.

Dehnhardt, G. (1994). Tactile size discrimination by a California sea lion *(Zalophus californianus)*using its mystacial vibrissae. *J Comp Physiol A*, 175, 791-800.

Dehnhardt, G. (2002). Sensory systems. In *Marine Mammal Biology An Evolutionary Approach*. ed. A.R. Hoelzel. pp. 116-141. Malden, MA: Blackwell Science Ltd.

Dehnhardt, G. and Kaminski, A. (1995). Sensitivity of the mystacial vibrissae of harbour seals (*Phoca vitulina*) for size differences of actively touched objects. *J. Exp. Biol*. 198, 2317-2323.

Dehnhardt, G. and B., Mauck. (2008). Mechanoreception in secondarily aquatic vertebrates. In: *Senses on the Threshold: Form and Function of the Sense Organs in Secondarily Aquatic Tetrapods*, J. G. M. Thewissen and Sirpa Nummela (editors). University of California Press, Berkeley, pp. 295-314.

Dehnhardt, G., Mauck, B. and Bleckmann, H. (1998a). Seal whiskers detect water movements. *Nature* 394, 235-236.

Dehnhardt, G., Mauck, B., and W. Hanke. (2004). Hydrodynamic perception in seals. In *Dynamic Perception, Workshop of the GI Section "Computer Vision"*. ed. U. Ilg, H. Bülthoff, and H. Mallot. p. 27-32. Tübugen: IOS press.

Dehnhardt, G., Mauck, B., Hanke, W. and Bleckmann, H. (2001). Hydrodynamic trail-following in harbor seals (*Phoca vitulina*). *Science.* 293, 102-104.

Dehnhardt, G., Mauck, B., and H. Hyvärinen. (1998b). Ambient temperature does not affect the tactile sensitivity of mystacial vibrissae in harbour seals. The Journal of Experimental Biology 201, 3023–3029.

Dehnhardt, G., Mauck, B. and Hanke, W. (2004). Hydrodynamic perception in seals. In *Dynamic Perception, Workshop of the GI Section "Computer Vision"* (ed. U. Ilg, H. Bülthoff, and H. Mallot), pp. 27-32. Tübugen: IOS Press.

Dykes, R.W. (1975). Afferent fibers from the mystacial vibrissae of cats and seals. *Journal of Neurophysiology.* 39, 650-662.

Fish, F. E., Howle, L. E. and Murray, M. M. (2008). Hydrodynamic flow control in marine mammals. *Integr. Comp. Biol.* 48, 788-800.

Ginter, C. G., Fish, F. E. and Marshall, C. D. (2010). Morphological analysis of the bumpy profile of phocid vibrissae. *Mar. Mammal. Sci.* 26, 733-745.

Gläser, N., Otter, C., Dehnhardt, G. and Hanke, W. (2010). Hydrodynamic trail following in a California sea lion (*Zalophus californianus*). *J. Comp. Physiol. A* 197, 141-151.

Hanke, W., Witte, M., Miersch, L., Brede, M., Oeffner, J., Michael, M., Hanke, F., Leder, A. and Dehnhardt, G. (2010). Harbor seal vibrissa morphology suppresses vortex-induced vibrations. *J. Exp. Biol.* 213, 2665-2672.

Hirons, A. C., Schell, D. M., & St. Aubin, D. J. (2001). Growth rates of vibrissae of harbor seals (*Phoca vitulina*) and Steller sea lions (*Eumetopias jubatus*). *Canadian Journal of Zoology*, *79*(6), 1053-1061.

Hyvärinen, H. (1989). Diving in darkness; whiskers as sense organs of the ringed seal (*Phoca hispida saimensis). J. Zool. (Lond.).* 218, 663-678.

Hyvärinen, H. (1995). Structure and function of the vibrissae of the ringed seal (Phoca hispida L.). *Sensory Systems of Aquatic Mammals*

Hyvärinen, H. and Katajisto, H. (1984). Functional structure of the vibrissae of the ringed seal *(Phoca hispida Schr.). Acta Zool. Fenn.*171, 27-30.

Hyvärinen, H., Palviainen, A., Strandberg, U. and Holopainen, I.J. (2009). Aquatic environment and differentiation of vibrissae: Comparison of sinus hair systems of ringed seal, otter and pole cat. *Brain Behav. Evol*. 4, 268–279.

Huber, E. (1930). Evolution of facial musculature and cutaneous field of trigeminus. Part I. *TheQuarterly Review of Biology*, *5*(2), 133–188.
Jin, T.-E., Witzemann, V., & Brecht, M. (2004). Fiber types of the intrinsic whisker muscle and whisking behavior. *The Journal of neuroscience*, *24*(13), 3386-93.

Kastelein, R., Stevens, S., & Mosterd, P. (1990). The tactile sensitivity of the mystacial vibrissae of a Pacific Walrus (Odobenus rosmarus divergens). Part 2: Masking. *Aquatic Mammals*, *16*, 78–87.

Kastelein, R., & Van Gaalen, M. (1988). The sensitivity of the vibrissae of a Pacific walrus (Odobenus rosmarus divergens) Part 1. *Aquatic Mammals*, *14*, 123–133.

Ladygina, T., Popov, V., & Supin, A. Y. (1985). Topical organization of somatic projections in the fur seal cerebral cortex. *Neurophysiology*, *17*(3), 246–252.

Ladygina, T., Popov, V., & Supin, A. Y. (1992). Micromapping of thr fur seal's somatosensory cerebral cortex. In J. Thomas & et al. (Eds.), *Marine Mammal Sensory Systems*. New York: Plenum Press.

Levenson, D. H., & Schusterman, R. J. (1999). Dark Adaptation and Visual Sensitivity in Shallow and Deep-Diving Pinnipeds. *Marine Mammal Science*, *15*(4), 1303-1313.

Ling, J.K. (1966). The skin and hair of the southern elephant seal, *Mirounga leonine* (Linn.) I. The facial vibrissae. *Australian Journal of Zoology.* 14, 855-866.

Ling, J. K. (1972). Vibrissa follicles of the ross seal. *Br. Antarct. Surv. Bull.*, *27,* 19-24.

Ling, J.K. (1977). Vibrissae of marine mammals. In *Functional Anatomy of Marine Mammals, Vol. 3* (ed. R. J. Harrison), pp. 387-415. London: Academic Press.

Marshall, C. D., Amin, H., Kovacs, K. M., & Lydersen, C. (2006). Microstructure and innervation of the mystacial vibrissal follicle-sinus complex in bearded seals, Erignathus barbatus (Pinnipedia: Phocidae). *The anatomical record. Part A, Discoveries in molecular, cellular, and evolutionary biology*, *288*(1), 13-25.

Mills, F. H. J. and D. Renouf. (1986). Determination of the vibration sensitivity of harbour seals (*Phoca vitulina*) vibrissae. *J. Exp. Mar. Biol. Ecol.* 100, 3-9.

Oliver, G. W. (1978). Navigation in Mazes by a Grey Seal , Halichoerus grypus (Fabricius). *Behaviour*, *67*(1/2), 97-114.

Peterson, R., & Bartholomew, G. A. (1967). The natural history and behavior of the California sea lion. *American Society of Mammalogists, Stillwater, Oklahoma, Special Pu*.

Pocock, R. (1914). On the Facial Vibrissæ of Mammalia. *Proceedings of the Zoological Society of London* (Vol. 84, pp. 889–912).

Reep, R.L., Marshall, C.D., and M.L. Stoll. (2002). Tactile hairs on the postcranial body in Florida manatees: a mammalian lateral line? *Brain Behavior and Evolution.* 59:141-154.

Reep, R.L., Stoll, M.L., Marshall, C.D., Homer, B.L. and D.A. Samuelson. (2001). Microanatomy of facial vibrissae in the Florida manatee: the basis for specialized sensory function and oripulation. *Brain Behavior and Evolution.* 58:1-14.

Renouf, D. (1979). Preliminary measurements of the sensitivity of the vibrissae of Harbour seals (*Phoca vitulina*) to low frequency vibrations. *J. Zool.* 188, 443-450.

Rice, F. L., Mance, A., & Munger, B. L. (1986). A comparative light microscopic analysis of the sensory innervation of the mystacial pad. I. Innervation of vibrissal follicle-sinus complexes. *The Journal of comparative neurology*, *252*(2), 154-74.

Roshko, A. (1954). On drag and shedding frequency of two-dimensional bluff bodies. N.A.C.A. Tech. Note No. 3169

Schulte-Pelkum, N., Wieskotten, S., Hanke, W., Dehnhardt, G., and B. Mauck. (2007). Tracking of biogenic hydrodynamic trails in harbour seals (*Phoca vitulina*). The Journal of Experimental Biology. 210, 781-787.

Stevens, R. J., Beebe, I. J. and Poulter, T. C. (1973). Innervation of the vibrissae of the California sea lion, *Zalophus californianus*. *Anat. Record*. 176, 421-442.

Vogel, S. (1994) *Life in moving fluids.* Princeton: Princeton University Press.

Watkins, W.A., and, D. Wartzok. (1985). Sensory biophysics of marine mammals. *Marine Mammal Science.* 1:219-260.

Wieskotten, S., Dehnhardt, G., Mauck, B., Miersch, L., and W. Hanke. (2010a). Hydrodynamic determination of the moving direction of an artificial fin by a harbour seal (*Phoca vitulina*). Journal of Experimental Biology. 213, 2194-2200.

Wieskotten S., Dehnhardt G., Mauck B., Miersch L., and W. Hanke. (2010b) The impact of glide phases on the trackability of hydrodynamic trails in harbour seals (*Phoca vitulina*). The Journal of Experimental Biology. 213, 3734-3740.

Wilson, Don E., et al. (1991). Geographic variation in sea otters, Enhydra lutris. *Journal of Mammalogy*. 22-36.

CHAPTER 1[1]: EFFECT OF ANGLE ON FLOW-INDUCED VIBRATIONS OF PINNIPED VIBRISSAE

Abstract

Two types of vibrissal surface structures, undulated and smooth, exist among pinnipeds. Most Phocidae have vibrissae with undulated surfaces, while Otariidae, Odobenidae, and a few phocid species possess vibrissae with smooth surfaces. Variations in cross-sectional profile and orientation of the vibrissae also exist between pinniped species. These factors may influence the way that the vibrissae behave when exposed to water flow. This study investigated the effect that vibrissal surface structure and orientation have on flow-induced vibrations of pinniped vibrissae. Laser vibrometry was used to record vibrations along the whisker shaft from the undulated vibrissae of harbor seals (*Phoca vitulina*) and northern elephant seals (*Mirounga angustirostris*) and the smooth vibrissae of California sea lions (*Zalophus californianus*). Vibrations along the whisker shaft were measured in a flume tank, at three orientations (0°, 45°, 90°) to the water flow. The results show that vibration frequency and velocity ranges were similar for both undulated and smooth vibrissae. Angle of orientation, rather than surface structure, had the greatest effect on flow-induced vibrations. Vibration velocity was up to

[1] Portions of these results have been previously published (Murphy, C.T., Eberhardt, W.C., Calhoun, B.H., Mann, K.A. and D.A. Mann (*in press*) Effect of angle on flow-induced vibrations of pinniped vibrissae. PLOS ONE)

60 times higher when the wide, flat aspect of the whisker faced into the flow (90°), compared to when the thin edge faced into the flow (0°). Vibration frequency was also dependent on angle of orientation. Peak frequencies were measured up to 270 Hz and were highest at the 0° orientation for all whiskers. Furthermore, CT scanning was used to quantify the three-dimensional structure of pinniped vibrissae that may influence flow interactions. The CT data provide evidence that all vibrissae are flattened in cross-section to some extent and that differences exist in the orientation of this profile with respect to the major curvature of the hair shaft. These data support the hypothesis that a compressed cross-sectional profile may play a key role in reducing self-noise of the vibrissae.

Introduction

Vibrissae, otherwise known as sinus hairs, sensory hairs, tactile hairs, or whiskers, are keratinous structures of epidermal origin that are present in nearly all mammals (Ling, 1977). These structures are especially well developed in pinnipeds (seals, sea lions, and walrus). The vibrissae are arranged in an array about the face and muzzle and connect to richly innervated follicle sinus complexes below the skin (Hyvärinen et al., 2009;Hyvärinen, 1989;Marshall et al., 2006). In pinnipeds, the vibrissae are known to function in both haptic touch and detection of waterborne disturbances from hydrodynamic stimuli (Dehnhardt and Kaminski, 1995;Dehnhardt et al., 1998;Dehnhardt et al., 2001;Gläser et al., 2011). The vibrissal system has been demonstrated to be highly sensitive and, in some seals, has been shown to detect water velocities as low as 245 μms^{-1} (Dehnhardt et al., 1998).

Two types of vibrissal surface structures, undulated and smooth, exist among pinnipeds. The vibrissae of all Phocidae (true seals), with the exception of the bearded seal (*Erignathus barbatus)* and monk seals (*Monachus spp.)*, have undulated surfaces. This surface profile has also been described as wavy, beaded, or corrugated in appearance and is characterized by repeating crests and troughs along the length of the shaft (Dehnhardt and Kaminski, 1995;Ling, 1966). In contrast, the vibrissae of all Otariidae (fur seals and sea lions) and Odobenidae (walrus) have smooth surfaces (Figure 1.1).

Pinnipeds are the only animal group known to possess undulated vibrissae (Ginter et al., 2010). The unique morphological differences in pinniped vibrissal surface structure have been noted by numerous investigators (Dehnhardt and Kaminski, 1995;Ginter et al., 2012;Hyvärinen et al., 2009;Ling, 1966;Watkins and Wartzok, 1985), but their functional relevance is unclear. It has been hypothesized that the undulated structure facilitates detection of hydrodynamic signals, possibly by enhancing sensitivity or reducing background noise on the sensor (Dehnhardt et al., 2001;Fish et al., 2008;Ginter et al., 2010;Ginter et al., 2012;Gläser et al., 2011). Hanke et al. (Hanke et al., 2010) and Miersch et al. (Miersch et al., 2011) recently reported experimental evidence suggesting that the undulations serve to minimize vortex shedding behind the whisker, thereby reducing vibrations that would be generated from movement through the water. The experiments utilized force measurements and computational fluid dynamics to compare the flow resistance between undulated and smooth vibrissae. Using piezoceramic transducers, the dynamic forces at the base of the shaft were compared between the undulated vibrissae of harbor seals and the smooth vibrissae of California sea lions, measured in a rotational flume with the hairs at one fixed angle relative to the flow. The

studies revealed forces up to 9.5 times lower at the base of the undulated vibrissae than at the base of the smooth vibrissae, as well as a lower signal to noise ratio on the harbor seal than the sea lion vibrissae. A subsequent study (Witte et al., 2012), which combined particle imaging techniques and numerical simulation, determined that the wake behind an undulated vibrissa is characterized by an unsteady vortex structure and resulted in reduced drag and lift forces, as compared to an infinite cylinder with a circular cross-section.

While previous experimental evidence (Hanke et al., 2010) suggests that undulated vibrissae may be more specialized for hydrodynamic detection, behavioral studies indicate that both species with smooth vibrissae and species with undulated vibrissae can effectively track hydrodynamic signals (Dehnhardt et al., 2001;Gläser et al., 2011). In addition, psychophysical testing has revealed that pinnipeds with either type of vibrissae can detect low amplitude waterborne vibrations. At certain frequencies, the smooth vibrissae of the California sea lion actually have better sensitivity than the undulated vibrissae of the harbor seal (Dehnhardt et al., 2004), suggesting that surface structure alone may not be the only factor influencing performance.

In addition to differences in surface structure, it is also important to consider that cross-sectional shape of the hair shaft may affect the behavior of vibrissae when exposed to water flow. While all terrestrial mammals have smooth vibrissae with a circular cross-section (Ginter et al., 2010), both undulated and smooth pinniped vibrissae are flattened in profile to some extent (Dehnhardt and Mauck, 2008;Hanke et al., 2010;Hyvärinen et al., 2009). It has been hypothesized that undulated vibrissae exhibit more extreme flattening, while the smooth vibrissae have an oval cross-section (Dehnhardt et al., 2004).

In addition, there may be variability between species in the degree of cross-sectional flattening; however, this has not been studied in detail. Due to the cross-sectional flattening that occurs in both whisker types, each vibrissa has a distinct broad and thin aspect. Slightly rotating the vibrissa will change which edge faces into the flow, thus making orientation of the vibrissa a potentially important consideration in understanding flow interactions.

In addition to structural differences, variations in positioning and orientation of the array may exist between pinniped groups. Pinnipeds have motor control over the vibrissae and can protract the sensors from a relaxed position, flat against the face, to an erect position, held nearly perpendicular to the axis of the body. Previous behavioral studies of hydrodynamic wake following indicate that both harbor seals and California sea lions hold the vibrissal array in the erect position while tracking signals underwater (Dehnhardt et al., 2001;Gläser et al., 2011). It is not currently understood how the vibrissae are oriented in awake, behaving animals and how this may differ between species. However, it is important to consider these factors as a biological framework for understanding flow interactions of vibrissae.

Previous researchers have demonstrated that water flow causes vibrations along the vibrissal shaft (Hyvärinen and Katajisto, 1984;Miersch et al., 2011). A recent study conducted in air also found that seal vibrissae vibrated in response to stimulation from low frequency sounds (Shatz and De Groot, 2013). When modeled with the appropriate drag coefficient for water, the vibrissae were predicted to be tuned to frequencies of 20 to 200 Hz. In addition, some prior data demonstrated that orientation of the vibrissae influences the vibrations elicited by movement through the water. Hyvärinen measured

the frequency of vibrations along the shaft of a single excised vibrissa of the Saimaa ringed seal and found that when held with the broad edge of the vibrissa facing into the flow, vibrations along the shaft were measured at up to 300 Hz (Hyvärinen, 1995). However, when the same vibrissa was held with the narrow edge of the hair shaft facing into the flow, no detectable vibrations were measured.

The goal of the present study was to measure the effect that orientation has on the vibrations of smooth and undulated pinniped vibrissae exposed to water flow in a flume tank. Vibrissae were tested from three species of pinnipeds, one with smooth vibrissae and two with undulated vibrissae. Samples were fixed at multiple angles to the flow and the velocity and frequency spectra of vibrations were analyzed with respect to orientation. In addition, CT scanning of vibrissal samples was conducted in order to quantify the cross-sectional shape of the vibrissae and understand how this may contribute to orientation effects on self-induced vibrations.

Materials and Methods

Sample collection

Testing was conducted on excised mystacial vibrissae samples collected from post-mortem stranded animals at the Marine Mammal Center in Sausalito, California. Samples were collected from three pinniped species: the Pacific harbor seal (*Phoca vitulina*), northern elephant seal (*Mirounga angustirostris*), and California sea lion (*Zalophus californianus*). Sample availability was restricted to juvenile animals due to the higher mortality rate of this age group and both male and female animals were

sampled. All samples were collected from the right side of the muzzle and one vibrissa from each individual was tested.

Vibrissal samples for flume testing were collected from 26 individuals (n=9 for California sea lions; n=8 for elephant seals; n=9 for harbor seals). In order to standardize size across samples, vibrissae of matching lengths were selected for testing. Mean length of 7.7 cm (s.d.=0.55 cm) was chosen because samples in this size class were present in all three species. Constraining sample length was prioritized over matching for follicle position on the vibrissal bed. Length was constrained as closely as sample availability would allow. Mean length by species was 7.7 cm (s.d.=0.4 cm) for California sea lions; 8.19 cm (s.d.=0.5 cm) for elephant seals; and 7.35 cm (s.d.=0.4 cm) for harbor seals.

During collection, vibrissae were clipped at the skin surface, rinsed in fresh water, and packaged in dry gauze for transport. Prior to testing, each specimen was rehydrated by immersion in fresh water for one hour. Rehydration as well as flume testing was conducted in fresh water due to constraints of the flume setup.

Vibrissal samples from an additional 9 individuals (n=3 for California sea lions; n=3 for elephant seals; n=3 for harbor seals) were collected for CT scanning in order to quantify the three-dimensional shapes of the vibrissae. Samples for this portion of the study were also selected based on the length criteria used in flume testing. Mean length for CT samples was 6.5 cm (s.d.=0.63 cm). All samples were collected from the right side of the muzzle, and one vibrissa from each individual was scanned. These samples were extracted from the capsule, leaving the subdermal portion of the hair shaft attached. Samples were rehydrated in fresh water prior to being mounted on a slide for CT scanning.

Flume apparatus and vibration recordings

Samples were tested in a Rolling Hills Research Company Model 1520 water flume (El Segundo, CA, USA). The test section of the flume measures 152 cm in length, 38 cm in width, and 46 cm tall. Flow in the test section was laminar with velocity uniformity outside the wall boundary layer of <+/-2%. Inside the flume, individual vibrissae were mounted on a sting apparatus composed of a stainless steel rod with a 90 degree bend (Figure 1.2), located in the center of the water column. The boundary layer thickness along the walls of the flume tank was 1.6 cm and did not extend into the location of the sample mount. The body of the sting mount was positioned downstream of the sample; therefore, it did not interfere with the flow around the whisker. For attachment to the sting, the sample was fixed inside a cylindrical, threaded aluminum sleeve. The base of each whisker was inserted 1 cm into the sleeve and set with epoxy. The threaded sleeve base allowed the whisker to be rotated on the sting in order to test various angles to the flow. All tests were conducted at a flow speed of 0.5 m/s, verified by particle image analysis (PIV). The flow speed was selected based on the constraints of the system, as higher flow rates caused secondary vibrations of the tank that would have affected the data collected from the vibrissae. Although 0.5 m/s represents a slow swimming speed for these animals, it is represented in the swimming behavior of the species studied and may be more typical of glide phases in swimming (Hassrick et al., 2007;Le Boeuf et al., 1992;Lesage et al., 1999;Ponganis et al., 1990;Williams and Kooyman, 1985).

Recordings were made with a Polytec model PDV 100 laser-Doppler vibrometer, measuring point velocities on the whisker (Waldbronn, Germany). The laser was focused

on the whisker shaft and vibrations in the cross-stream direction were recorded for 6 seconds using the Polytec Vibrometer Software (version 4.6). Pilot recordings were conducted to determine the optimal location along the whisker shaft to record vibrations. Vibration frequency remained consistent along the whisker length, while velocity increased with distance from the base. Vibration velocity was maximal at the distal end of the vibrissa. However, recording quality degraded at the tip because the large whisker displacement sometimes moved it out of the plane of the laser (Figure 1.3). All comparative recordings were therefore collected at the midpoint of the whisker's length, where the recording equipment collected a strong, consistent signal.

Each sample was tested at vibrissae orientations of 0°, 45°, and 90° to the flow. Vibration measurements were recorded in the cross-stream direction for all vibrissae orientations. Definition of orientation was based on the angle of attack, or angle of the major cross-sectional axis of the vibrissa, at the base of the sample. Caliper measurements were taken at the base of the sample to determine the position of the minimum caliper width. This position was defined as 0° and the thin edge of the base of the vibrissa faced into the flow at this orientation. As the sample was rotated to 45° and then 90°, the broad edge of the vibrissa was oriented into the flow. In the 0° condition, the major curvature of the hair shaft was generally in the downstream direction for the harbor and elephant seal samples and in the cross-stream direction for the California sea lion samples (Figure 1.4). Based on behavioral observations, we hypothesize that the 0° condition closely corresponds to the natural orientation of the vibrissae in each species when the array is protracted (Figure 1.5).

Signals from the laser vibrometer were digitized at 1200 Hz and signal processing was conducted in MATLAB (Mathworks, Inc.). Peak frequency and corresponding peak vibration velocity were determined by performing fast Fourier transform (FFT) averaging with a 240 point FFT, yielding a frequency resolution of 5 Hz. Analysis was conducted on the entire 6 second length for most recordings. For some recordings that showed sections of reduced signal quality, shorter segments were analyzed with fewer power spectra averaged. One sea lion recording and three harbor seal recordings were removed from the analysis due to large vibrations in the stream-wise direction causing the whisker to move out of line with the laser taking measurements in the cross-stream direction.

A linear regression analysis was performed in order to analyze the variation in frequency and velocity that was attributable to length of the vibrissal sample. Repeated-measures two-factor ANOVA analyses with Tukey post-hoc tests were conducted to examine the effect of species and angle of orientation on frequency and velocity of whisker vibration (GraphPad Prism Software version 6, San Diego, CA). As statistical tests did not allow for uneven sample size within repeated measures analyses, subjects that had dropped values at the 90° orientation due to poor laser vibrometer signal were removed from the analysis. The resulting sample size for statistical tests was n=8 for California sea lions; n=8 for elephant seals; and n=6 for harbor seals.

Calculated theoretical vibration frequency

The recorded whisker vibration frequency was compared to calculated theoretical vortex shedding frequency for a cylinder of similar size, with a circular cross-section. The theoretical cylinder used for modeling was based on the diameter of the vibrissa facing into the flow at the corresponding angle of orientation. Theoretical cylinders

modeled only the stream-wise diameters of the whiskers and not the surface structure. In addition, calculations modeled only frequency and not velocity of vibrations.

The theoretical vibration frequency is based on the Reynolds number calculation:

$$\mathrm{Re} = \frac{Ud}{v}$$

$$f = \frac{U}{d} * 0.198 * (1 - \frac{19.7}{\mathrm{Re}})$$

where Re=Reynolds number, U=fluid velocity, d=vibrissae cross-sectional length perpendicular to the flow, ν=kinematic viscosity, f=frequency (Roshko, 1954a;b).

Theoretical frequency was calculated for each vibrissa at the 0° and 90° orientations based on the width of the profile facing into the flow at each orientation. These stream-wise diameters were measured at the centroid of the vibrissa. For undulated vibrissae, a maximum and minimum width was measured at points closest to the centroid, due to the variations in thickness of the shaft created by the crests and troughs. The 45° orientation was omitted from these calculations because there was potential for error in the measurement of the stream-wise diameter, due to the fact that the profile facing into the flow was an angled plane.

CT Scanning of vibrissal structure

Samples were rehydrated in fresh water for one hour and taped flat onto an acrylic slide, without compromising the natural curvature of the hair shaft. Samples were scanned in air using a micro-CT scanner (SCANCO, Wayne, NJ) at 30 μm isotropic resolution. Three dimensional reconstructions and digital cross-section images were created in ImageJ (version 1.47d) (Schneider et al., 2012). Cross-sectional properties (cross-sectional area, maximum and minimum caliper width, and theta or the angle of the

principal cross-sectional axis) were determined using BoneJ (version1.3.7) (Doube et al., 2010). Based on the maximum and minimum chord dimensions, eccentricity or ellipticity (a measure of how much an ellipse deviates from being circular) was calculated for each cross-sectional slice. Eccentricity *(e)* is based on the equation:

$$e = \frac{\sqrt{\max\text{radius}^2 - \min\text{radius}^2}}{\max\text{radius}}$$

with the eccentricity of a circle being 0 and the eccentricity of an ellipse being >0 but <1.

Underwater photographic images

Images of the vibrissae in a live, free-swimming harbor seal and California sea lion were captured at Long Marine Laboratory at the University of California Santa Cruz, using the Phantom Flex high speed underwater video camera (Vision Research Inc., Wayne, NJ). Images were recorded at 400 to 1000 frames per second and still shots were isolated using the Vision Research PCC software.

Ethics statement

The use of marine mammal samples was authorized under the National Marine Fisheries Service, letter of authorization to C. Murphy. Research with live marine mammals was authorized under National Marine Fisheries Service permit 14535 and conducted with the approval of the Institutional Animal Care and Use Committee at the University of California Santa Cruz.

Results

Whiskers vibrated strongly with a distinct fundamental frequency. Harmonics were observed in some recordings but were not consistently seen for all samples. The vibration of the sting apparatus, on which the sample was mounted, was recorded and did not overlap with the frequency range of the vibrissae vibration (Figure 1.6). The sting apparatus consistently vibrated under 50 Hz, with a peak frequency of 15 Hz, and peak velocity less than .005 m/s.

Vibration frequency and velocity ranges were similar for both undulated and smooth vibrissae (Table 1.1 and Table 1.2). At each angle of orientation, similar values were observed across whisker types. Angle of orientation affected the peak frequency and peak velocity of vibrations. For all whisker types, peak frequency was highest at the 0° orientation and decreased as the vibrissa was rotated to 45° and then 90° (Figure 1.7, Figure 1.8A). Theoretical frequency, calculated based on Reynolds number for a cylinder of similar size, (Table 1.1) revealed the same trend in values. The theoretical frequency calculations based on stream-wise diameter alone yielded average predicted values that were within 21% of the corresponding measured value. For all whisker types, peak velocity was minimal at the 0° orientation and increased as the vibrissa was rotated to 45° and then 90° (Figure 1.7, Figure 1.8B).

For frequency data, a repeated-measures two-factor ANOVA showed a significant effect of angle of orientation on frequency of whisker vibration ($p<0.0001$). However, the main effect analysis for species did not reach the criterion for statistical significance ($p=0.0582$). There was a significant interaction between species and angle of orientation ($p < 0.0001$) (Table 1.3). The results of Tukey post-hoc tests are shown in Table 1.4. A

linear regression analysis showed that very little of the variation in frequency (b=-20.164 Hz/cm; r^2 =0.074) was explained by length.

For velocity data, a repeated-measures two-factor ANOVA showed a significant effect of angle of orientation ($p < 0.0001$), but no significant effect of species ($p=0.1732$), on the velocity of whisker vibration. There was no statistically significant interaction between the effect of species and angle of orientation ($p=0.1669$) (Table 1.5). The results of Tukey post-hoc tests are shown in Table 1.6. A linear regression analysis showed that very little of the variation in velocity (b=0.0067 mm/s·cm; r^2=0.003) was explained by length.

CT scanning of vibrissal samples allowed for digital cross-sectioning of the hair shafts (Figure 1.9, S1, S2, S3). Cross-sectional area was tracked along the length of the shaft and maximum caliper width was measured for each cross-section (Figure 1.10). For all vibrissae, the cross-sectional area gradually decreased from the base of the shaft towards the tip. For the elephant seal and harbor seal vibrissae, the cross-sectional area remained relatively consistent between the crests and troughs, while the maximum caliper width increased and decreased with each undulation. For these undulated vibrissae, although each crest and trough caused the major axes to alternate, the total cross-sectional area was relatively consistent across neighboring undulations.

For all vibrissae, the cross-sectional profile became increasingly flattened towards the tip. In addition to this overall trend, local differences in cross-sectional shape were observed between the crest and trough sections of undulated vibrissae. The elephant and harbor seal vibrissae oscillated between more and less compressed ellipsoid cross-sectional shapes from troughs to crests, while the California sea lion vibrissae maintained

consistent shape in cross-section between neighboring points along the shaft. These trends can be observed by tracking the measure of eccentricity along the whisker shafts of each individual sample (Figure 1.11). Theta, the angle of the major axis from horizontal, was calculated for each cross-section (Figure 1.12). As samples were scanned lying flat against a slide, theta measurements represent the deviation from the axis of the major curvature of the vibrissa. In the undulated vibrissae, theta centered about zero and remained relatively stable from hair base to tip. In contrast, theta in the smooth vibrissae deviated from zero and showed variations along the length of the hair shaft. Theta for these vibrissae ranged from a minimum of -14° to a maximum of 45°. In undulated vibrissae, the orientation of the flattened profile is in-line with the overall curvature of the vibrissa, while in the smooth vibrissae the orientation of the flattened profile is off-axis of the major curvature.

It is difficult to quantify orientation of the vibrissae in live pinnipeds. Underwater photos and high-speed videos of the vibrissal array of a freely swimming harbor seal and California sea lion provide some qualitative comparison between these species. These recordings indicate that differences may occur between species in the direction of vibrissal curvature with respect to the rostro-caudal axis of the body (Figure 1.5, S4, S5, S6, S7). In footage of the California sea lion swimming with the array protracted, the vibrissae appear to curve ventrally. In contrast, when the harbor seal is swimming with the array protracted, the vibrissae appear straight because the curvature is directed caudally.

Discussion

When exposed to water flow, both the undulated vibrissae of the seals and the smooth vibrissae of the sea lions showed similar ranges in vibration frequency and velocity. When the vibrissae were tested across a range of orientations, no distinguishing difference was observed as a function of surface structure. Within each angle of orientation, similar values were observed across whisker types. Angle of orientation, rather than species differences and thus surface structure of the vibrissa, had the greatest effect on the frequency and velocity of flow-induced vibrations.

Angle of orientation had a large effect on vibration velocity (Figure 1.8). For all vibrissal types, peak velocity was lowest at the 0° orientation and corresponded to when the thin edge of the hair was angled into the flow. Rotating the orientation of the vibrissa away from 0° increased the velocity of vibrations along the shaft. In terms of wake tracking, we hypothesize that the 0° orientation would reduce vibrations from forward swimming motion and that the vibrissae would be more sensitive to flow disturbances impinging on the whisker from 90°. It is important to note that flow-disturbances could impinge on the vibrissae from any direction. Self-induced vibrations that could be considered noise to the animal would be minimized, potentially allowing for a greater chance of detecting signals in the water.

While the present study did not find differences between the vibrations of the undulated and smooth vibrissae, previous research by Hanke et al. did find differences between vibrissal types (Hanke et al., 2010). One possible explanation for this discrepancy is that samples in the previous study were held at one fixed orientation based on the curvature of the vibrissal shaft. If the test positions used in the previous study

differed in orientation (i.e., if the thin edge of the vibrissa faced into the flow for the harbor seal, while the broad edge faced into the flow for the sea lion), then more extreme differences could have been observed.

Frequency was also markedly affected by angle of orientation for both the smooth and undulated vibrissae (Figure 1.8). Measured peak frequency was highest at the 0° orientation, when the thin edge of the hair faced into the flow, and decreased as the vibrissa was rotated to the 90° orientation. This trend is similar to that observed in the calculated frequency of theoretical cylinders that model only the stream-wise diameters of the whiskers and not the surface structure (Table 1.1). As a vibrissa is rotated from the 0° to the 90° orientation, the broader edge of the vibrissa faces into the flow and the size of the stream-wise diameter increases. This yields higher Reynolds number flow and consequently a lower vibrational frequency. Theoretical values based on stream-wise diameter were within an average of 14% of corresponding measured values for each vibrissa. The similarity in frequency response between measured and theoretical values suggests that a key variable influencing the frequency of vibration is the diameter of the portion of the whisker facing into the flow. This implies that the cross-sectional flattening of the vibrissae, rather than the surface structure, may explain most of the trend observed in measured vibration frequency at the flow speed tested.

CT scanning and digital cross-sectioning of the vibrissae confirmed that this flattening is present in both undulated and smooth vibrissae. Eccentricity calculations revealed that the vibrissae of all species tested were cross-sectionally flattened to some degree and became increasingly flattened toward the distal end (Figure 1.11). In addition to this overall trend, undulated vibrissae showed oscillating eccentricity values with each

crest and trough. Surprisingly, the smooth and undulated vibrissae exhibited similar overall degree of flattening at comparable regions along the vibrissal length, which may be important in reducing self-induced vibration of the sensor. Although it was previously assumed that the undulated vibrissae were more severely compressed in profile (Dehnhardt et al., 2004), these data make it apparent that the smooth vibrissae are also considerably compressed. In addition, the undulated vibrissae showed an interesting compensation along the whisker where the cross-sectional areas of adjacent sections were consistent despite the undulations. Maintaining consistent cross-sectional area might minimize variability in vibrations that would be generated by the hair shaft when exposed to water flow.

Theta, or angle of the major cross-sectional axis from horizontal, was analyzed in order to better understand the relationship between curvature of the vibrissal shaft and the orientation of the cross-sectional profile (Figure 1.12). For the undulated vibrissae from harbor seals and elephant seals, theta measurements centered around zero along the entire length of the shaft. This indicates that the direction of cross-sectional flattening is in the same plane as the curvature of the hair shaft. In contrast, theta measurements for the smooth vibrissae from sea lions deviated from zero. This indicates that, if the whisker is positioned based on the overall curvature of the hair shaft, the orientation of the flattened profile does not lie directly in this plane. The CT data show that the sea lion whisker would need to be rotated about 10-20 degrees from the plane of the whisker lying flat to have the thinnest edge oriented into the flow.

It is difficult to quantify how these parameters relate to the positioning of the array in a live animal. However, images obtained using high speed recordings provide

some qualitative biological framework for understanding these data (Figure 1.5, S4, S5, S6, S7). These video recordings of a harbor seal and a California sea lion during active swimming allow the overall positioning of the array to be compared between these species. In both subjects, the array remains stable in its protracted position and the vibrissae do not become depressed or swept back as the animal moves through the water. This stable positioning suggests that the vibrissae are able to resist the water pressure from forward movement and we hypothesize that the flattened cross-sectional profile may streamline the vibrissae and aid in the process.

One difference between the harbor seal and the sea lion, which can be seen in the video images, is the curvature of the vibrissae with respect to the rostro-caudal axis of the body. The vibrissae of both species have a distinct major curvature. Comparing the protracted array between these subjects, the vibrissae of the harbor seal appear to be curved caudally, while the vibrissae of the California sea lion appear to be curved ventrally. Taking this into consideration with the theta measurements from CT scanning, it is possible that this positioning may allow the thin edge of the vibrissae to face into the flow. Considering that the laser vibrometer measurements in the flume indicated that the self-induced noise on the vibrissae is minimized at an angle of attack of zero, we can speculate that this array positioning aids in noise reduction. Detailed effort still needs to be made to determine the precise rotational orientation of the array during underwater tracking tasks. However, considering the range of motion of the array in each species, we hypothesize that the 0° condition used in this study is an appropriate generalization of natural orientation.

From the present data, the function of the undulations in pinniped vibrissae is unclear. Under the conditions tested, the undulated surface structure does not appear to minimize self-induced noise on the sensor to a greater degree than vibrissae with a smooth surface. To determine the function of the undulations, subsequent testing should include the introduction of hydrodynamic disturbances and consideration of vibrissal curvature, length, and additional flow speeds. The undulations may provide some advantage in filtering or amplification of a signal when the sensor is exposed to salient hydrodynamic stimuli. Taking into account evidence from previous research using theoretical modeling (Hanke et al., 2010) and behavioral testing (Dehnhardt et al., 2001;Gläser et al., 2011), pinniped species with undulated vibrissae may be more specialized for hydrodynamic detection. However, the smooth vibrissae should not be considered an inefficient sensor. As can be seen from the comparative laser vibrometer recordings, when oriented at the same angle of orientation, smooth vibrissae exhibit the same capacity as undulated vibrissae to minimize flow-induced vibrations as well as respond strongly to flow in other planes. We hypothesize that this is attributable to the compressed cross-sectional shape of the vibrissal shaft, a shared characteristic between both undulated and smooth vibrissae.

Tables

Table 1.1 Measured and theoretical vibration frequency values pooled across subjects for each species group.

		Measured Peak Frequency (Hz)			Theoretical Frequency (Hz)			
	Angle of orientation	0°	45°	90°	0°	0° % difference	90°	90° % difference
California sea lion	**Mean**	**204.4**	**156.7**	**112.5**	**201.1**	4.9%	**122.2**	14.6%
(Smooth vibrissae)	S.E.	9.4	13.4	4.6	8.7		5.3	
	Range	175.0 – 270.0	115.0 – 230.0	95.0 - 130.0	159.0 - 233.4		98.9 - 137.1	
Elephant seal	**Mean**	**151.3**	**140.0**	**121.3**	**176.3**	18.3%	**102.6**	14.8%
(Undulated vibrissae)	S.E.	5.9	7.3	5.2	5.7		2.0	
	Range	130.0 - 185.0	115.0 - 170.0	105.0 - 140.0	154.5 - 201.9		94.5 - 111.2	
Harbor seal	**Mean**	**202.8**	**157.2**	**95.0**	**241.8**	20.9%	**103.4**	9.4%
(Undulated vibrissae)	S.E.	7.3	17.6	4.3	7.9		2.8	
	Range	175.0 - 240.0	70.0 - 245.0	80.0 - 110.0	195.5 - 271.9		93.4 - 112.7	

Overall range, mean, and SE of the measured peak frequency and calculated theoretical frequency for all vibrissae sampled. Measured values were obtained from laser vibrometer recordings and theoretical values are based on the Reynolds number calculation for a cylinder with a circular cross-section and matching stream-wise diameter. The percent difference between the absolute value of the measured and theoretical frequency was calculated for each vibrissa. The “% difference” column is the mean of the percent differences pooled across subjects for the specified species and angle of orientation. Samples that had dropped values at the 90° orientation due to poor laser vibrometer signal were removed from the data set. The resulting sample size was n=9 at 0°, n=9 at 45°, and n=8 at 90° for California sea lions; n=8 at 0°, n=8 at 45°, and n=8 at 90° for elephant seals; and n=9 at 0°, n=9 at 45°, and n=6 at 90° for harbor seals.

Table 1.2 Measured vibration velocity values pooled across subjects for each species group.

		Measured Peak Velocity (m/s)		
	Angle of orientation	0°	45°	90°
California sea lion	**Mean**	**0.0087**	**0.0426**	**0.1099**
(Smooth vibrissae)	S.E.	0.0029	0.0142	0.0172
	Range	0.0036 -0.0316	0.0051 - 0.1452	0.0535 - 0.2018
Elephant seal	**Mean**	**0.0029**	**0.0559**	**0.1745**
(Undulated vibrissae)	S.E.	0.0010	0.0280	0.0226
	Range	0.0007 -0.0091	0.0034 -0.1842	0.0909 -0.3083
Harbor seal	**Mean**	**0.0069**	**0.0484**	**0.1192**
(Undulated vibrissae)	S.E.	0.0038	0.0167	0.0175
	Range	0.0009 - 0.0361	0.0022 - 0.1481	0.0484 - 0.1745

Overall range, mean, and SE of the measured peak velocity from laser vibrometer recordings for all vibrissae sampled. Samples that had dropped values at the 90° orientation due to poor laser vibrometer signal were removed from the data set. The resulting sample size was n=9 at 0°, n=9 at 45°, and n=8 at 90° for California sea lions; n=8 at 0°, n=8 at 45°, and n=8 at 90° for elephant seals; and n=9 at 0°, n=9 at 45°, and n=6 at 90° for harbor seals.

Table 1.3 ANOVA table for vibration frequency.

Source	SS	DF	MS	F (DFn, DFd)	P value
Angle of orientation	62950	2	31475	F (2, 38) = 74.62	< 0.0001
Species	6690	2	3345	F (2, 19) = 3.315	0.0582
Interaction	14293	4	3573	F (4, 38) = 8.472	< 0.0001
Subjects (matching)	19173	19	1009	F (19, 38) = 2.392	0.0109
Residual	16028	38	421.8		

ANOVA table showing the results of the repeated-measures two-factor analysis of variance, demonstrating the effect of species and angle of orientation on frequency of whisker vibration. A significant effect of angle of orientation and a significant interaction is observed. No significant effect of species is observed. Sample size for statistical tests was n=8 for California sea lions; n=8 for elephant seals; and n=6 for harbor seals at all angles of orientation.

Table 1.4 Tukey post-hoc analysis of the effect of angle of orientation on vibration frequency, within each species.

Group	Mean diff.	P-value
California sea lion (CSL)		
CSL 0° vs. 45°	45.63	0.0002
CSL 0° vs. 90°	93.13	< 0.0001
CSL 45° vs. 90°	47.5	0.0001
Elephant seal (ES)		
ES 0° vs. 45°	11.25	0.5227
ES 0° vs. 90°	30	0.0157
ES 45° vs. 90°	18.75	0.1749
Harbor seal (HS)		
HS 0° vs. 45°	17.5	0.3137
HS 0° vs. 90°	101.7	< 0.0001
HS 45° vs. 90°	84.17	< 0.0001

“Mean diff.” is the mean difference between the first and second angle listed. “P Value” is the adjusted p-value.

Table 1.5 ANOVA table for vibration velocity.

Source	SS	DF	MS	F (DFn, DFd)	P value
Angle of orientation	0.1873	2	0.09363	F (2, 38) = 51.15	P < 0.0001
Species	0.009278	2	0.004639	F (2, 19) = 1.925	P = 0.1732
Interaction	0.01255	4	0.003138	F (4, 38) = 1.715	P = 0.1669
Subjects (matching)	0.04578	19	0.00241	F (19, 38) = 1.316	P = 0.2298
Residual	0.06955	38	0.00183		

ANOVA table showing the results of the repeated-measures two-factor analysis of variance, demonstrating the effect of species and angle of orientation on velocity of whisker vibration. A significant effect of angle of orientation is observed. No significant effect of species or interaction is observed. Sample size for statistical tests was n=8 for California sea lions; n=8 for elephant seals; and n=6 for harbor seals at all angles of orientation.

Table 1.6 Tukey post-hoc analysis of the effect of angle of orientation on vibration velocity, within each species.

Group	Mean diff.	P-value
California sea lion (CSL)		
CSL 0° vs. 45°	-0.03359	0.2707
CSL 0° vs. 90°	-0.1008	< 0.0001
CSL 45° vs. 90°	-0.06722	0.0089
Elephant seal (ES)		
ES 0° vs. 45°	-0.05295	0.046
ES 0° vs. 90°	-0.1715	< 0.0001
ES 45° vs. 90°	-0.1186	< 0.0001
Harbor seal (HS)		
HS 0° vs. 45°	-0.01882	0.7283
HS 0° vs. 90°	-0.1101	0.0002
HS 45° vs. 90°	-0.09124	0.002

“Mean diff.” is the mean difference between the first and second angle listed. “P Value” is the adjusted p-value.

Figures

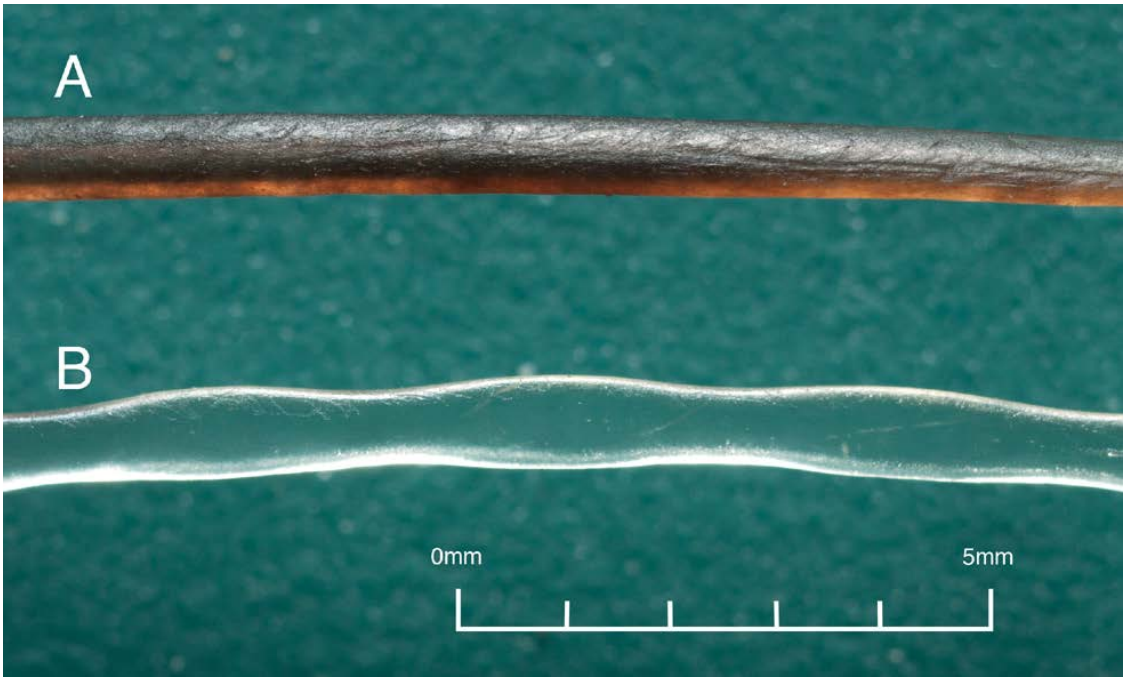

Figure 1.1 Undulated and smooth vibrissal surface structures. Surface structure of (A) a smooth vibrissa (California sea lion) and (B) an undulated vibrissa (harbor seal).

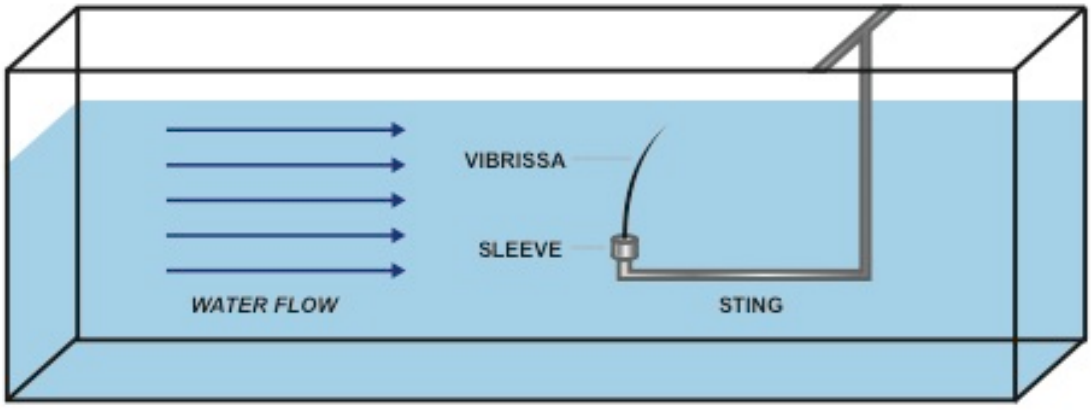

Figure 1.2 Diagram of a vibrissal sample mounted in the test section of the water flume. Schematic (figure not drawn to scale) of the recording area of the flume. The vibrissa was mounted on the sting apparatus in the center of the water column. The laser vibrometer (not pictured) was focused on the vibrissal shaft from outside the test enclosure, with the beam passing through the water column, perpendicular to the flow.

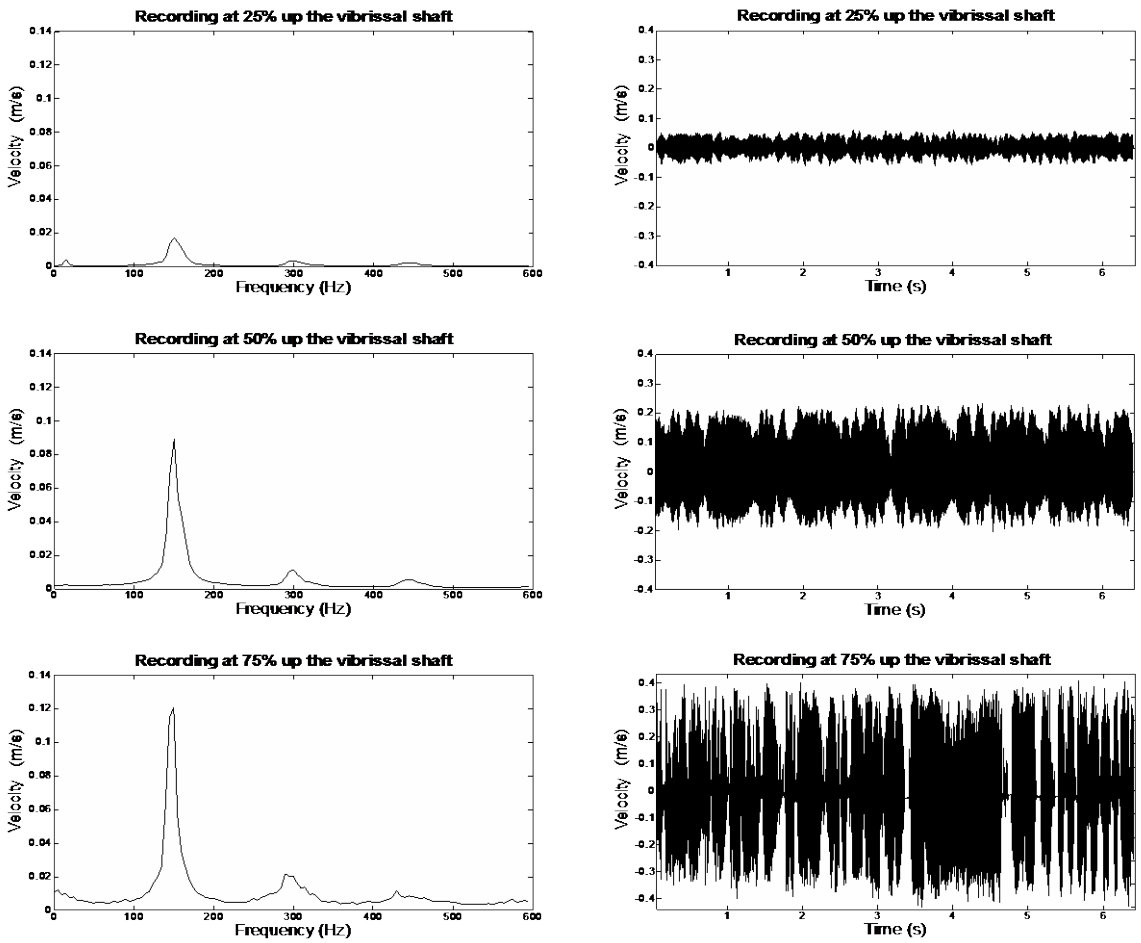

Figure 1.3 Vibrational signal with distance up the vibrissal shaft. Comparison of three example laser vibrometer recordings taken at different points along the shaft of a single vibrissal sample. Recordings were taken at 25% (top row), 50% (middle row), and 75% (bottom row) up the length of the whisker shaft and are shown as FFTs (left) and waveforms (right). The 50% recording position was determined to be optimal for signal quality and all subsequent data were recorded at this position.

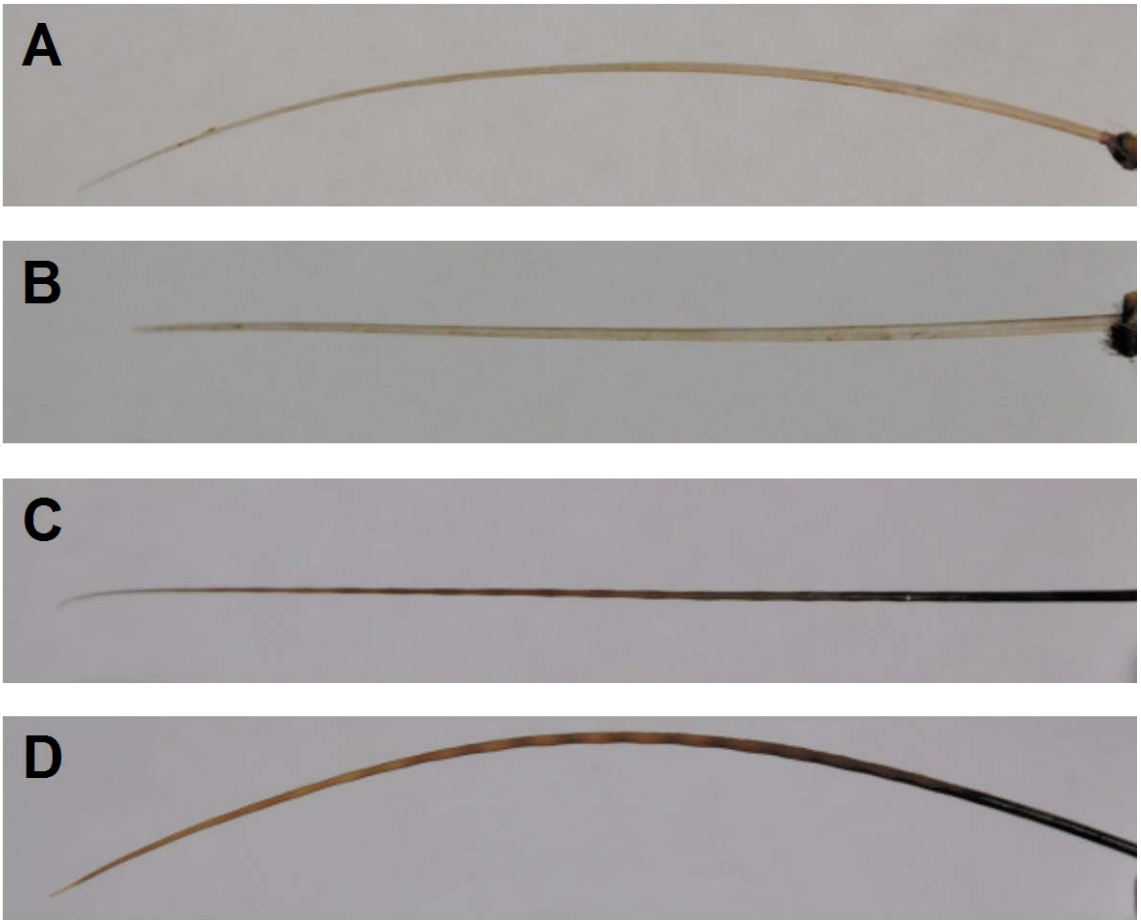

Figure 1.4 Vibrissal orientation for laser vibrometer recordings. (A) Smooth (California sea lion) vibrissa at the 0° orientation. Thin edge of the vibrissa faces into the flow. (B) The same vibrissa at the 90° orientation. Broad edge of the vibrissa faces into the flow. (C) Undulated vibrissa (elephant seal) at the 0° orientation. Thin edge of the vibrissa faces into the flow. (D) The same vibrissa at the 90° orientation. Broad edge of the vibrissa faces into the flow. In these images, the direction of flow is into the page. Total length of the vibrissa in A and B is 8.1 cm, total length of the vibrissa in C and D is 9.2 cm.

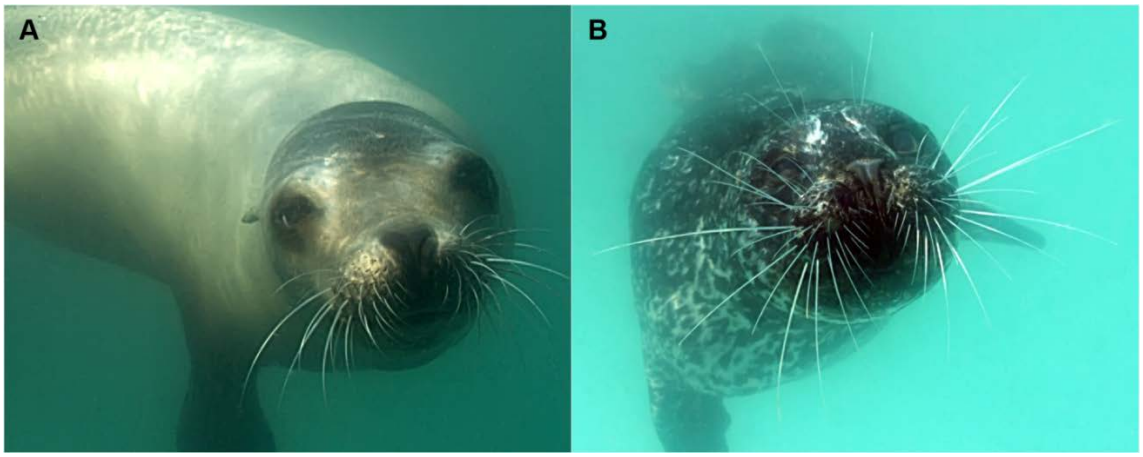

Figure 1.5 Position of the vibrissal array during active swimming. (A) California sea lion with the vibrissal array protracted. In this position the vibrissae are curved ventrally. (B) Harbor seal with the vibrissal array protracted. In this position the vibrissae are curved caudally.

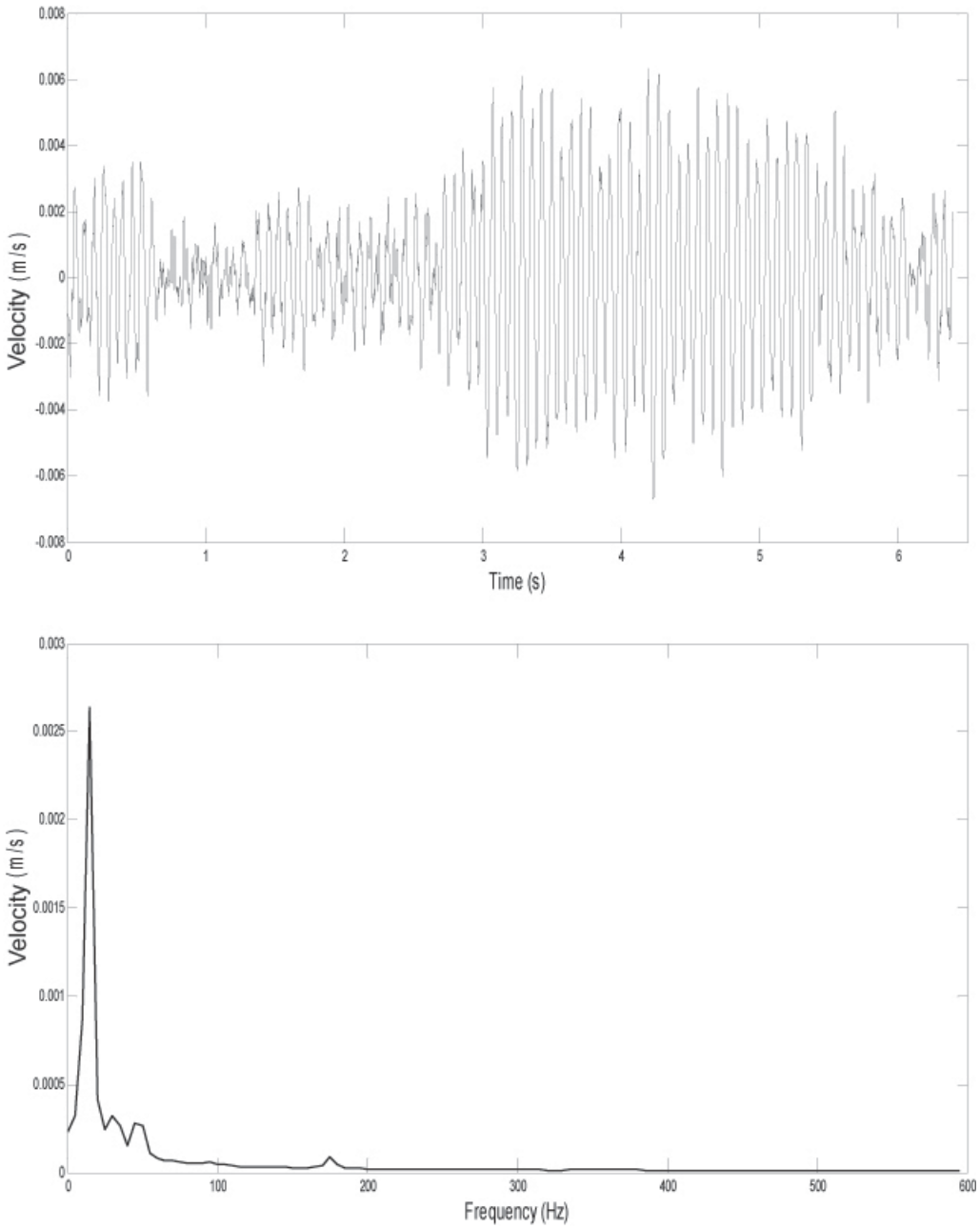

Figure 1.6 Vibrational signal recorded from the sting mount. Vibration of the sting apparatus, shown as a waveform (top) and FFT (bottom). The peak frequency of the vibration of the sting apparatus was consistently at 15 Hz and did not overlap with the frequency range of the signal from the vibrissae. Note that the scale used here to view the sting vibration is approximately 50 times smaller than the scales used for the vibrissae vibrations in Figures 1.3 and 1.7.

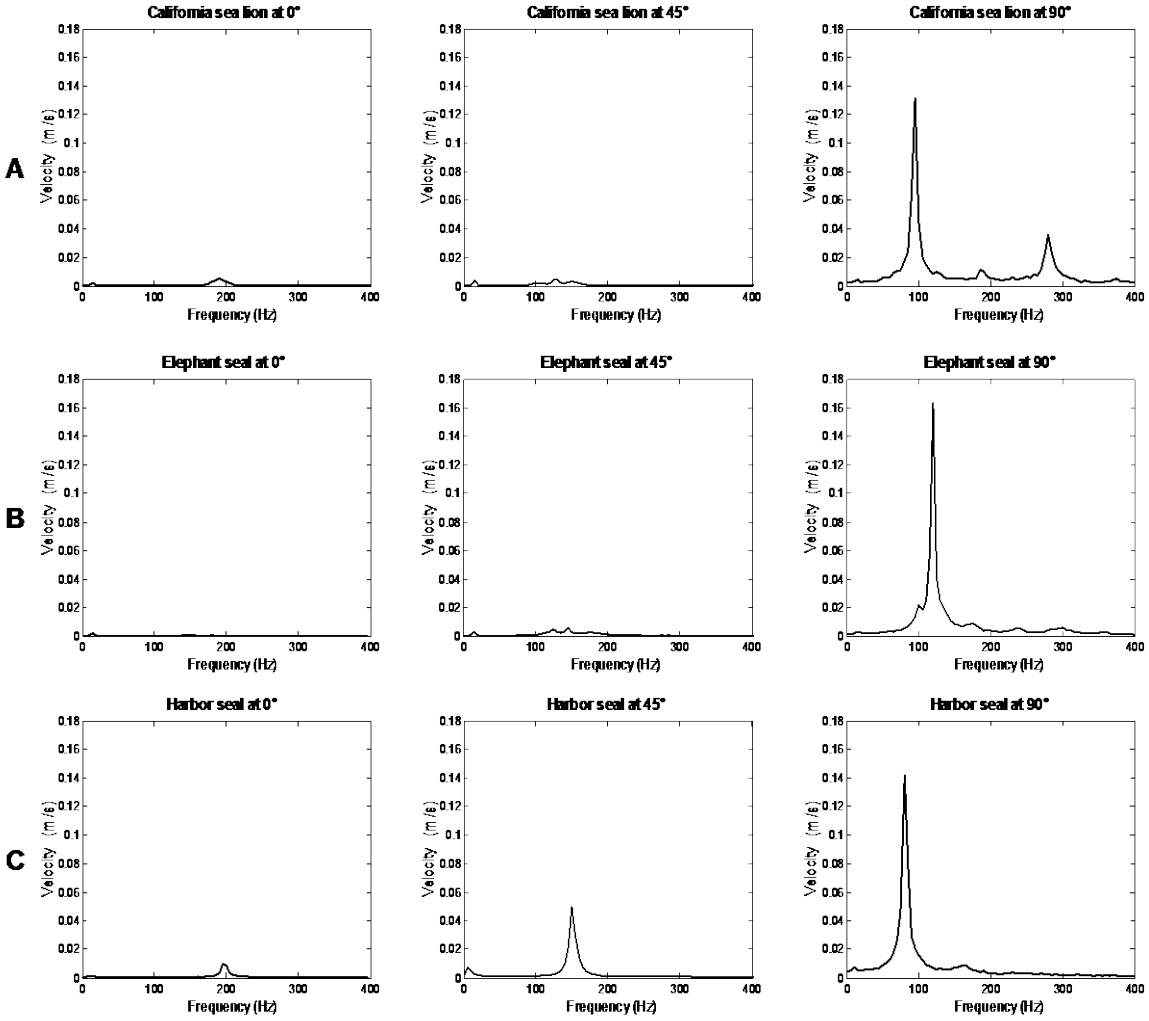

Figure 1.7 Effect of angle of orientation on vibrational signal. Comparison of FFTs at 0°, 45°, and 90° for one individual (A) California sea lion, (B) elephant seal and (C) harbor seal. In all vibrissae, peak velocity was minimal at the 0° orientation and increased as the vibrissa was rotated to 45° and then 90°.

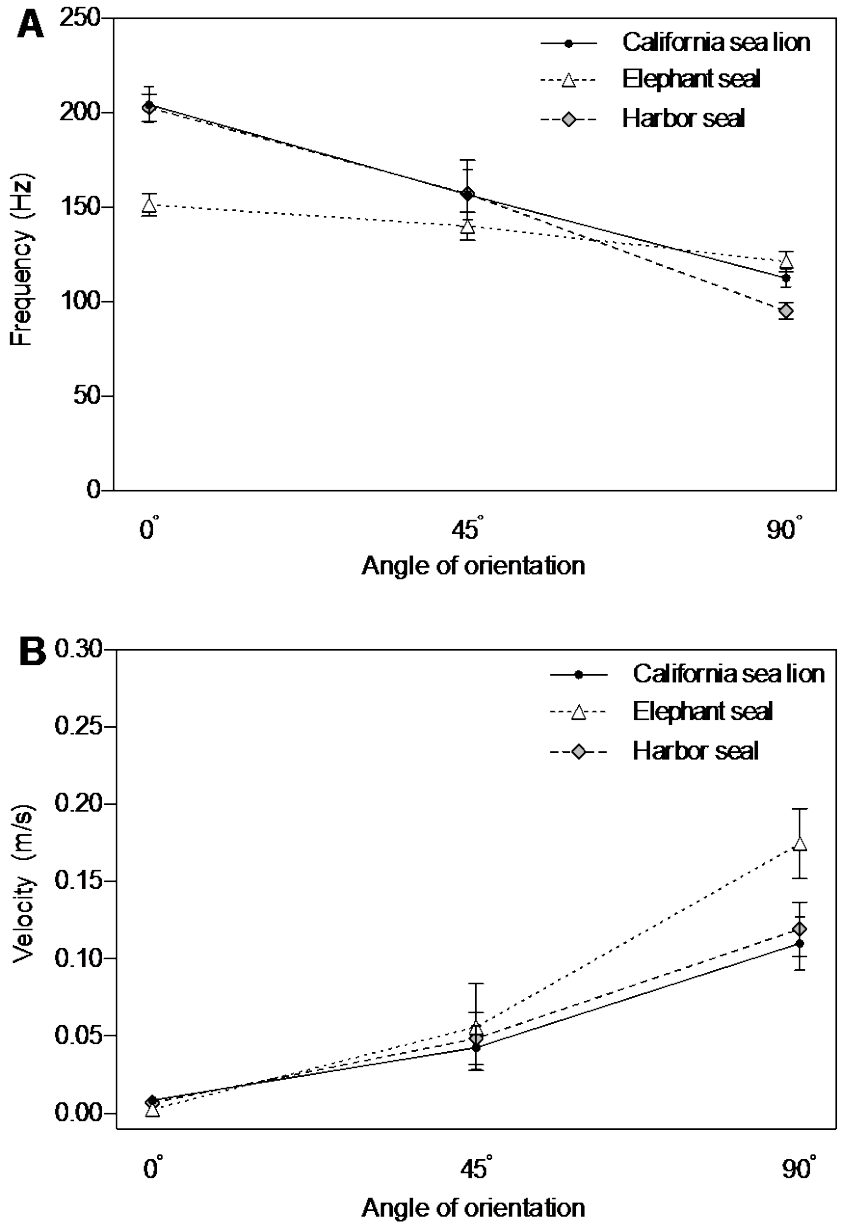

Figure 1.8 Effect of angle of orientation on mean peak frequency and velocity of vibration. (A) Mean peak frequency across species at three angles of orientation. For all whisker types, peak frequency was highest at the 0° orientation and decreased as the vibrissa was rotated to 45° and then 90°. (B) Mean peak velocity across species at three angles of orientation. In all vibrissae, peak velocity was lowest at the 0° orientation and increased as the vibrissa was rotated to 45° and then 90°. Both graphs show pooled data for each species with +/- SE.

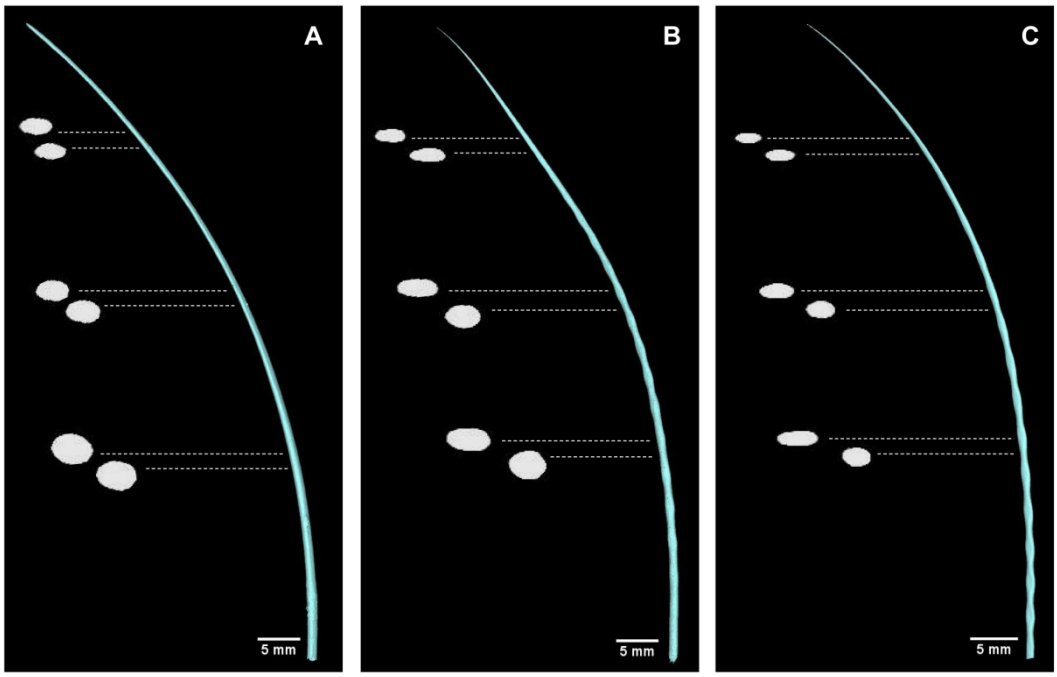

Figure 1.9 Comparative digital cross-sections from CT data. Reconstructions of vibrissae from CT scan data. (A) California sea lion; (B) elephant seal; (C) harbor seal. Enlarged digital cross-sections are shown at six points along the whisker length. Scale bar represents scaling for whole whisker image. Cross-sections are approximately 4-5x enlarged. In smooth vibrissae, the cross-sectional shape is consistent between neighboring points along the shaft, while undulated vibrissae vary in cross-sectional shape between troughs to crests. The cross-sections of all vibrissae show increased flattening toward the tip.

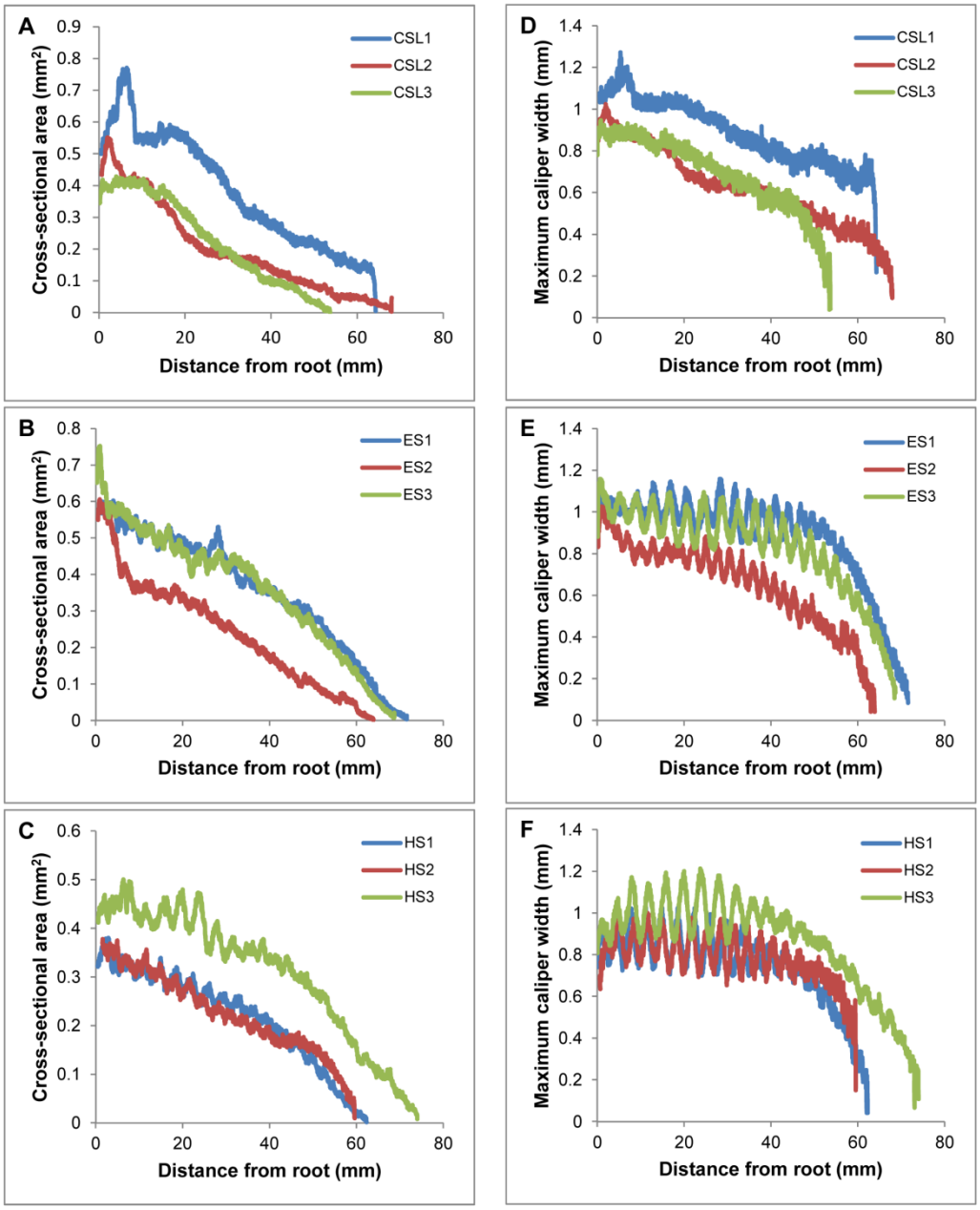

Figure 1.10 Cross-sectional area and maximum caliper width of vibrissal cross-sectional profiles from CT data. Calculated cross-sectional area along the vibrissal length for three subjects of each species. (A and D) California sea lion; (B and E) elephant seal; (C and F) harbor seal. In all vibrissae, the cross-sectional area gradually decreased from the base of the shaft towards the tip. In undulated vibrissae, the cross-sectional area remained relatively consistent between the crests and troughs, while the maximum caliper width increased and decreased with each undulation.

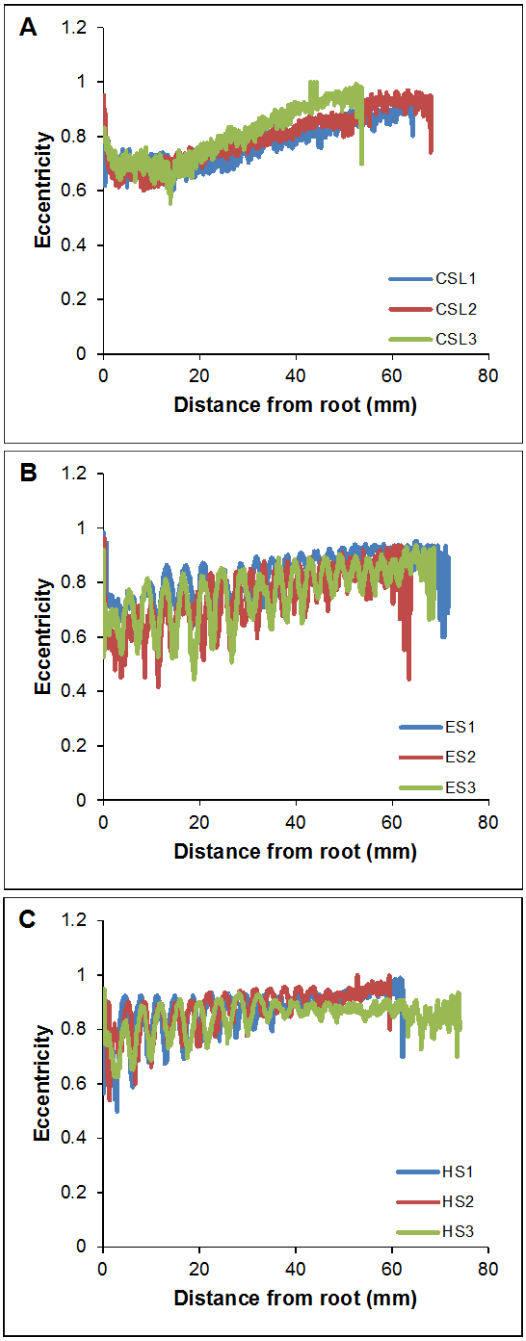

Figure 1.11 Eccentricity of vibrissal cross-sectional profiles from CT data. Measure of eccentricity, or ellipticity, along the vibrissal length for three subjects of each species. (A) California sea lion; (B) elephant seal; (C) harbor seal. The eccentricity of a perfect circle is 0, while the eccentricity of an ellipse would be >0 but <1. Overall, both smooth and undulated vibrissae show similar degrees of eccentricity. In smooth vibrissae, eccentricity is consistent between neighboring points along the shaft, while in undulated vibrissae eccentricity oscillates with each trough and crest.

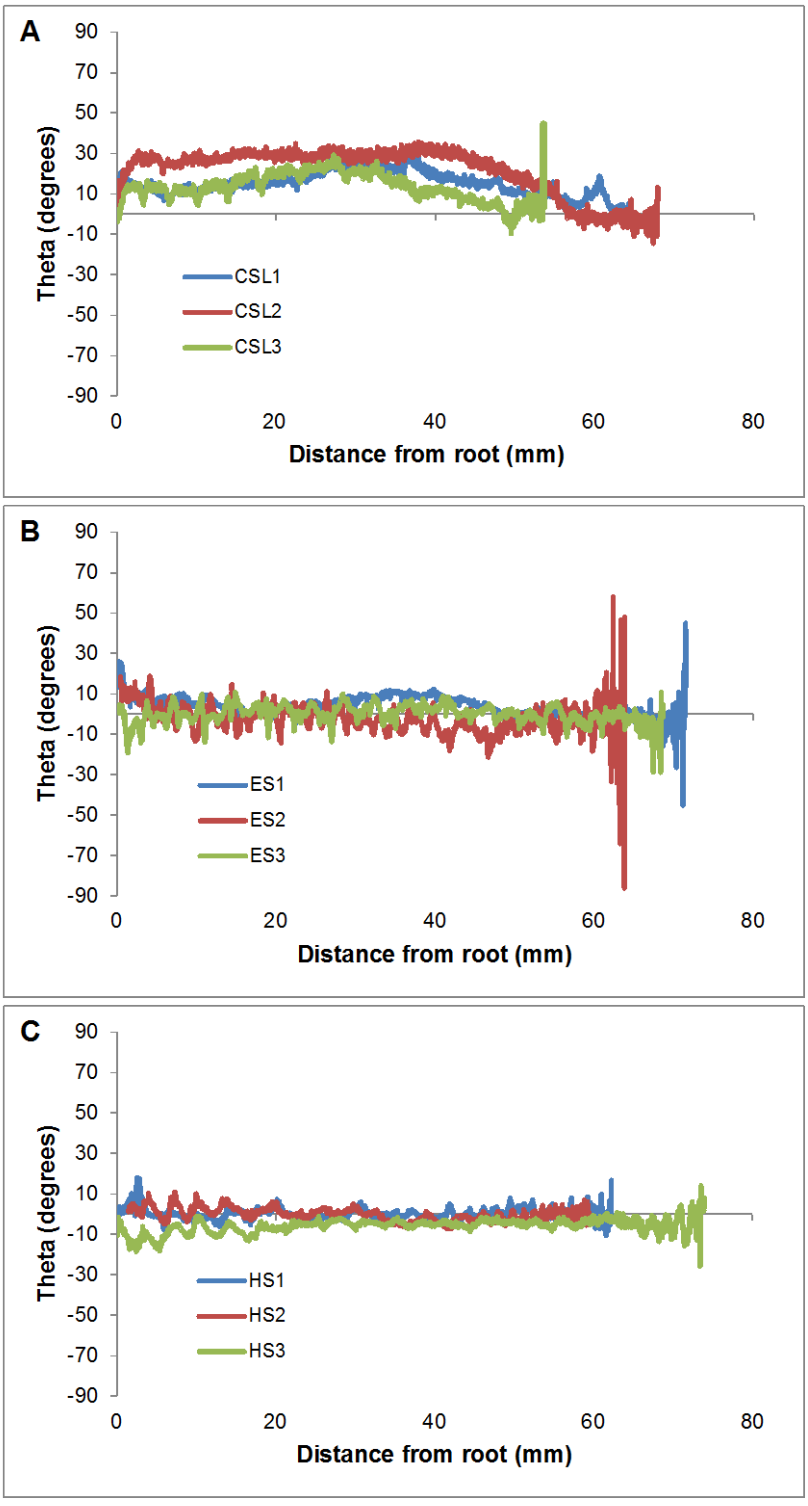

Figure 1.12 Theta of vibrissal cross-sectional profiles from CT data. Angle of the major axis of the cross-section from horizontal. (A) California sea lion; (B) elephant seal; (C) harbor seal. For smooth vibrissae, theta measurements deviate from zero, while in undulated vibrissae theta measurements centered around zero across the entire length of the vibrissa.

Description of Supplementary Material

(please see external links)

S1. CT scan of a California sea lion vibrissa. A slice-by-slice animation of the CT scan showing successive cross-sections from the vibrissal base to the tip. Slice thickness is 0.03 mm.

S2. CT scan of an elephant seal vibrissa. A slice-by-slice animation of the CT scan showing successive cross-sections from the vibrissal base to the tip. Slice thickness is 0.03 mm.

S3. CT scan of a harbor seal vibrissa. A slice-by-slice animation of the CT scan showing successive cross-sections from the vibrissal base to the tip. Slice thickness is 0.03 mm.

S4. Frontal view of a California sea lion vibrissal array. This view, filmed during active swimming and orientation, shows the array held in the protracted position with the curvature of the vibrissae directed ventrally.

S5. Profile view of a California sea lion vibrissal array. This view, filmed during active swimming and orientation, shows the array held in the protracted position with the curvature of the vibrissae directed ventrally.

S6. Frontal view of harbor seal vibrissal array. This view, filmed during active swimming and orientation, shows the array held in the protracted position with the curvature of the vibrissae directed caudally.

S7. Profile view of harbor seal vibrissal array. This view, filmed during active swimming and orientation, shows the array held in the protracted position with the curvature of the vibrissae directed caudally.

References

Dehnhardt, G. and Kaminski, A. (1995) Sensitivity of the mystacial vibrissae of harbour seals (Phoca vitulina) for size differences of actively touched objects. *J Exp Biol* 198(11), 2317-2323.

Dehnhardt, G., Mauck, B. and Bleckmann, H. (1998) Seal whiskers detect water movements. *Nature* 394(6690), 235-236.

Dehnhardt, G., Mauck, B., Hanke, W. and Bleckmann, H. (2001) Hydrodynamic trail-following in harbor seals *(Phoca vitulina*). *Science* 293(5527), 102-104.

Dehnhardt, G., Mauck, B. and Hanke, W. (2004) Dynamic perception, workshop of the GI section "computer vision" Ilg, U., Bülthoff, H. and Mallot, H. (eds), pp. 27-32.

Dehnhardt, G. and Mauck, B. (2008) Sensory evolution on the threshold: adaptations in secondarily aquatic vertebrates. Thewissen, J. and Nummela, S. (eds), pp. 295-314, University of California Press, Berkeley.

Doube, M., Kłosowski, M.M., Arganda-Carreras, I., Cordelières, F.P., Dougherty, R.P., Jackson, J.S., Schmid, B., Hutchinson, J.R. and Shefelbine, S.J. (2010) BoneJ: Free and extensible bone image analysis in ImageJ. *Bone* 47(6), 1076-1079.

Fish, F.E., Howle, L.E. and Murray, M.M. (2008) Hydrodynamic flow control in marine mammals. *Integr Comp Biol* 48(6), 788-800.

Ginter, C.C., Fish, F.E. and Marshall, C.D. (2010) Morphological analysis of the bumpy profile of phocid vibrissae. *Mar Mammal Sci* 26(3), 733-743.

Ginter, C.C., DeWitt, T.J., Fish, F.E. and Marshall, C.D. (2012) Fused traditional and geometric morphometrics demonstrate pinniped whisker diversity. *PloS one* 7(4), e34481.

Gläser, N., Wieskotten, S., Otter, C., Dehnhardt, G. and Hanke, W. (2011) Hydrodynamic trail following in a California sea lion (*Zalophus californianus*). *J Comp Physiol A* 197(2), 141-151.

Hanke, W., Witte, M., Miersch, L., Brede, M., Oeffner, J., Michael, M., Hanke, F., Leder, A. and Dehnhardt, G. (2010) Harbor seal vibrissa morphology suppresses vortex-induced vibrations. *J Exp Biol* 213(15), 2665-2672.

Hassrick, J.L., Crocker, D.E., Zeno, R.L., Blackwell, S.B., Costa, D.P. and Le Boeuf, B.J. (2007) Swimming speed and foraging strategies of northern elephant seals. *Deep Sea Res Part 2 Top Stud Oceanogr* 54(3), 369-383.

Hyvärinen, H. and Katajisto, H. (1984) Functional structure of the vibrissae of the ringed seal (*Phoca hispida Schr*.). *Acta Zool Fenn* 171, 27-30.

Hyvärinen, H. (1995) Sensory Systems of Aquatic Mammals Kastelein, R., Thomas, J. and Nachtigall, P. (eds), pp. 429-445, De Spil Publishers, Woerden.

Hyvärinen, H., Palviainen, A., Strandberg, U. and Holopainen, I. (2009) Aquatic environment and differentiation of vibrissae: comparison of sinus hair systems of ringed seal, otter and pole cat. *Brain Behav Evol* 74(4), 268-279.

Hyvärinen, H. (1989) Diving in darkness: whiskers as sense organs of the ringed seal (*Phoca hispida saimensis*). *J Zool (Lond)* 218(4), 663-678.

Le Boeuf, B.J., Naito, Y., Asaga, T., Crocker, D. and Costa, D.P. (1992) Swim speed in a female northern elephant seal: metabolic and foraging implications. *Can J Zool* 70(4), 786-795.

Lesage, V., Hammill, M.O. and Kovacs, K.M. (1999) Functional classification of harbor seal (Phoca vitulina) dives using depth profiles, swimming velocity, and an index of foraging success. *Can J Zool* 77(1), 74-87.

Ling, J.K. (1966) The skin and hair of the southern elephant seal, *Mirounga leonina* (Linn.) I. The facial vibrissae. *Australian J Zool* 14(5), 855-866.

Ling, J.K. (ed) (1977) Vibrissae of marine mammals, Academic Press, London.

Marshall, C.D., Amin, H., Kovacs, K.M. and Lydersen, C. (2006) Microstructure and innervation of the mystacial vibrissal follicle-sinus complex in bearded seals, *Erignathus barbatus* (Pinnipedia: Phocidae). *Anat Rec A Discov Mol Cell Evol Biol* 288A(1), 13-25.

Miersch, L., Hanke, W., Wieskotten, S., Hanke, F., Oeffner, J., Leder, A., Brede, M., Witte, M. and Dehnhardt, G. (2011) Flow sensing by pinniped whiskers. *Philosl Trans R Soc Lond B Biol Sci* 366(1581), 3077-3084.

Ponganis, P.J., Ponganis, E.P., Ponganis, K.V., Kooyman, G.L., Gentry, R.L. and Trillmich, F. (1990) Swimming velocities in otariids. *Can J Zool* 68(10), 2105-2112.

Roshko, A. (1954a) On the development of turbulent wakes from vortex streets, N.A.C.A. Report No. 1191.

Roshko, A. (1954b) On the drag and shedding frequency of two-dimensional bluff bodies, N.A.C.A. Tech. Note No. 3169.

Schneider, C.A., Rasband, W.S. and Eliceiri, K.W. (2012) NIH Image to ImageJ: 25 years of image analysis. *Nat Methods* 9(7), 671-675.

Shatz, L.F. and De Groot, T. (2013) The frequency response of the vibrissae of harp seal, *Pagophilus groenlandicus*, to sound in air and water. *PloS one* 8(1), e54876.

Watkins, W.A. and Wartzok, D. (1985) Sensory biophysics of marine mammals. *Mar Mammal Sci* 1(3), 219-260.

Williams, T. and Kooyman, G. (1985) Swimming performance and hydrodynamic characteristics of harbor seals *Phoca vitulina*. *Physiol Zool* 58, 576-589.

Witte, M., Hanke, W., Wieskotten, S., Miersch, L., Brede, M., Dehnhardt, G. and Leder, A. (2012) Nature-inspired fluid mechanics. Tropea, C. and Bleckmann, H. (eds), pp. 271-289, Springer, Berlin.

CHAPTER 2: SENSITIVITY OF THE VIBRISSAL SYSTEM OF A HARBOR SEAL (PHOCA VITULINA) TO DIRECTLY COUPLED SINUSOIDAL VIBRATIONS

Abstract

This study measured the sensitivity of the vibrissal system of a harbor seal (*Phoca vitulina*) to directly coupled sinusoidal stimuli delivered by a vibrating plate. A trained seal was tested in a psychophysical paradigm in order to determine the smallest velocity that was detectable at nine test frequencies ranging from 10 Hz to 1000 Hz. The stimulus plate was driven by a vibration shaker and the velocity of the plate at each frequency-amplitude combination was calibrated with a laser vibrometer. To prevent cueing from other sensory stimuli, the seal was fitted with a blindfold and headphones playing broadband masking noise during testing. The seal's performance in this stimulus detection task showed that the vibrissal array was sensitive to directly coupled vibrations across the range of frequencies tested, with best sensitivity of 0.09 mm/s at 80 Hz. Velocity thresholds as a function of frequency showed a characteristic U-shaped curve for this subject with decreasing sensitivity below 20 Hz and above 250 Hz. For comparative purposes, human subjects were tested in the same experimental paradigm using their thumb to contact the vibrating plate. Threshold measurements for the human thumb were similar to those of the seal vibrissae, demonstrating comparable tactile

sensitivity for these structurally different mechanoreceptive systems. The thresholds measured for the harbor seal in this study were about 100 times more sensitive than previous in-air measures of vibrissal sensitivity for this species. The results were similar to those reported by others for the detection of waterborne vibrations, but show an extended range of frequency sensitivity.

Introduction

The vibrotactile sense of pinnipeds relies on sturdy, specialized vibrissae and supporting neural architecture apparently designed for the reception of waterborne vibrations. The vibrissal system in pinnipeds is highly innervated and strongly represented in the somatosensory cortex (Ladygina et al., 1985;Marshall et al., 2006). At least some pinnipeds are capable of using their vibrissae to detect and follow hydrodynamic trails and likely rely on this system during the pursuit and capture of swimming prey (Dehnhardt et al., 2001;Gläser et al., 2011). Although behavioral and histological evidence suggests that the vibrissal systems of pinnipeds are highly sensitive, the abilities of this sensory modality are not fully understood. One fundamental approach used to understand the capabilities of a sensory system is to measure its sensitivity at a range of frequencies. A limited number of studies have attempted to systematically evaluate the vibrissal systems of pinnipeds in this manner. These prior studies have utilized differing methods to examine the functional characteristics of this sensory modality and have yielded conflicting results.

The earliest study of vibrissal sensitivity in pinnipeds utilized direct recordings from the infraorbital nerve to investigate responses of the vibrissae to mechanical

stimulation. Dykes (1975) measured neural responses in anesthetized grey seals (*Halichoerus grypus*) and harbor seals (*Phoca vitulina)* to deflection of individual vibrissae that had been clipped near the skin surface and coupled to a mechanical transducer. Extracellular recordings were taken from individual nerve fibers as the vibrissae were stimulated in air by sinusoidal oscillations from a mechanical transducer. The resulting tuning curves suggested that most of the frequency-responsive fibers are broadly tuned, while a very small proportion of the fibers may be tuned to a frequency of approximately 80 to 100 Hz. The study also examined frequency sensitivity by contacting vibrissae with tuning forks of different resonances (from 128 to 1024 Hz) and recording the percentage of fibers that phase-locked to the stimulus frequency. The percentage of responsive fibers decreased as stimulus frequency increased and only a small proportion of the fibers were responsive at the highest test frequency. This suggests that the best sensitivity for the seal is at or below 128 Hz. Although Dykes did not directly measure response thresholds to stimulation, he concluded that the vibrissae of seals were relatively insensitive and implied that the system was likely to be responsive only to direct stimulation and unable to detect waterborne stimuli. However, based on later experimental findings (Dehnhardt et al., 1998;Dehnhardt et al., 2001), this appears to be an underestimate of the vibrissal system's sensitivity.

Subsequent studies utilized less invasive psychophysical methods to investigate vibrissal sensitivity in trained seals. Renouf (1979) and Mills and Renouf (1986) used a psychophysical procedure to test the sensitivity of the vibrissal system of the harbor seal to vibrations in air. Vibrissae were directly stimulated by contact with a metal rod vibrating at frequencies from 50 to 2500 Hz. Best sensitivity for the seals was measured

at frequencies of 750 and 1000 Hz (with minimum detectable velocity of approximately 4 mm/s). The seals were least sensitive to vibrations at frequencies of 500 Hz below (with thresholds between 17 and 95 mm/s reported) The authors concluded that the vibrissae were insensitive at low frequencies. Furthermore, they speculated that pinnipeds were specialized for detecting high frequencies in order to sense fine texture differences during active touch.

Dehnhardt , Mauck, and Bleckmann (1998) were the first to demonstrate that a seal can use its vibrissae to detect low-amplitude water movements. Their study employed a psychophysical task to measure the sensitivity of a trained harbor seal to low frequency (10 to 100 Hz) waterborne vibrations produced by an oscillating sphere. The particle motion component in the nearfield of the stimulus was used to simulate hydrodynamic signals and signal amplitude was estimated based on the distance from the source to the seal's vibrissae. The seal was able to detect low-amplitude vibrations transmitted through the water and, in contrast to previous in-air measures, displayed best sensitivity at low frequencies. The frequency of the seal's maximum sensitivity was 50 Hz with minimal detected water velocity of .25 mm/s and corresponding minimum particle displacement of 0.0008 mm . The velocity threshold curves depicting underwater sensitivity showed a steep roll-off by 100 Hz, indicating a sharp decrease in sensitivity for frequencies above this point. This identifies a range of best sensitivity that overlaps with the frequency components of most hydrodynamic stimuli, that are likely biologically relevant stimuli for this system(Bleckmann et al., 1991).

Through comparison with other known biological systems for mechanoreception, it is possible to better understand the pinniped vibrissal system. Unfortunately, there are

limited data on vibrotactile sensitivity of other whiskered animals. Although a great deal is known about the intricacies of the neural pathways of the vibrissal system in rats, comparable psychophysical thresholds are not available across a wide range of frequencies (Adibi and Arabzadeh, 2011;Gibson and Welker, 1983;Hutson and Masterton, 1986;Stüttgen et al., 2006). In contrast, the vibrotactile sensitivity of the human hand has been studied in numerous psychophysical experiments (Gilmer, 1935;Sherrick, 1953;Verrillo, 1963;1966). The sensitivity of the human hand to vibrations is well documented and has been studied for over a century (Dunlap, 1911). The vibrotactile thresholds for the hand are known to have a U-shaped curve with best sensitivity at 250 Hz (Gilmer, 1935;Sherrick, 1953;Verrillo, 1963;1966).

The aim of the present study was to investigate the absolute sensitivity of the vibrissae of the harbor seal to directly coupled vibrations, delivered in air. By physically coupling the stimulus to the vibrissae, we directly measured the sensitivity of the mechanoreceptive system to vibrissal movement at each frequency of interest. This allowed for careful control of the experimental stimuli without confounding factors from propagation through a medium. Prior measures of vibrissal sensitivity in seals provide conflicting views on the capabilities of this system (Dehnhardt et al., 1998;Dykes, 1975;Mills and Renouf, 1986;Renouf, 1979). In order to allow for comparison with previous measures of sensitivity in seals, we utilized test stimuli overlapped in frequency range with all of the aforementioned experiments. Furthermore, we compared the vibrotactile thresholds for the seal's vibrissae to those of the human thumb measured in an identical paradigm. In this study, the human tactile system served as a model for

comparison to the pinniped system and also provided a standard for comparison that demonstrated the reliability of the experimental setup.

Materials and Methods

Subjects

The primary subject was a captive-born, 24-year-old, adult, male Pacific harbor seal (*P. v. vitulina*) identified as *Sprouts* (NOA0001707). This seal had extensive prior training relevant to the current experiment, including experience participating in a variety of psychophysical auditory and visual experiments. He had normal hearing capabilities (Reichmuth et al., 2013) but had poor vision due to chronic bilateral cataracts. Prior to the current study, he had been trained to perform behavioral tasks while wearing either headphones or a blindfold, similar to those used in the current procedure. *Sprouts* consumed ~5 kg of freshly thawed capelin (*Mallotus villosus*) and herring (*Clupea spp.)* each day, a quarter of which was provided during daily training and testing for this study. His diet was not constrained for experimental purposes and he was maintained at a healthy weight throughout the study. Testing was conducted from May to July 2012, prior to the summer molt. The seal's vibrissal array was fully-grown and intact during this period.

Four human subjects were also tested in the current study during the same time period. These were one male and three female subjects, aged 20 to 24 years with no significant sensory deficits. The human subjects were assistants at Long Marine Laboratory who volunteered to participate in the experiment.

Ethics statement

Animal research was authorized under National Marine Fisheries Service permit 14535 and conducted with the approval of the Institutional Animal Care and Use Committee at UCSC. Research with human subjects was conducted under a Category 2 exemption by the UCSC Internal Review Board.

Experimental design

The harbor seal and human subjects were tested using a psychophysical procedure to measure velocity thresholds for vibrational stimuli, detected from a calibrated oscillating contact plate. The harbor seal contacted the plate with his vibrissae and each human subject contacted the plate with the pad of their thumb. A go/no-go behavioral response paradigm, conducted using a modified method of limits (staircase procedure), was used to measure absolute vibrotactile sensitivity to sinusoidal stimuli at nine frequencies from 10 to 1000 Hz.

Testing environment

The experiment was conducted at Long Marine Laboratory in Santa Cruz, California in a custom-designed, hemi-anechoic, experimental chamber (*Eckel Industries*) that was located near the seal's living enclosure. This chamber, designed for audiometric testing, was subdivided into a *testing room* suitable for large animals and an adjacent, sound-isolated *control room* with space for controlling equipment and an experimenter. A detailed description of the testing chamber is provided by Southall et al. (2003) and a general schematic of the experimental set-up is provided in Figure 2.1.

Stimulus generation

Sinusoidal waveforms were used to drive oscillatory movements of a rectangular Plexiglas contact plate (1140 mm high x 760 mm wide x 2.8 mm thick). The generated vibratory stimuli had a frequency of 10, 20, 40, 80, 100, 250, 500, 800 or 1000 Hz and a total duration of 1000 ms, including 25 ms linear rise/fall times. Signals were generated with an RP2 real-time processer (*Tucker-Davis Technologies, Alachua, FL, USA*) controlled with a custom-written MATLAB script on a PC computer, attenuated via a PA5 programmable attenuator (*Tucker-Davis Technologies Alachua, FL, USA*), amplified by a Pyle Pro PPA200 power amplifier (*Pyle Audio, Brooklyn, NY, USA*), and used to drive a SignalForce GW-V4 shaker system (*Data Physics Corp., San Jose, CA*). The shaker motor was coupled to an aluminum rod (750 mm long x 4 mm diameter) that was attached to the rear of the contact plate by a tee nut glued to a metal fixed-angle hinge that held the plate at a rigid 45˚ angle to the axis of the rod.

The stimulus generation equipment was located in the control room of the experimental chamber. The shaker motor was vibration isolated from the surrounding substrate using foam and Sorbothane shock absorption padding (*IsolateIt, Burlington, NC, USA*). The aluminum rod that extended from the shaker passed through the wall of the control room into the test room through the center of a 50 cm long PVC conduit that was encased on the control room side with sound isolating foam. To maintain the rod at a parallel angle to the floor as it entered the test room, the rod was suspended with elastic rubber bands where it exited the conduit through a 1.2 cm diameter hole in the conduit cap. No portion of the vibration driven components were in direct contact with any portion of the testing room.

Stimulus calibration

A single-point laser vibrometer (CLV1000 controller with CLV700 sensor) (*Polytech Inc., Irvine, CA, USA*) was used to measure the velocity (v) in mm/s of the contact plate during stimulation by the sinusoidal test signals. The laser vibrometer was positioned at a 45˚ angle to the plate surface, so that the laser beam was in line with the axis of the oscillating rod; consequently, the laser beam was in line with the axis of the movement of the plate. Velocity measurements were obtained before and after every session from the center point of the contact plate. During calibration, the frequency of the signal was held constant, while velocity was measured at 12 discrete amplitudes, starting at a supra-threshold level and attenuating in 6 dB steps until the signal was buried in the noise floor. This amplitude range included all stimulus levels used during testing at each frequency. Displacement (d) values in mm and acceleration (a) values in mm/s^2 of the test stimuli were calculated from the velocity measurements, with d determined as $v/2\pi f$ and a determined as $v2\pi f$ (where f = frequency in Hz).

Stimulus mapping

In order to map the consistency of vibration levels across the surface of the plate, fine-scale spatial mapping was conducted before and after the experimental term. For each test frequency, recordings were obtained from 15 evenly spaced points across the surface of the plate. At each point, recordings were made at the same 12 amplitudes used during daily calibrations. Within each recording point, attenuation was determined to be linear across all stimulus amplitudes. Therefore, calculations of spatial variability and determination of vibration modes were based on the starting (highest) amplitude level.

Modes of vibration, or resonance patterns, were quantified by calculating the difference in velocity between each mapping point and the center point of the plate (daily calibration position). Spatial variation of signal amplitude for each test frequency was quantified by a Coefficient of Variation (*CV*). The *CV* was calculated by dividing the standard deviation of velocities across the plate by the average of velocities across the plate.

In order to characterize the movement of the plate in multiple planes, mapping was carried out with the laser vibrometer positioned at two orientations. For each of the 15 spatial positions, recordings were made with the laser oriented at a 45˚ angle to the plate surface (in line with the axis of vibration, as in daily calibration) and with the laser oriented at a 90˚ angle to the plate surface (45˚ angle to the axis of vibration).

Experimental controls

Controls were put in place to ensure that subjects responded only to the vibrational test stimuli. These controls included evaluating and eliminating any extraneous vibrotactile, visual, and acoustic artifacts associated with stimulus generation as well as preventing the possibility of behavioral cueing from human experimenters.

The presence of confounding vibrotactile cues in the testing area was systematically evaluated using laser vibrometer measurements. Recordings were made from all surfaces that the subjects came in contact with while the stimulus was generated at each frequency at supra-threshold levels. These recordings confirmed that the stimulus plate was the only surface with any detectable movement.

To eliminate any possibility of visual cues during testing, the seal wore a soft, customized blindfold made of opaque neoprene during testing. Human subjects were

oriented in such a way during testing that the contact plate was not visible. Even so, it is notable that at all frequencies, movement of the plate was not visually detectable to humans at the stimulus levels used during testing at all frequencies. Independent human observers, not touching the contact plate but visually observing the plate during stimulus generation, confirmed that the test signals could not be identified on the basis of visual cues.

To mask potential acoustic artifacts associated with vibration of the contact plate, broadband masking noise was played through headphones worn by the subjects. The masking stimulus consisted of a Gaussian noise distribution with the frequency of greatest energy centered at the test frequency. The masking signal was generated by an RP2 real-time processer (*Tucker-Davis Technologies, Alachua, FL, USA*), amplified by a VP1000 voltage preamplifier (*RESON Inc., Goleta, CA, USA*), and transmitted through TDH-39 headphones (*Telephonics Corporation, Farmingdale, New York, USA*) that were seated in rubber ear cushions. The seal wore a custom-made neoprene headband that held the headphones snugly in place over the ears. Prior to testing at each frequency, an ER-7C probe microphone (*Etymotic Research, Elk Grove Village, IL, USA*) was used to record the spectrum and level of the acoustic artifact associated with supra-threshold signal generation in the absence of the masker, from beneath the ear cushion of the headphones while placed on the seal. This information was used to determine the appropriate shape and amplitude of the masking sound for each test frequency based on published critical ratio values for harbor seals (Southall et al., 2003). The characteristics of the masker were then verified by recording the masking noise from beneath the headphones, in the presence and absence of supra-threshold signals, to confirm sufficient

masking levels to prevent the detection of acoustic cues. Human subjects were provided with foam earplugs that they wore beneath HDA 200 headphones (*Sennheiser Electronic Corporation, Old Lyme, CT, USA*) that presented the same masking noise given to the seal. Since humans have similar or higher critical ratios than seals (Hawkins and Stevens, 1950), the seal's maskers should have been more than adequate to mask the signal artifacts presented to human subjects. Independent human observers, who listened for the signal during trials while wearing headphones but not touching the contact plate, confirmed that the test signals could not be acoustically detected at the stimulus levels used during threshold testing.

For the seal trials, an assistant was present inside the testing chamber with the animal. This assistant was "blind" to the presentation of the test signal and received instructions from the experimenter via headphones following each trial. For human sessions, the subjects were alone in the testing room.

Psychophysical procedure

The seal was trained using operant conditioning with positive (fish) reinforcement to participate in the experiment. At the start of each session, he was cued by an assistant to move from his living enclosure to enter the testing chamber and allow the door to be closed behind him. Once in the chamber, he was fitted with the headphones and the blindfold by the assistant, and then was cued to rest his lower jaw on a contoured chin rest. In this stationing position, the whiskers on his right muzzle touched the surface of the contact plate, as shown in Figure 2.2. He was able to flex his whiskers forward to obtain firmer contact with the plate but was not permitted to move his jaw from the station or contact the plate with any part of the skin.

During the session, an experimenter controlled the test trials and viewed the session on a closed-circuit video system. A go/no-go response paradigm was used in which the seal reported detection of a vibratory signal by pressing a response target to his left and the absence of a vibratory signal by remaining in position at the chin station. Prior to every trial, the assistant checked the placement of the headphones and blindfold and then cued the seal to position at the station. Once the seal was correctly positioned, the experimenter initiated the acoustic masker for a 5-second interval. This delineated the trial interval for the subject. Both signal-present and signal-absent trials were used. During a signal-present trial, the vibratory signal was delivered via the plate at a variable point during the trial window. During a signal-absent, or "catch" trial, only the acoustic masker was played.

Correct responses included pressing the response paddle after the presentation of a vibratory signal (*hit*) and remaining motionless in the station for the entire trial interval in the absence of a vibratory signal (*correct rejection*). Correct responses of either type were marked for the seal by a brief whistle followed by one piece of fish given by the assistant. Incorrect responses included failing to respond during the trial interval to the presentation of a vibratory signal (*miss*) and touching the response paddle on a signal-absent trial (*false alarm*). Following incorrect responses of either type, the masker was terminated and the subject was prompted to reposition at the station.

Sessions included approximately 60 trials and were conducted 1-2 times per day. The order of signal and catch trials in a session were counterbalanced using a MATLAB-generated pseudorandom schedule that constrained the maximum run length of a particular trial type to four. A signal was presented during the trial interval on 50 to 60%

of the trials. This trial ratio maintained a consistent false alarm rate throughout the experiment. On signal-present trials, the frequency of the vibratory signal was the same throughout the session and the amplitude of the signal was varied using an adaptive up-down descending methods of limits (e.g. a descending staircase procedure) (Cornsweet, 1962). A session began with several easily detectable "warm-up" trials at supra-threshold level. The velocity of the signal was then attenuated by 4 dB after each successful trial until the subject's first miss. The velocity was then increased by 4 dB after each miss and decreased by 2 dB following each subsequent hit. A session continued until five consecutive hit-to-miss transitions within 6 dB of attenuation were completed. Sessions were conducted at the same frequency until the seal maintained stable performance for at least three consecutive sessions as described below. The nine test frequencies were tested in non-consecutive order. At the conclusion of the experiment, the threshold for the first test frequency was re-measured as a reliability check. The re-measured threshold was within 3% of the original threshold and ensured that no practice effect had occurred during the course of the experiment.

Human subjects were tested in the same experimental chamber as the seal with only a few differences in procedure. Humans received written and verbal instructions regarding the testing procedure prior to the initiation of the experiment. At the start of each session, the human subject was fitted with earplugs and headphones, and then seated at a 90˚ angle to the seal's chin cup. The subject's left hand was placed in the seal's chin cup, with the weight of the hand resting in the cup and the fleshy pad of the thumb touching the center of the contact plate. Subjects reported detection of a signal on a trial by raising their right hand and the absence of a signal by remaining still. For each correct

answer, subjects were presented a flashing white light at the termination of the masker. For incorrect responses, the masker was terminated with no additional feedback. A signal was presented during the trial interval on 70% of the trials. All other aspects of the procedure and signal presentation were identical to those used for the seal.

Threshold calculation

Following each session, the calibration data were used to convert signal attenuation in dB to velocity in mm/s. A session threshold, defined as the 50% detection probability threshold for rms velocity, was calculated as the mean of the velocities of the last five hit-to-miss transitions on signal-present trials. To calculate an overall threshold for a given frequency, three consecutive sessions with stable performance were required. The last five hit-to-miss transitions within each of these sessions needed to show a plateau (no significant slope) and the thresholds for each session needed to fall within 6 dB of each other. Usable sessions were also constrained on the basis of false alarm rate. For the seal, false alarm rates of greater than 0 and less than 30% were accepted. For humans, false alarm rates of greater than or equal to 0 and less than 30% were accepted. At the end of the experiment, an overall threshold for each test frequency was calculated as the mean of the thresholds from the three sessions meeting these criteria.

The velocity threshold value determined for each frequency based on the seal's performance on the task was ultimately corrected to account for the spatial variation of the signal across the contact plate at that frequency. Although only the center point of the plate was used for daily calibration of the velocity threshold, the mapping data (quantified as the *CV*) revealed frequency-dependent non-linearities across the surface of the plate caused by modes of vibration. Therefore, a threshold correction factor was

identified and applied to account for spatial variability in velocities on the contact plate. This factor was calculated as the maximum velocity at any point on the plate divided by the velocity at the daily calibration position. The threshold determined for each test frequency was multiplied by this correction factor, so that the final reported threshold was referenced to the maximum vibration velocity anywhere on the plate. This ensured a conservative estimation of performance and compensated for points of vibrissal contact other than the center point of the plate. Threshold corrections were based on spatial mapping of stimuli with the laser beam oriented at a 45˚ angle to the plate surface, as in daily calibrations. No correction factor was necessary for the human data, as the thumb contacted only the center point of the plate, where the daily calibration was based.

Results

The vibrating plate used to measure sensitivity to directly coupled vibrations allowed multiple vibrissae to contact the surface of the plate during testing. These vibrissae contacted the plate over much of its surface, as shown in Figure 2.2. The spatial patterns of velocity caused by modes of vibration on the surface of the plate are depicted as relative intensity plots for each test frequency (Figure 2.3). These intensity plots show that spatial variation in signal amplitude was minimal at lower frequencies (between 10 and 80 Hz) and maximal at highest frequencies (800 and 1000 Hz). This is confirmed quantitatively by the *CV* measure (Table 2.1), which was ≤ 0.07 below 80 Hz and ≥ 0.53 above 800 Hz. The stimuli were further characterized by examining the surface vibrations measured with the laser vibrometer from two angles: 45˚ and 90˚ relative to the surface of the plate. The CV values were similar between the two laser angles were similar for

frequencies up to 500 Hz, providing a relatively consistent view of the vibrational patterns on the plate. Greater inconsistencies between orientations were measured at frequencies above 500 Hz, reflecting an elliptical path of plate movement at high frequencies.

To ensure that the measured threshold sensitivity was not biased by spatial variability across the vibrating surface, the reported thresholds are referenced to the highest velocity measured on the contact plate. Threshold corrections were based on spatial mapping of stimuli with the laser beam oriented at a 45˚ angle to the plate surface, as in daily calibrations.

The velocity thresholds and false alarm rates for the seal at each test frequency are provided in Table 2.1. The vibrotactogram of these velocity thresholds had a U-shape (Figure 2.4B), with best sensitivity at 80 Hz and decreasing sensitivity below 20 Hz and above 250 Hz. An irregularity in the tactogram curve is seen between 500 and 800 Hz. The measured velocity thresholds were converted to displacement (Figure 2.4A) and acceleration (Figure 2.4C), for which the curves showed decreasing and increasing thresholds, respectively, as a function of frequency.

Threshold measurements for the human subjects were similar to those of the seal (Table 2.2 and Figure 2.5). Performance was generally consistent between individual subjects and was in agreement with previous measures of the sensitivity of the human hand. Frequency of best sensitivity was at 250 Hz when the thresholds were considered in terms of velocity or displacement. When thresholds were considered in terms of acceleration, minimum threshold varied from 10 and 80 Hz across subjects. A notch in the tactogram curve is seen at 20 Hz.

Discussion

The harbor seal tested in the present study was sensitive to vibrations across the entire range of frequencies tested (10 to 1000 Hz). The velocity thresholds showed a characteristic U-shaped curve with a gradual low-frequency roll-off below 80 Hz and a steeper high-frequency roll-off above 250 Hz. Best velocity sensitivity was measured at 80 Hz, with a minimum absolute threshold of 0.09 mm/s.

In order to obtain the most accurate estimation of vibrotactile threshold levels, great care was taken to accurately characterize the test signal delivered to the subject. This was achieved by careful calibration and mapping of the test stimuli. Mapping of the spatial variability of signal amplitude across the surface of the plate yielded a measure of confidence in threshold estimation. At the frequencies of best sensitivity, reliable estimation of these threshold levels was achieved due to the minimal variation across the plate. The greatest spatial variation occurred at the higher frequencies in the test range, particularly at 800 and 1000 Hz. Although the thresholds for the seal are based on the point of highest vibration on the plate, the complex modes of vibration that occur at these high frequencies result in a less constrained threshold estimate. This spatial variability may account for the irregularity in the curve shape that occurs between 500 and 800 Hz in the velocity threshold curve (Figure 2.4B). The irregularity likely does not represent a true increase in sensitivity from 500 to 800 Hz, rather it suggests that the threshold at one of these frequencies may be underestimated or overestimated. This variation across the plate affects only the threshold measurements for the seals, as whisker contact was spread

out across the entire surface of the plate, while human subjects contacted only the center point of the plate during testing.

While the data are considered primarily with respect to the velocity metric, the relevant component of motion that the vibrissal system senses is unknown. Therefore, it is advantageous to visualize the sensitivity thresholds in terms of the displacement and acceleration parameters of motion, as well as velocity. Furthermore, no standard exists for which parameter to report thresholds in and the metric used varies between studies. Considering the thresholds in all three parameters of motion therefore allows for comparisons to be easily made between other work.

When converted to displacement and acceleration, the minimum threshold value for the harbor seal subject remained at 80 Hz. The displacement curve showed a sharp decrease in threshold level between 10 and 80 Hz. Above the frequency of best sensitivity, the displacement thresholds were similarly low, showing a plateau in the slope of the sensitivity curve. Conversely, the acceleration thresholds showed a plateau below 80 Hz and a sharp increase in threshold level above this frequency.

The shapes of the sensitivity curves reported in this study (in displacement, velocity, and acceleration metrics) are in agreement with those reported by Dehnhardt et al. (1998) for a harbor seal tested underwater. The hydrodynamic receptors of several other aquatic species also show similar threshold curve shapes when considered as a function of these different motion parameters (Bleckmann, 1994). Although the shapes of the curves allow for inter-species comparisons, they may not always indicate the parameter of motion that is biologically salient to the receptor system. The relevant component of motion that the vibrissal system senses cannot be determined using

absolute threshold data from sinusoidal stimuli. Previous work conducted with rats has suggested that velocity is the salient component of the stimulus for the vibrotactile system of the rat. This conclusion was based on performance of rats in a vibrotactile discrimination task in which the combination of amplitude and frequency in two stimuli were varied. Rats could not discriminate between two stimuli if the product of amplitude and frequency were constant; therefore, the investigators concluded that rats sense the composite of these features, which is proportional to velocity (Adibi et al., 2012). Given these findings with rats, it is plausible that velocity is also the relevant parameter of motion for the seal's vibrissal system; however, future studies would need to employ non-sinusoidal stimuli to test this hypothesis.

In order to ground truth the methods used to understand the sensitivity of the seal's vibrissal system in this study, the procedure was adapted with few modifications for comparison to the human mechanoreceptive system. The tactile sensitivity of the human hand to vibration as a function of frequency is well understood. It is known that human vibrotactile thresholds, have a U-shaped curve with best sensitivity around 250 Hz (Gilmer, 1935;Sherrick, 1953;Verrillo, 1963;1966). Although threshold amplitude differs slightly depending on the portion of the hand being stimulated, the overall shape of the curve is maintained (Verrillo, 1962). The data presented in the current study are in agreement with previous measures of sensitivity for the human hand. The four human subjects showed best sensitivity at 250 Hz. The notch at 20 Hz in the human sensitivity curves is consistent with the data from previous studies and is representative of a shift in receptors (Gescheider et al., 2002;Morioka and Griffin, 2005). The parallel performance between the present study and prior measures of tactile sensitivity in humans

demonstrates the accuracy of the experimental method used is in this study and provides confidence in the measured thresholds for the seal.

Prior measures of vibrissal sensitivity in seals provide conflicting views on the capabilities of this system. The results of the present study agree with Dykes (1975) regarding frequency of best sensitivity, but not in overall assessment of sensitivity of the system. The electrophysiological data collected by Dykes identified best sensitivity at or below 128 Hz, which closely corresponds to the frequency of best sensitivity identified in this study. Based on the stimulus amplitude required to induce phase-locked neural firing, Dykes also concluded that the seal vibrissal system was relatively insensitive overall. In contrast, the present study reports good sensitivity across a range of frequencies. The present study is likely a more accurate assessment of the capabilities of the vibrissal system as Dykes did not collect absolute threshold data and the methodology that he utilized to identify phase locking of fibers does not necessarily indicate minimum detectable stimulus level.

The thresholds measured for the harbor seal in this study are dramatically lower than those reported in previous in-air psychophysical measures of vibrissal sensitivity in this species (Mills and Renouf, 1986;Renouf, 1979). Renouf (1979) and Mills and Renouf (1986) reported high threshold values overall and concluded that the seal vibrissae are insensitive at low frequencies. The present study reported good sensitivity overall, with threshold levels an average of 100 times lower than the prior measures. Furthermore, Renouf and Mills and Renouf reported best sensitivity at high frequencies (above 500 Hz), while the present study reports best sensitivity at low frequencies (below 250 Hz).

The response bias of a subject, which is experimentally constrained by the false alarm rate, can affect the thresholds measured in a behavioral experiment. While the current data set differs from previous in-air measures, the observed differences in reported thresholds between the two studies cannot be explained by response bias. In comparison to the current study's false alarm constraint of less than 30%, Mills and Renouf (1986) utilized a false alarm rate averaging 50%; thus, it would have resulted in a response bias that would have driven the thresholds down, generating an overestimation of sensitivity.

In order to accurately measure a vibrotacticle threshold, it is imperative that there are no extraneous cues available to other sensory modalities. The present study thoroughly measured all acoustic artifacts and took precautions to adequately mask any confounding cues. The thresholds reported by Renouf (1979) were criticized for not having adequate acoustic controls (Mills and Renouf, 1986;Watkins and Wartzok, 1985). In the follow up measurements by Mills and Renouf (1986), enhanced acoustic controls were established; however, it is possible that some acoustic artifacts may have cued the animal.

The threshold levels reported here are most similar to those measured underwater by Dehnhardt et al. (1998). The ranges of threshold amplitudes are similar, although different frequencies of best sensitivity are reported. Notably, the present study reports a wider range of frequency sensitivity, with good sensitivity extending above 100 Hz, where Dehnhard's measures indicate a roll-off. However, it is difficult to determine if the upper range of frequency sensitivity reported indicates a limitation of the sensory system or a limitation imposed by hydrodynamic coupling of the stimuli to the sensors. While it

is unlikely that the receptor itself functions differently in air and underwater, it is probable that the way the stimulus interacts with the whisker differs between mediums. Because the present study directly coupled vibrations to the sensors, the points of contact on the vibrissae were moved at relatively the same rate as the stimulus. In the experiment by Dehnhardt et al., the animal was detecting vibrations that were propagating through the water. It is possible that as frequency increased, the waterborne vibrations did not stimulate movement of the whisker adequately to excite the receptors.

The present research utilized carefully controlled measures to assess the sensitivity of the vibrissal system of the harbor seal and lends to a more complete understanding of the capabilities of this system. The thresholds obtained in the current study are in line with what would be expected for an animal that is highly reliant on its mechanoreceptive system. Interestingly, the thresholds collected for the seal were similar to the sensitivity for the human thumb. The similarities in performance between the seal vibrissae and the human thumb demonstrate good tactile sensitivity for these structurally different mechanoreceptive systems. In addition, the frequency of range best sensitivity identified in the present study closely agrees with the probable frequency range of biologically relevant stimuli, as hydrodynamic stimuli are considered to be below 100 Hz (Bleckmann et al., 1991;Bleckmann, 1994) and vibrations measured from vibrissae of harbor seals in laboratory studies were are at frequencies below 300 Hz (as seen in chapter 1).

Tables

Table 2.1 Velocity thresholds for the harbor seal

Frequency (Hz)	Velocity threshold (mm/s)	CV	FA rate	Test order
10	1.06	0.06	26%	7
20	0.42	0.02	22%	6
40	0.25	0.05	25%	1
80	0.09	0.07	17%	2
100	0.17	0.45	22%	3
250	0.42	0.24	26%	4
500	1.99	0.48	18%	5
800	1.55	0.69	18%	8
1000	3.90	0.52	21%	9

CV = Coefficient of variation (calculated from stimulus variation across the plate at each frequency), FA rate = False alarm rate

Table 2.2 Velocity thresholds (mm/s) for individual human subjects

Frequency (Hz)	Subject 1	Subject 2	Subject 3	Subject 4
10	0.73	0.76	0.81	1.36
20	0.95	1.35	1.49	1.62
40	0.17	0.96	0.32	0.61
80	0.14	0.09	0.10	0.21
100	0.13	0.26	0.10	0.18
250	0.07	0.10	0.04	0.14
500	0.54	0.37	0.17	0.41
800	2.06	1.09	0.77	1.38
1000	1.90	3.54	1.14	1.34

Figures

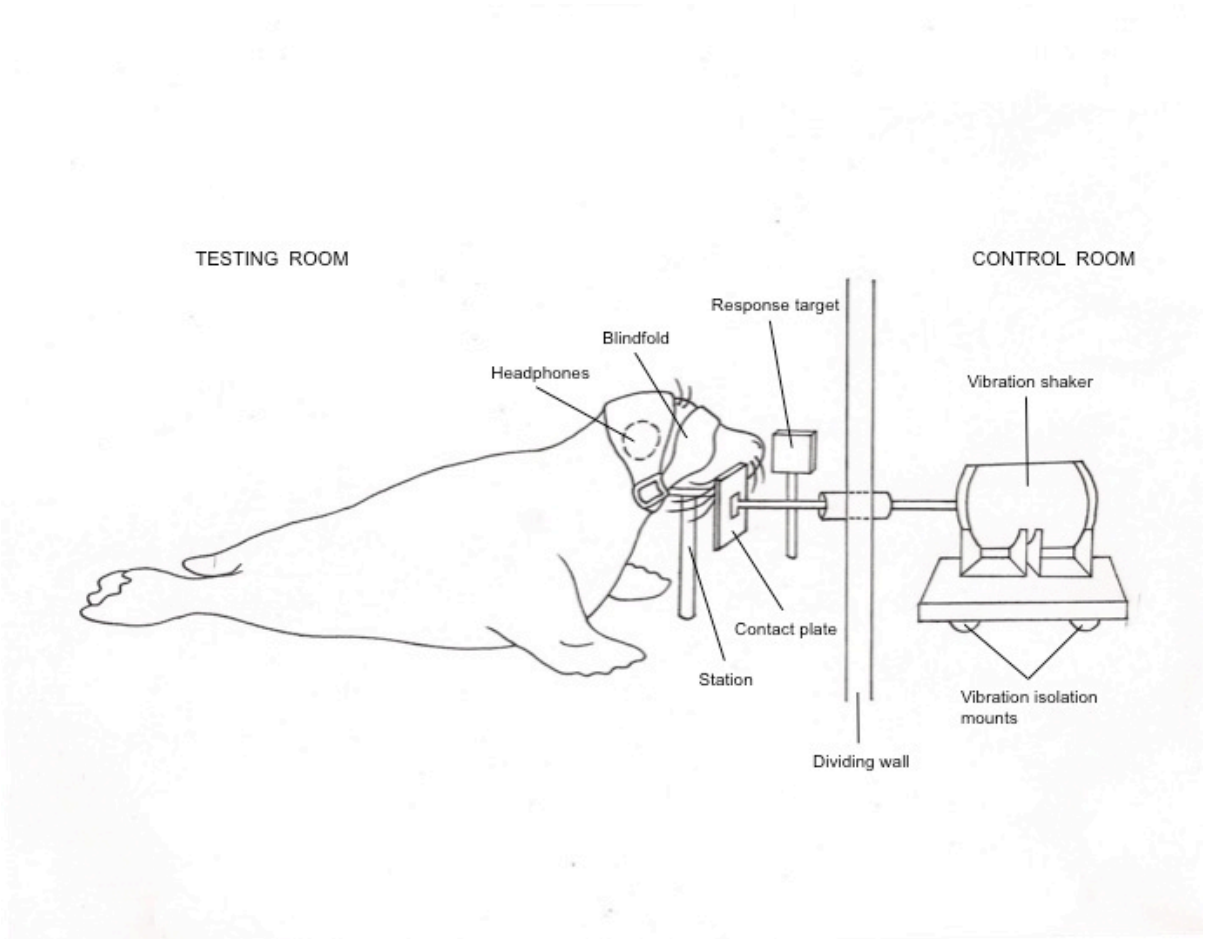

Figure 2.1 Schematic of the study area showing the seal in position on the experimental setup. The experimental chamber is divided into a testing room, where the stimulus is delivered to the subject and a control room, where signal generation is operated by an experimenter. The figure is not drawn to scale and for simplification purposes, only the central components of experimental setup are illustrated here.

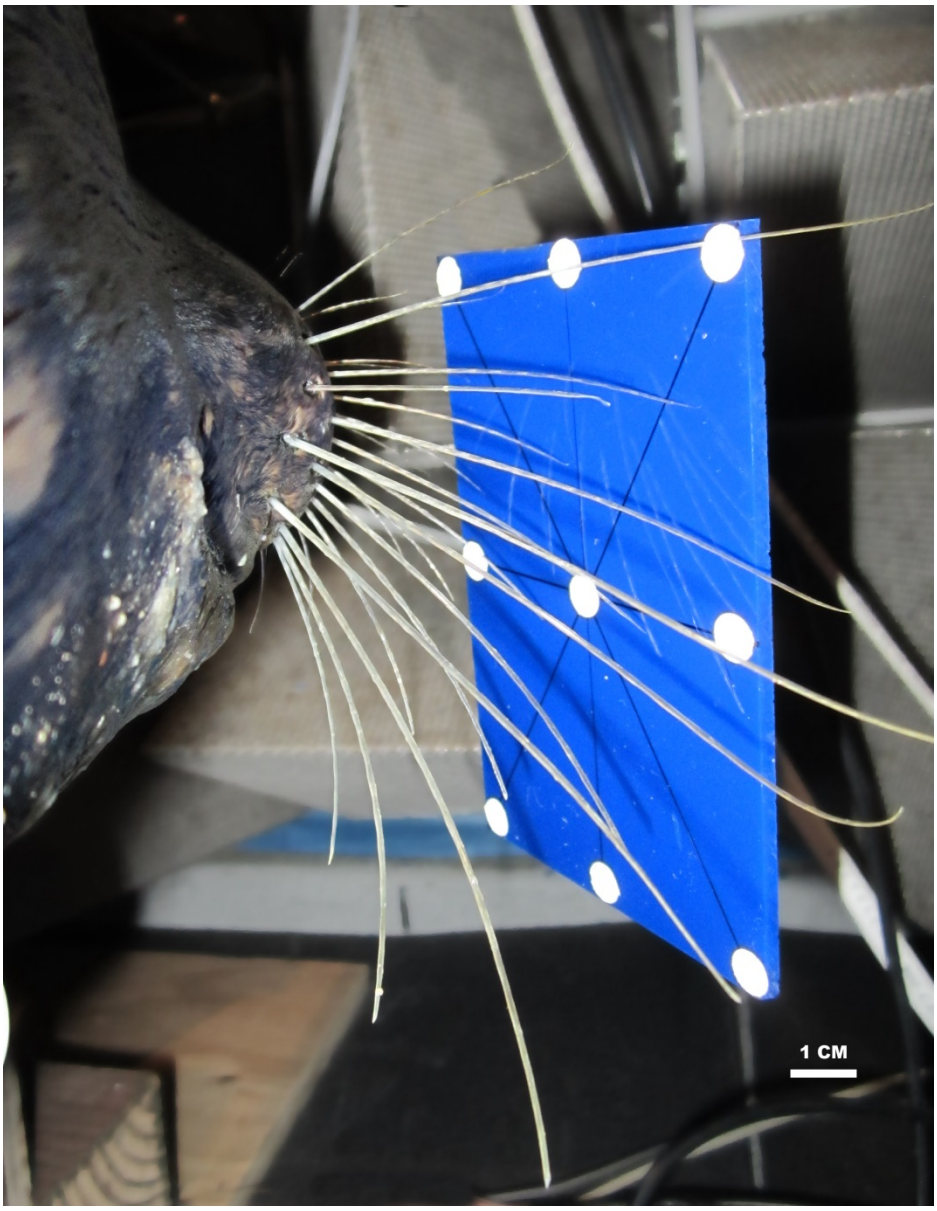

Figure 2.2 Photograph showing whisker contact on the stimulus plate during testing. When stationed in the chin cup, the whiskers of the seal's right vibrissal bed contacted the plate. Plate dimensions were customized to maximize the number of vibrissae contacting the plate. The dimensions of the plate are 1140 mm high x 760 mm wide x 2.8 mm thick.

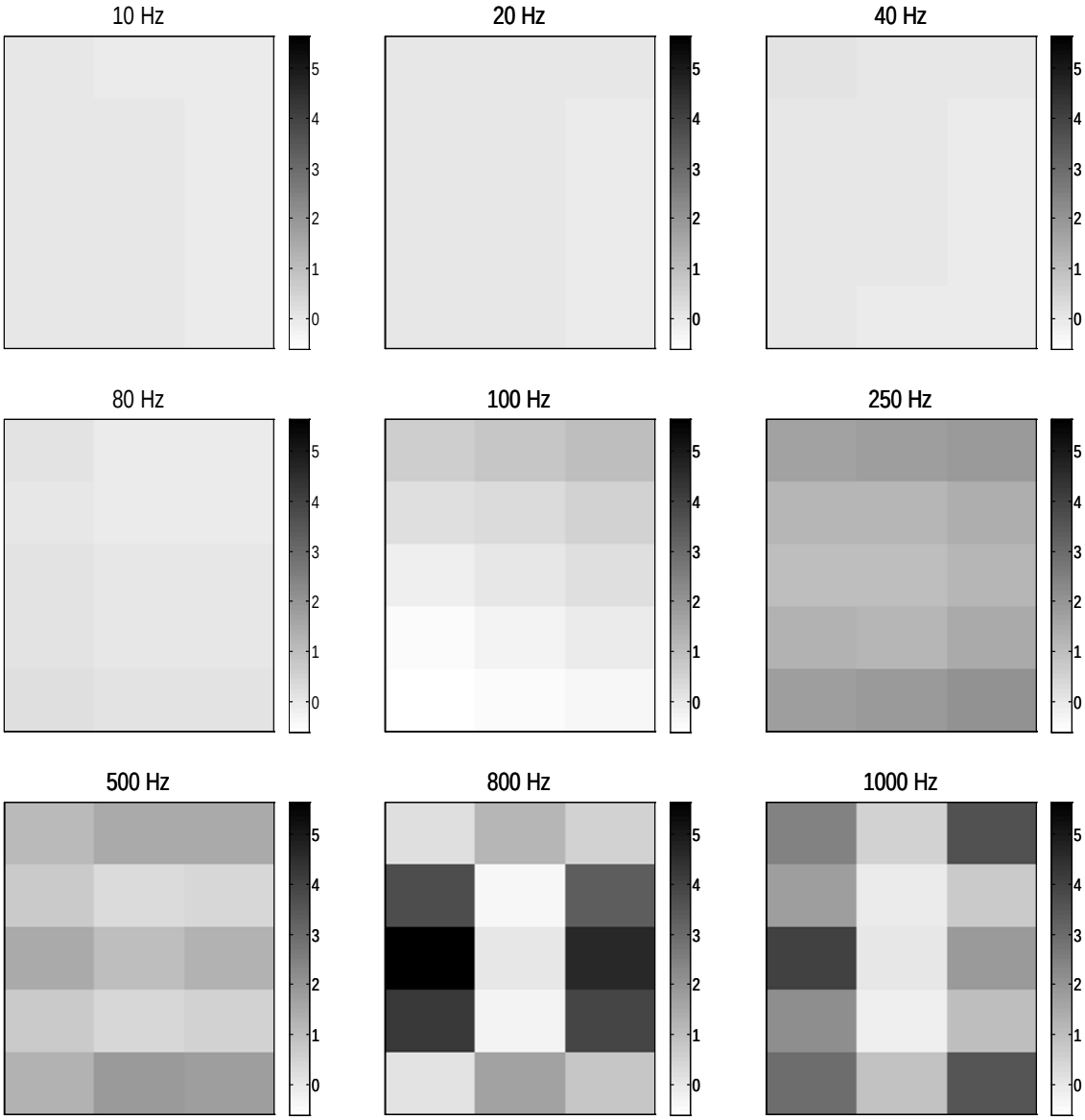

Figure 2.3 Relative intensity plots illustrating spatial variation in signal amplitude for each test frequency. Signal velocity was recorded at 15 discrete points across the surface of the plate, with the laser oriented at a 45˚ angle to the plate surface (in line with the axis of vibration), as in daily calibration. The color intensity at each point on the grid illustrates the difference in velocity between that point and the center of the plate, divided by the velocity at the center of the plate. The color scale is expressed in terms of this ratio number and color intensity reflects higher (darker) and lower (lighter) deviations from the center position. Vibration amplitude is relatively spatially consistent for low frequencies, while distinct modes of vibrations visible for 800 and 1000 Hz.

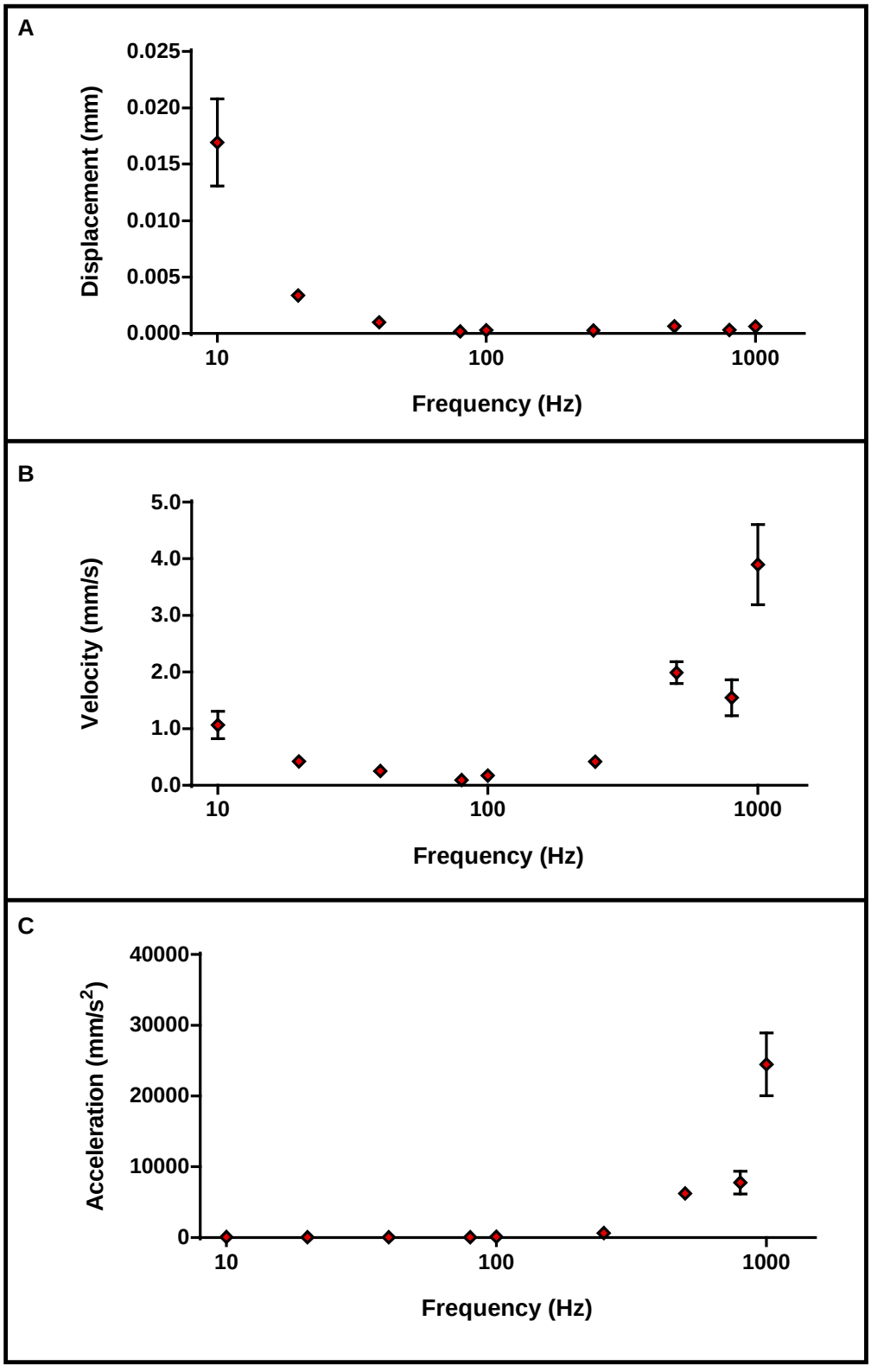

Figure 2.4 Mean vibrotactile thresholds for the seal at each test frequency. Thresholds are shown in terms of (A) displacement, (B) velocity, and (C) acceleration. Error bars represent +/- s.d. of thresholds from 3 sessions at each frequency.

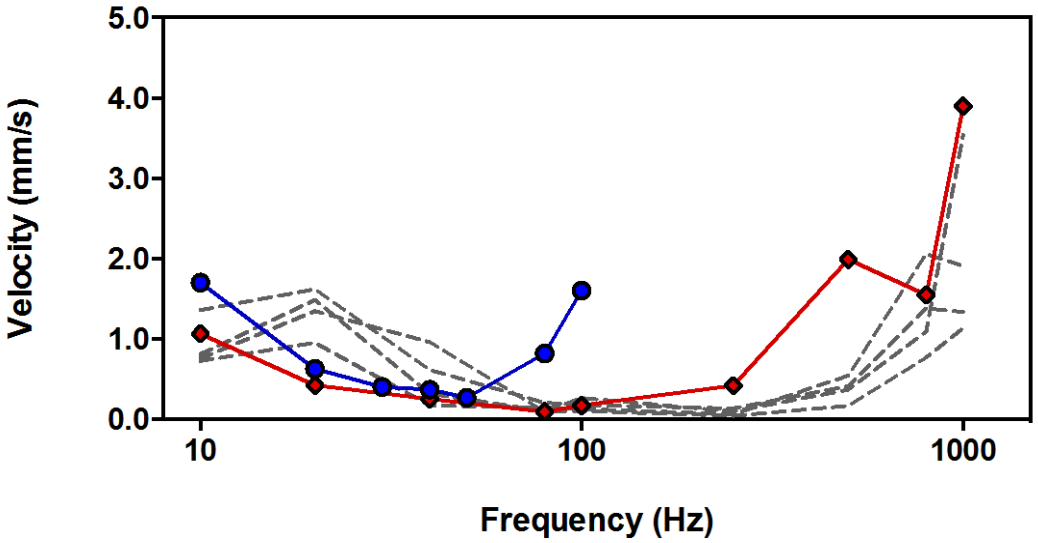

Figure 2.5 Velocity thresholds from the present study, overlaid a previous measure of vibrissal sensitivity in the harbor seal. Velocity thresholds for the harbor seal (diamonds) tested in the current study, shown with the same measurements obtained for four human subjects (dashed lines). The sensitivity thresholds of another harbor seal to underwater stimuli (reported by Dehnhardt et al. 1988) are shown for comparison (circles). The only other available sensitivity data for harbor seals (reported by Renouf (1979) and Mills and Renouf (1986)) are not shown here as those aerial thresholds, when converted from displacement to velocity range from 3.6 to 110 mm/s and cannot be accommodated by the scale of this figure.

References

Adibi, M. and Arabzadeh, E. (2011) A comparison of neuronal and behavioral detection and discrimination performances in rat whisker system. *Journal of neurophysiology* 105(1), 356-365.

Adibi, M., Diamond, M.E. and Arabzadeh, E. (2012) Behavioral study of whisker-mediated vibration sensation in rats. *Proceedings of the National Academy of Sciences* 109(3), 971-976.

Bleckmann, H., Breithaupt, T., Blickhan, R. and Tautz, J. (1991) The time course and frequency content of hydrodynamic events caused by moving fish, frogs, and crustaceans. *Journal of Comparative Physiology A* 168(6), 749-757.

Bleckmann, H. (1994) Reception of Hydrodynamic Stimuli in Aquatic and Semiaquatic Animals *Progress in Zoology* 41.

Cornsweet, T.N. (1962) The staircase-method in psychophysics. *The American journal of psychology* 75(3), 485-491.

Dehnhardt, G., Mauck, B. and Bleckmann, H. (1998) Seal whiskers detect water movements. *Nature* 394(6690), 235-236.

Dehnhardt, G., Mauck, B., Hanke, W. and Bleckmann, H. (2001) Hydrodynamic trail-following in harbor seals *(Phoca vitulina*). *Science* 293(5527), 102-104.

Dunlap, K. (1911) Palmesthetic difference sensibility for rate. *American Journal of Physiology--Legacy Content* 29(1), 108-114.

Dykes, R.W. (1975) Afferent fibers from mystacial vibrissae of cats and seals. *Journal of neurophysiology* 38(3), 650-662.

Gescheider, G.A., Bolanowski, S.J., Pope, J.V. and Verrillo, R.T. (2002) A four-channel analysis of the tactile sensitivity of the fingertip: frequency selectivity, spatial summation, and temporal summation. *Somatosensory & motor research* 19(2), 114-124.

Gibson, J.M. and Welker, W.I. (1983) Quantitative studies of stimulus coding in first-order vibrissa afferents of rats. 1. Receptive field properties and threshold distributions. *Somatosensory & motor research* 1(1), 51-67.

Gilmer, B.v.H. (1935) The measurement of the sensitivity of the skin to mechanical vibration. *The Journal of General Psychology* 13(1), 42-61.

Gläser, N., Wieskotten, S., Otter, C., Dehnhardt, G. and Hanke, W. (2011) Hydrodynamic trail following in a California sea lion (*Zalophus californianus*). *J Comp Physiol A* 197(2), 141-151.

Hawkins, J. and Stevens, S. (1950) The masking of pure tones and speech by white noise. *Journal of the Acoustical Society of America* 22, 6-13.

Hutson, K. and Masterton, R. (1986) The sensory contribution of a single vibrissa's cortical barrel. *Journal of neurophysiology* 56(4), 1196-1223.

Ladygina, T., Popov, V. and Supin, A.Y. (1985) Topical organization of somatic projections in the fur seal cerebral cortex. *Neurophysiology* 17(3), 246-252.

Marshall, C.D., Amin, H., Kovacs, K.M. and Lydersen, C. (2006) Microstructure and innervation of the mystacial vibrissal follicle-sinus complex in bearded seals, *Erignathus barbatus* (Pinnipedia: Phocidae). *Anat Rec A Discov Mol Cell Evol Biol* 288A(1), 13-25.

Mills, F.H. and Renouf, D. (1986) Determination of the vibration sensitivity of harbour seal *Phoca vitulina* vibrissae. *Journal of experimental marine biology and ecology* 100(1), 3-9.

Morioka, M. and Griffin, M.J. (2005) Thresholds for the perception of hand-transmitted vibration: Dependence on contact area and contact location. *Somatosensory & motor research* 22(4), 281-297.

Reichmuth, C., Holt, M.M., Mulsow, J., Sills, J.M. and Southall, B.L. (2013) Comparative assessment of amphibious hearing in pinnipeds. *Journal of Comparative Physiology A*, 1-17.

Renouf, D. (1979) Preliminary measurements of the sensitivity of the vibrissae of harbour seals (Phoca vitulina) to low frequency vibrations. *Journal of Zoology* 188(4), 443-450.

Sherrick, C.E. (1953) Variables affecting sensitivity of the human skin to mechanical vibration. *Journal of experimental psychology* 45(5), 273-282.

Southall, B.L., Schusterman, R.J. and Kastak, D. (2003) Auditory masking in three pinnipeds: Aerial critical ratios and direct critical bandwidth measurements. *The Journal of the Acoustical Society of America* 114(3), 1660-1666.

Stüttgen, M.C., Rüter, J. and Schwarz, C. (2006) Two psychophysical channels of whisker deflection in rats align with two neuronal classes of primary afferents. *The Journal of neuroscience* 26(30), 7933-7941.

Verrillo, R.T. (1962) Investigation of some parameters of the cutaneous threshold for vibration. *The Journal of the Acoustical Society of America* 34(11), 1768-1773.

Verrillo, R.T. (1963) Effect of contactor area on the vibrotactile threshold. *The Journal of the Acoustical Society of America* 35(12), 1962-1966.

Verrillo, R.T. (1966) Effect of spatial parameters on the vibrotactile threshold. *Journal of experimental psychology* 71(4), 570-475.

Watkins, W.A. and Wartzok, D. (1985) Sensory biophysics of marine mammals. *Mar Mammal Sci* 1(3), 219-260.

CHAPTER 3: SEAL WHISKER VIBRATIONS ARE DISRUPTED BY HYDRODYNAMIC FIELDS

Abstract

The seal whisker is an advanced hydrodynamic sensor that has been shaped by evolutionary processes. The present research aims to learn what signals are available to the seal during hydrodynamic tracking in order to better understand the functioning of this sensory system. We developed a novel, animal-borne tagging device, wLogger, which uses a miniature digital accelerometer to measure signals directly from a seal's whisker. Laboratory testing using excised whiskers in a water flume confirmed that the tag is capable of recording vibrational signals without hampering the natural movement of the whisker. In a laminar flow in the flume, the whisker vibration was dominated by vortex shedding in a narrow frequency range. When a hydrodynamic disturbance from a cylinder placed upstream was added, this peak diminished in amplitude and the frequencies of vibration broadened. Live animal testing with a trained seal showed similar results, where there was a narrow-bandwidth peak in vibration in the absence of a hydrodynamic trail that diminished in the presence of a trail generated by moving objects. Based on these results, we suggest that the seal vibrissal system could rely on the disruption of whisker's natural vortex shedding to detect hydrodynamic trails.

Introduction

Hydrodynamic stimuli, generated by perturbations of a fluid medium, are ubiquitous in the marine environment and are salient to many biological sensory systems. A variety of hydrodynamic receptors exist among marine organisms, including the lateral line organs of fishes, sensory hairs of crustaceans, and whiskers (vibrissae) of marine mammals (Dehnhardt and Mauck, 2008;Engelmann et al., 2000). Hydrodynamic detection has been observed to function in prey capture, predator avoidance, rheotaxis, navigation, and object discrimination (Bleckmann, 1994). Hydrodynamic trails, or wakes, are created when an object moves though the water or when flow passes over a stationary object. These trails contain complex spatial and temporal information that can allow organisms to detect stimuli at distances from the source and up to several minutes after the disturbance has been generated (Vogel, 1994).

Seals use their whiskers, or vibrissae, to detect hydrodynamic stimuli (Hanke et al., 2012). Although all pinnipeds (seals, sea lions and walrus) possess well-developed vibrissal arrays, the hydrodynamic detection abilities of the true seals (*Phocidae*) have been best studied and it is thought that species of this taxonomic group are specialized for detecting hydrodynamic signals. Seals have dense vibrissal arrays about the face, consisting of mystacial vibrissae on the muzzle, rhinal vibrissae above the nose, and supraorbital vibrissae above the eyes. The vibrissal system in seals is highly innervated, vascularized, and has extensive cortical representation (Ladygina et al., 1985;Marshall et al., 2006), suggesting an important role for this sensory modality.

Seals can use their vibrissae to detect low-amplitude waterborne vibrations and track biogenic and artificial wakes (Dehnhardt et al., 1998;Dehnhardt et al.,

2001;Schulte-Pelkum et al., 2007). In addition, seals can determine the direction of movement of a trail generator (Wieskotten et al., 2010) and discriminate between the wakes generated by objects of different size and shapes (Wieskotten et al., 2011). Although it is clear that seals can use their vibrissal array to extract important information from complex flow fields, how this is accomplished is not known.

The capacity of this biological system for hydrodynamic signal detection exceeds that of any artificial system; consequently, there is much interest in biomimetic modeling of the vibrissal system of seals (Stocking et al., 2010). Before one can effectively generate artificial sensors based upon this system, the biological function of the vibrissae must first be fully understood. Scientific understanding of hydrodynamic receptor systems is limited as compared to our knowledge of other sensory modalities. There is a lack of fundamental understanding of how hydrodynamic detection by the vibrissal system functions, especially at the level of signal reception. The physical properties of hydrodynamic stimuli that are biologically relevant are also poorly understood (Bleckmann, 1994).

It has been shown that seal whiskers vibrate when exposed to water flow (Hyvärinen, 1995;Murphy, *in press*). We hypothesize that the spectral characteristics of the vibrations of the whisker may carry information on the characteristics of fluid flow fields. Understanding this sensory system at a signal level would have beneficial implications for advances in sensor development as well as improved understanding of the ecology of these animals.

Tagging devices allow for in-situ measurements to be obtained from live animals, yielding insights into behavior and physiology. Rapid advances in technology and the

accompanying miniaturization of sensors have allowed for complex suites of instrumentation to be carried by marine mammals in the wild (Cooke et al., 2004). The use of accelerometers is becoming increasingly common in these biologging devices (Viviant et al., 2010;Watanabe and Takahashi, 2013) and has been effective in measuring parameters such as diving and feeding behavior. In this study, we develop a novel animal-borne recording tag, wLogger, which utilizes an accelerometer fixed to the base of a seal's whisker to record the vibrational signal directly from the sensory structure. This approach aims to investigate the signals received by these biological sensors and better understand the relevant signal components involved in hydrodynamic detection.

To assess the effect of the tag on the natural movement of the whisker, laboratory testing in a water flume was performed on excised whiskers instrumented with the accelerometer. A laser vibrometer was used to measure vibrations of single vibrissae, with and without the accelerometer attached, when exposed to laminar water flow and hydrodynamic disturbances. The tag was then used to record vibrations of an excised vibrissa in a test pool, in the presence and absence of hydrodynamic trails. Finally, animal-borne testing was conducted in a captive setting on a free-swimming harbor seal. A trained seal was instrumented with the accelerometer fit to a supraorbital vibrissa and recordings were obtained as the animal engaged in active swimming and tracked hydrodynamic disturbances.

Materials and Methods

Instrumentation

The wLogger tag incorporates an Arduino-based datalogger connected to an external digital ADXL345 accelerometer (*Analog Devices, Norwood, MA, USA*), fixed to the base of a whisker. The accelerometer and attached PCB surface mount board measures 6.0 x 3.0 x 1.0 mm. For attachment to the vibrissa, the external accelerometer was fixed with epoxy to a small piece of flexible polyolefin shrink tubing and slid onto the vibrissa to be tested. In order to achieve a secure fit on the tapered form of the vibrissal shaft, the tubing was pre-shrunk on a sample vibrissa of comparable dimensions. During live animal testing, a small amount of synthetic rubber adhesive tack was applied to the attachment tubing in order to avoid slippage during active swimming.

The accelerometer is attached by four thin (32 gauge) wires to a main recording unit, mounted on the head of the animal. The base of the main recording unit is comprised of an OpenTag board (*Loggerhead Instruments, Sarasota, FL, USA*) and is powered by a 3.7V 1300 mAh Li-Polymer cell rechargeable battery (product number 30108-1, *TENERGY, Freemont, CA*). Data are archived onto an 8 GB microSD card. For laboratory testing, the recording unit was sealed inside an acrylic tube. For live animal testing, the recording unit was waterproofed by potting in epoxy (*MG Chemicals, Surrey, B.C., Canada*). When potted, the recording unit measured 5.4 cm x 3.3 cm 1.8 cm and weighed 51 g (Figure 3.1).

Excised whisker flume testing

Laboratory testing in a water flume was conducted on two excised mystacial vibrissa samples. Vibrissae were obtained from post-mortem stranded harbor seals (*Phoca vitulina*) at the Marine Mammal Center in Sausalito, California and stored in dry sample containers. Prior to testing, each specimen was rehydrated by immersion in fresh water for one hour. Rehydration as well as flume testing was conducted in fresh water due to constraints of the flume setup.

Experiments were conducted in a Rolling Hills Research Company Model 1520 water flume (*El Segundo, CA, USA*) with a testing area measuring 152 cm in length, 38 cm in width, and 46 cm in height. For mounting in the flume tank, the base of each sample was fixed inside a cylindrical, threaded aluminum sleeve. The bottom 1 cm of the vibrissal shaft was inserted into the sleeve and set with epoxy. Samples were attached to a sting apparatus, composed of a stainless steel rod with a 90 degree bend. The sting apparatus held the sample in the testing area in center of the water column (Figure 3.2). Flow in the test area was laminar and the boundary layer (1.6 cm) along the walls of the flume tank did not extend into the location of the sample mount. The body of the sting mount was positioned downstream of the sample and therefore did not interfere with the flow around the mounted sample.

Laser vibrometry was used to measure vibrations of the excised whisker, fitted with the accelerometer board and after the board was removed, without moving the whisker. Recordings were made with a Polytec model PDV 100 laser-Doppler vibrometer (calibration accuracy +/- 0.1%), measuring point velocities on the whisker (*Waldbronn, Germany*). Vibrations were recording from the accelerometer placed at 12% up the

vibrissal shaft and from the identical point on the shaft, without the instrumentation. These points are referred to respectively as *tagged whisker* and *untagged whisker*. Recordings were also taken from the sting mount to measure vibrations induced by the apparatus. The laser was focused on the recording point, and vibrations in the cross-stream direction were recorded for 12 seconds at 1,200 Hz using the Polytec Vibrometer Software (version 4.6).

Recordings were made in the *tagged whisker* and *un-tagged whisker* configurations under two conditions termed *free-flow* and *disturbance*. In the *free-flow* condition, the sample was exposed to undisturbed, laminar water flow. In the *disturbance* condition, the sample was exposed to a hydrodynamic disturbance, generated by inserting a 2 cm diameter metal cylinder upstream of the sample (Figure 3.3). All tests were conducted at a flow speed of 0.5 m/s, verified by particle image velocimetry (PIV) analysis.

Excised whisker pool testing

Additional measurements were taken with an excised vibrissa in a 22,000 salt water test pool. The vibrissa was fitted with instrumentation and mounted on a PVC pole with a 90 degree bend (Figure 3.4A). The pole mount was dragged through the water, so that the body of the pole did not interfere with the signal on the whisker. The mounted vibrissa was dragged through the water to simulate a free-stream condition and also exposed to hydrodynamic stimuli generated by submerged objects moving through the water (Figure 3.4B and C). Hydrodynamic signals were generated using a sphere (6.7 cm diameter) on the end of a pole extension (2 cm diameter), as well as a radio-controlled

model submarine (76 cm length x 67 cm diameter) (*model Neptune SB-1, Thunder Tiger Corp, Taichung, Taiwan*).

Live animal testing

A trained adult male harbor seal (*P. v. vitulina*), identified as *Sprouts* (NOA0001707) served as the subject for this study. The subject was captive-born and aged 24 years at the time of testing. Experiments were conducted in an 8 m diameter saltwater pool surrounded by adjacent haul-out decks, which was part of the animal's living enclosure at Long Marine Laboratory in Santa Cruz, California.

The seal was trained using standard operant conditioning techniques to wear a soft neoprene blindfold over its eyes and follow the hydrodynamic wake generated by a submerged object moving through the water. Hydrodynamic signals were generated by the same objects used during excised vibrissa pool testing.

During test sessions, the recording unit was mounted on the seal's head by placement in the pocket of a soft neoprene headband. The accelerometer was securely and temporarily fixed to one of the subject's supraorbital vibrissae (Figure 3.5). Supraorbital vibrissae were used in these measurements for ease of attachment and behavioral constraints. Recordings were made in the Z-axis of the accelerometer (direction normal to whisker and circuit board) with a 600 Hz sample rate. During experimental sessions the animal located a hydrodynamic disturbance and tracked the wake from an offset of approximately 0.5 m for the duration of the trial. In order to characterize the background signal on the vibrissa elicited by swimming motion, trials were also conducted with the animal free swimming at varying speeds without an additional hydrodynamic disturbance. In order to match the vibrissal signal with known

behavioral events, a synchronized overhead video feed was concurrently recorded with the datalogger measurements (Figure 3.6). The accelerometer was synchronized to the video by a pulse recorded on both instruments.

Data analysis

Signal processing of both laser vibrometer and tag recordings were conducted in MATLAB (Mathworks, Inc.). A Hanning window was applied to the data and fast Fourier transform (FFT) averaging was conducted. A 150 point FFT was used for vibrometer recordings and a 75 point FFT was used for tag recordings to maintain a frequency resolution of 8 Hz for both data sets. Spectrograms were generated using the velocity data from vibrometer recordings and acceleration data from tag recordings with an 8 Hz frequency resolution. For further calculations, the frequency spectrum of the acceleration signal from the tag was converted to velocity by dividing by $2\pi f$ (where f = frequency in Hz).

The velocity spectra for both vibrometer and tag recordings were analyzed by performing FFTs on sequential (125 ms) segments from each recording. This was done because peak frequency could change throughout the course of each trial, and therefore FFT averaging was not appropriate. Peak frequency and corresponding -6 dB bandwidth was calculated for each segment. This is equivalent to identifying the darkest section on the spectrogram for each sequential 125 ms segment. Peak frequency calculations were restricted to frequencies above 60 Hz to avoid signals from the sting apparatus used in flume testing. The peak frequency of each time slice was divided by the bandwidth to yield a measure of Q, a dimensionless parameter describing the bandwidth of a signal

relative to its center frequency. Results were shown as distributions of bandwidth and Q, with each value identified as a count within its corresponding peak frequency and Q bin.

Results

Excised whisker flume testing

Laser vibrometer recordings revealed distinct differences in whisker vibration in the *free-flow* condition compared to the *disturbance* condition (Figure 3.7). In free-flow the vibrational signal of the whisker is relatively narrowband. When exposed to the hydrodynamic disturbance, the energy of the signal was spread out over a broader range of frequencies. This can be seen quantitatively in the 6 dB bandwidth and Q measurements (Figure 3.8). In the *disturbance* condition, the bandwidth measurements were larger and the Q values were shifted lower than in the free-stream condition. Note that in the *free-flow* condition, there were no values in the Q of 1 bin, while in the *disturbance* condition there were relatively high values in this bin. This illustrates the shift from a narrowband signal in free-flow to a broadband signal in the *disturbance* condition.

Attachment of the tag accelerometer to the whisker had little effect on its vibration. This can be seen in the comparable patterns on the spectrograms (Figure 3.7) as well as the closely matched power spectra for the whisker without the tag (Figure 3.9). The power spectra also illustrate the effect of the hydrodynamic disturbance on whisker vibrations and demonstrate that the *tagged whisker* shows the same effect of flow disturbance as the *whisker* alone.

Excised whisker pool testing

Excised whisker recordings provide an additional controlled comparison of the whisker signal under different hydrodynamic conditions (Figure 3.10). When the excised whisker was moved through the water without a hydrodynamic disturbance, the signal was narrowband. The bandwidth values in this condition were lower and Q values were higher than in any of the hydrodynamic disturbance conditions. When a hydrodynamic disturbance from the ball or submarine was introduced, the bandwidth increased and the Q values shifted lower. An extreme example of this shift was when the whisker was held stationary behind the submarine. In this case, the energy in the signal was spread across a wide range of frequencies. The Q values were shifted low, with the largest count in the lowest bin. Note that, because the duration of trials varied, the absolute count for each recording also varies. However, the relative contribution of each frequency bin and the spread of values is an informative comparison across trials.

Live animal testing

The wLogger tag recorded vibration from a whisker of an actively swimming seal. Differences were observed in the signal recorded during free swimming, as compared to when tracking a hydrodynamic signal (Figure 3.11). These spectral trends were similar to those observed for the excised whisker in the water flume. Trials where the subject was tracking the hydrodynamic wake from the ball and submarine had a wider bandwidth and a lower spread of Q values than when the subject was free swimming. Note that, because the duration of trials varied, the absolute count for each recording also varies. However, the relative contribution of each frequency bin and the spread of values is an informative comparison across trials.

Discussion

This is the first study to record and measure signals received by the whiskers of a live seal. The wLogger tag successfully measured vibrations from the supraorbital vibrissae of a harbor seal during active swimming and hydrodynamic detection. Laser vibrometer recordings from instrumented vibrissae confirmed that the attachment of the accelerometer had minimal effect on the vibration of the whisker. Animal-borne and laboratory testing demonstrated that the recording unit was effective in capturing the vibrissal signal.

Laser vibrometer and tag accelerometer recordings demonstrate that seal whiskers vibrate when moving through the water and when exposed to hydrodynamic stimuli. The vibrissal signal under all test conditions was predominantly less than 300 Hz, which is the frequency range of best sensitivity of the harbor seal (as seen in chapter 2). We hypothesize that vibration of the vibrissal shaft and modulations in this vibrational signal are detectable to the seal and provide salient information on the presence and nature of hydrodynamic stimuli.

The data revealed that hydrodynamic disturbances disrupt the vibrational signal on the whisker. Whiskers in undisturbed flow had a relatively narrowband signal. When the whisker was exposed to a hydrodynamic disturbance, the energy of the vibrational signal became spread across a wider range of frequencies. This is reflected by the trends in bandwidth and Q values between conditions. This effect is seen clearly in excised vibrissae tested under controlled laboratory conditions in the water flume and in a more variable setting in the test pool. While similar trends in bandwidth and Q values are

observed in the live animal data, the trend is less clear. This is likely due to uncontrolled factors such as residual flow disruptions and variations in the animal's swim speed.

The patterns observed in the whisker signal suggest that modulation of the whisker's natural vibration may be the key to hydrodynamic detection. Seals may rely on disruption of the baseline narrowband vibration to indicate that the whisker has encountered a hydrodynamic disturbance. Furthermore, the vibrissae of seals are arranged in a complex array and we hypothesize that comparison of the signal between points on the array may aid hydrodynamic detection. This warrants future research involving simultaneous recordings from multiple vibrissae. The present testing method could be expanded to record from multiple excised vibrissae arranged in a deliberate geometric positioning or from multiple points on the vibrissal array of a live animal. Furthermore, this research opens up the opportunity for field measurements on free swimming animals in order to characterize the whisker signal across the vibrissal array in naturally occurring hydrodynamic flow fields. Continued data collection in this area can aid in the characterization of the vibrissal system at a signal level and aid in understanding the underlying functioning of these advanced biological sensors and potentially aid in the development of biomimetic systems.

Figures

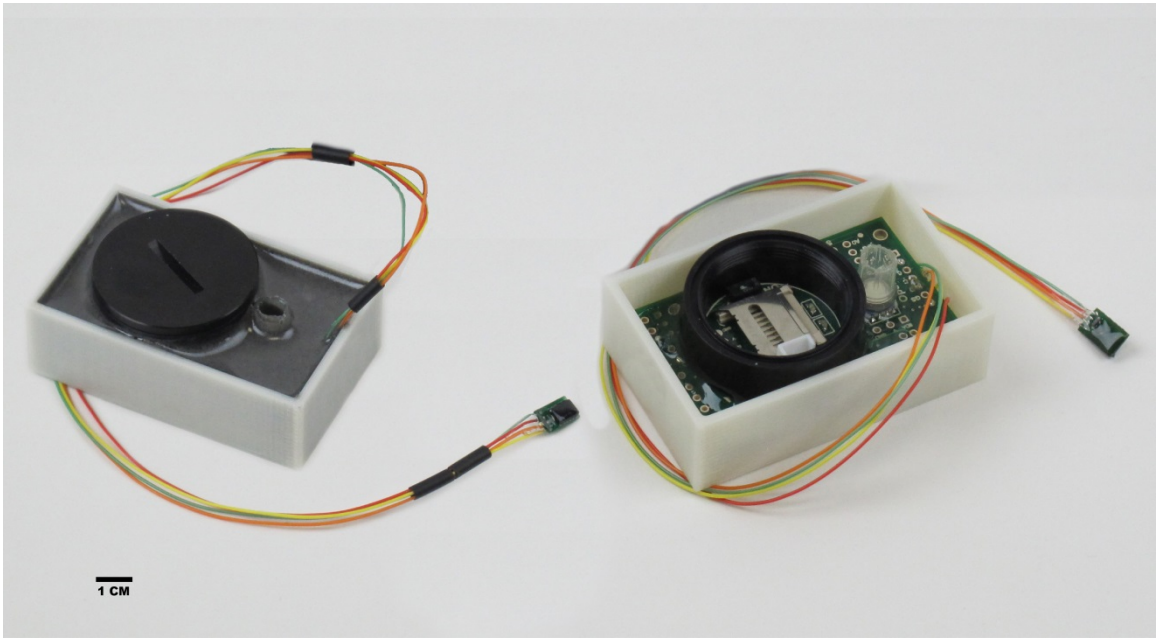

Figure 3.1 Photograph of the wLogger tag. The wLogger tag is shown here potted and sealed in its waterproof housing (left) and prior to potting with the internal components visible (right). Four wires connect the main recording unit to an external accelerometer that will be attached to a whisker.

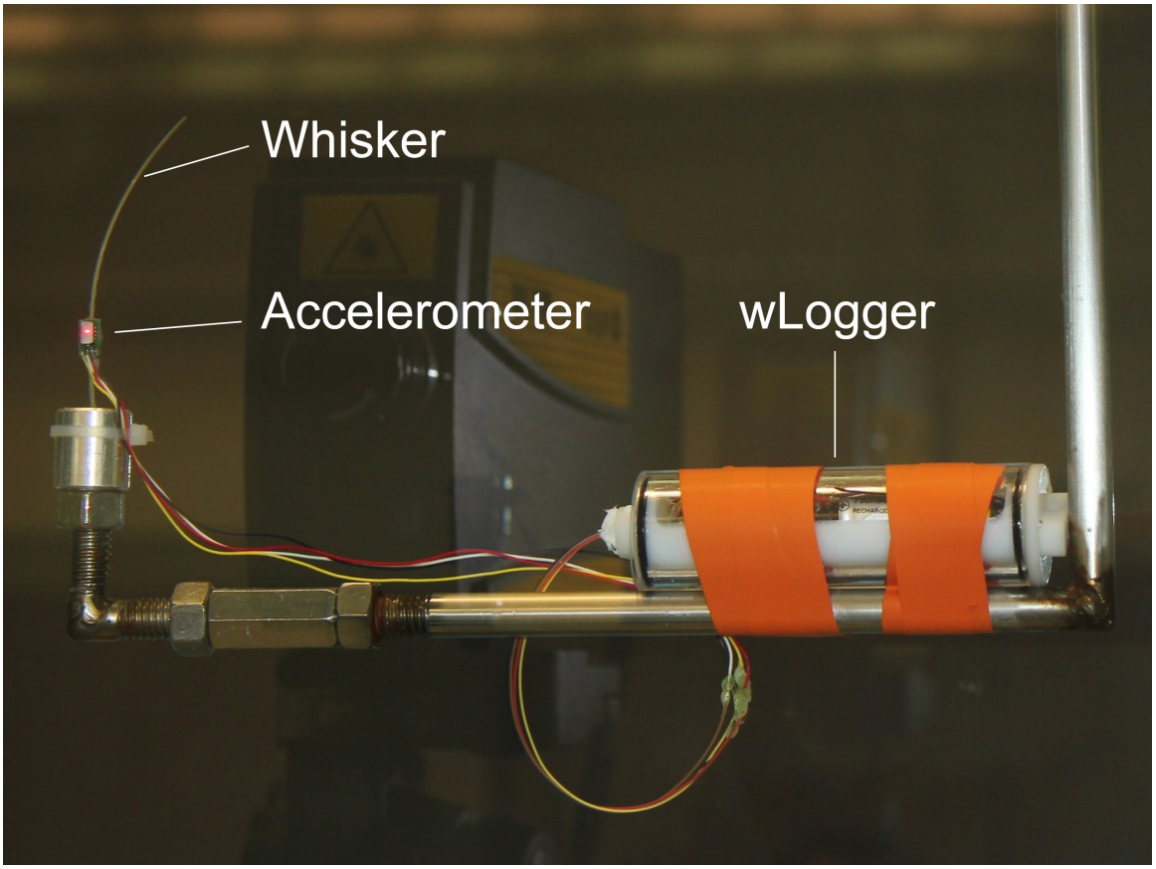

Figure 3.2 Cross-stream view of an instrumented excised vibrissa mounted on the sting apparatus inside the water flume. For this image, direction of water flow is from the left to right of the page. The accelerometer is positioned at 12% up the length of the whisker shaft and the laser is focused on the accelerometer (visible in this photograph as a red dot on the center of the accelerometer).

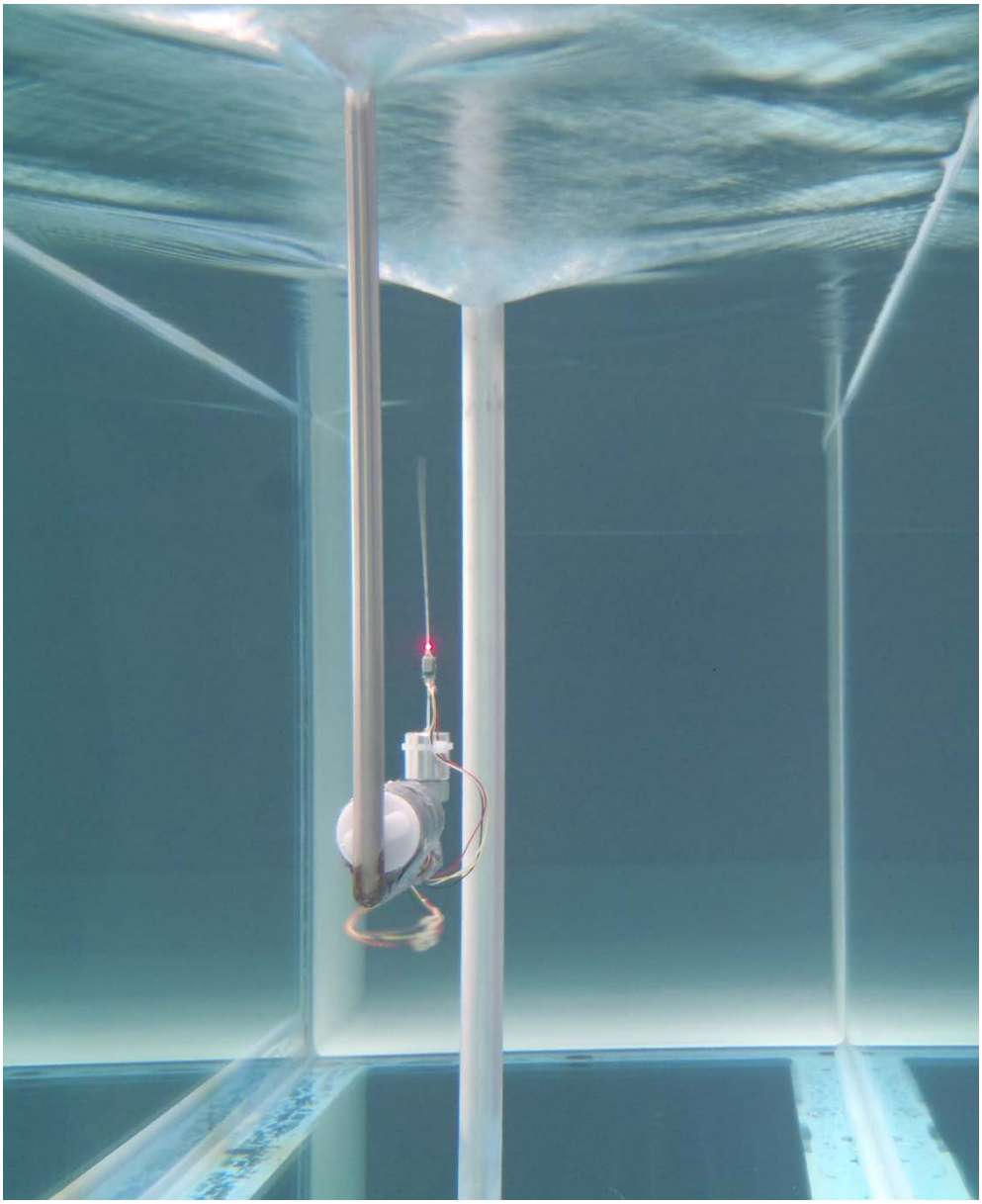

Figure 3.3 Down-stream view of an instrumented excised vibrissa mounted on the sting apparatus inside the water flume. A metal cylinder is positioned upstream to generate a hydrodynamic disturbance. The tip of the whisker is out of focus in this photograph due to strong vibrations in the cross-stream direction. For this image, direction of water flow is coming out of the page.

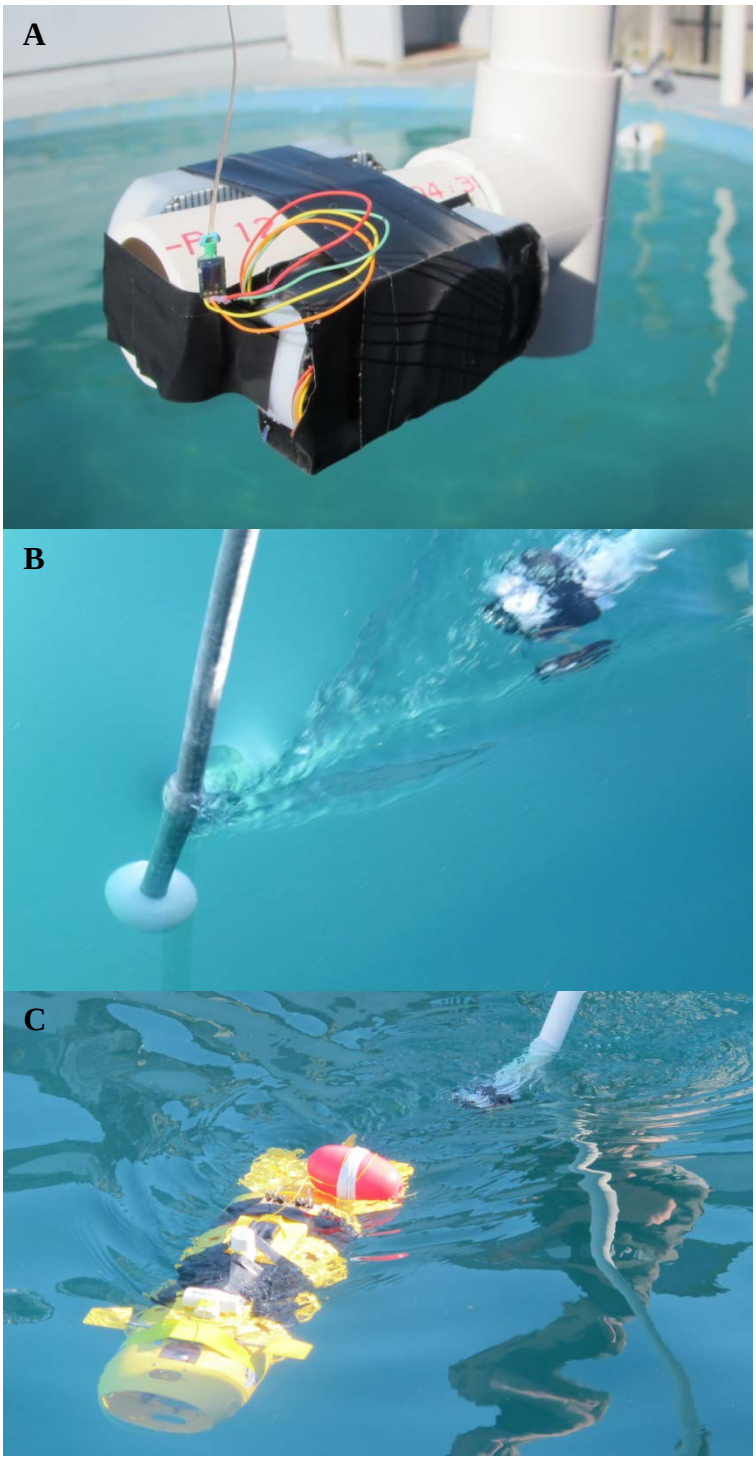

Figure 3.4 Excised whisker pool testing. **(A)** The wLogger tag attached to an excised whisker on a PVC mount for pool testing. **(B)** E*xcised whisker tracking ball* condition. An instrumented excised whisker moving through the water behind the wake of a dragged object. **(C)** E*xcised whisker tracking submarine* condition. An instrumented excised whisker moving through the water behind the wake of a radio controlled submarine. These conditions **(B and C)** simulate hydrodynamic trail following.

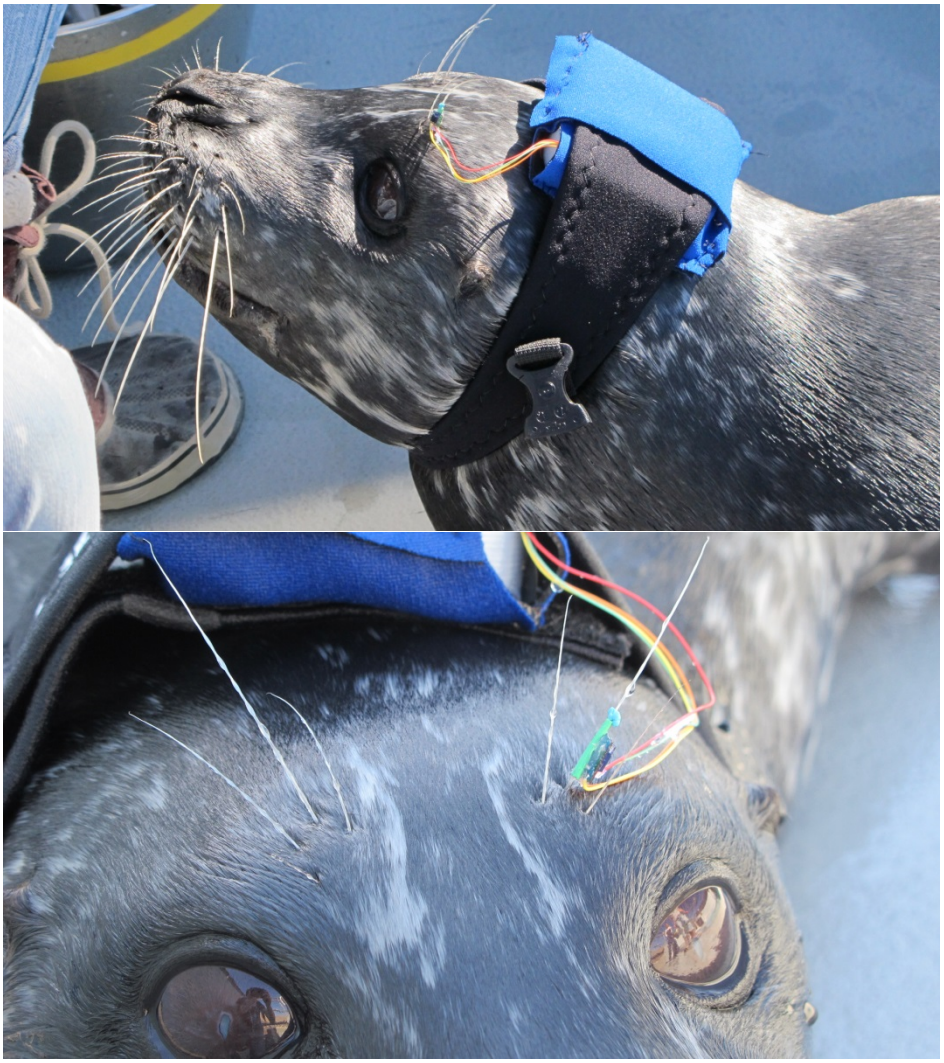

Figure 3.5 Photographs of the trained harbor seal wearing the wLogger tag. The accelerometer is attached to a supraorbital whisker. The main recording unit is fitted to the animal's head by placement inside a pocket of the neoprene headband.

Figure 3.6 Photograph of the seal tracking a radio-controlled submarine while wearing the wLogger tag. This photograph was obtained from the overhead video camera system used to synchronize tag recordings to behavioral events.

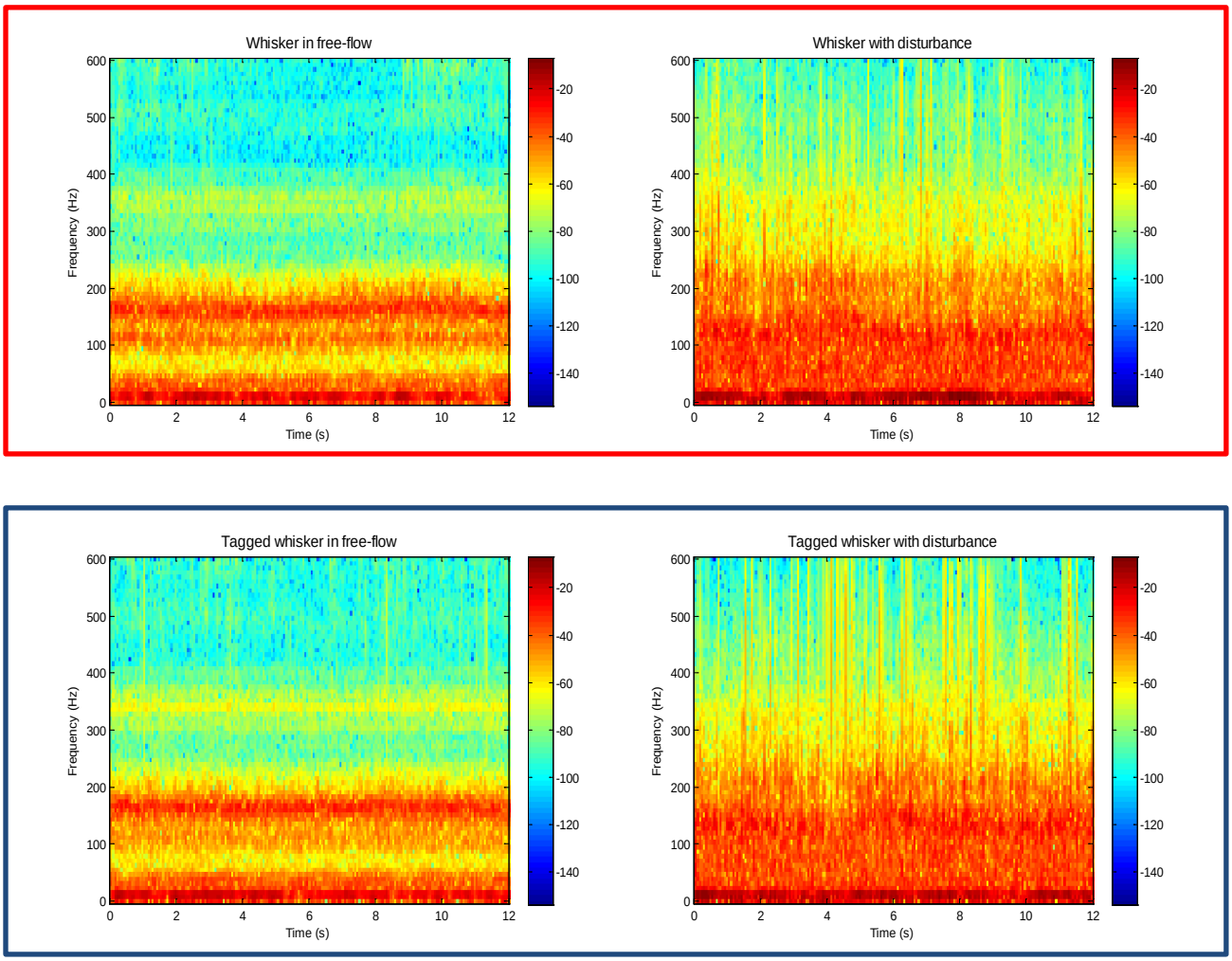

Figure 3.7 Spectrograms of recordings from excised whisker flume testing. Example spectrograms of laser vibrometer recordings from an excised whisker (*Whisker*) (top row: red box) and the same whisker fitted with the tag (*Tagged whisker*) (bottom row: blue box). Both sample conditions were exposed to identical *free-flow* and hydrodynamic *disturbance* conditions. For *whisker* recordings, the laser was focused on the vibrissal shaft at 12% up the length of the whisker. For *tagged whisker* recordings, the accelerometer was positioned on the identical point on the vibrissal shaft and the laser was focused on the surface of the accelerometer. Color bar indicates relative amplitude in terms of dB re: 1 m/s.

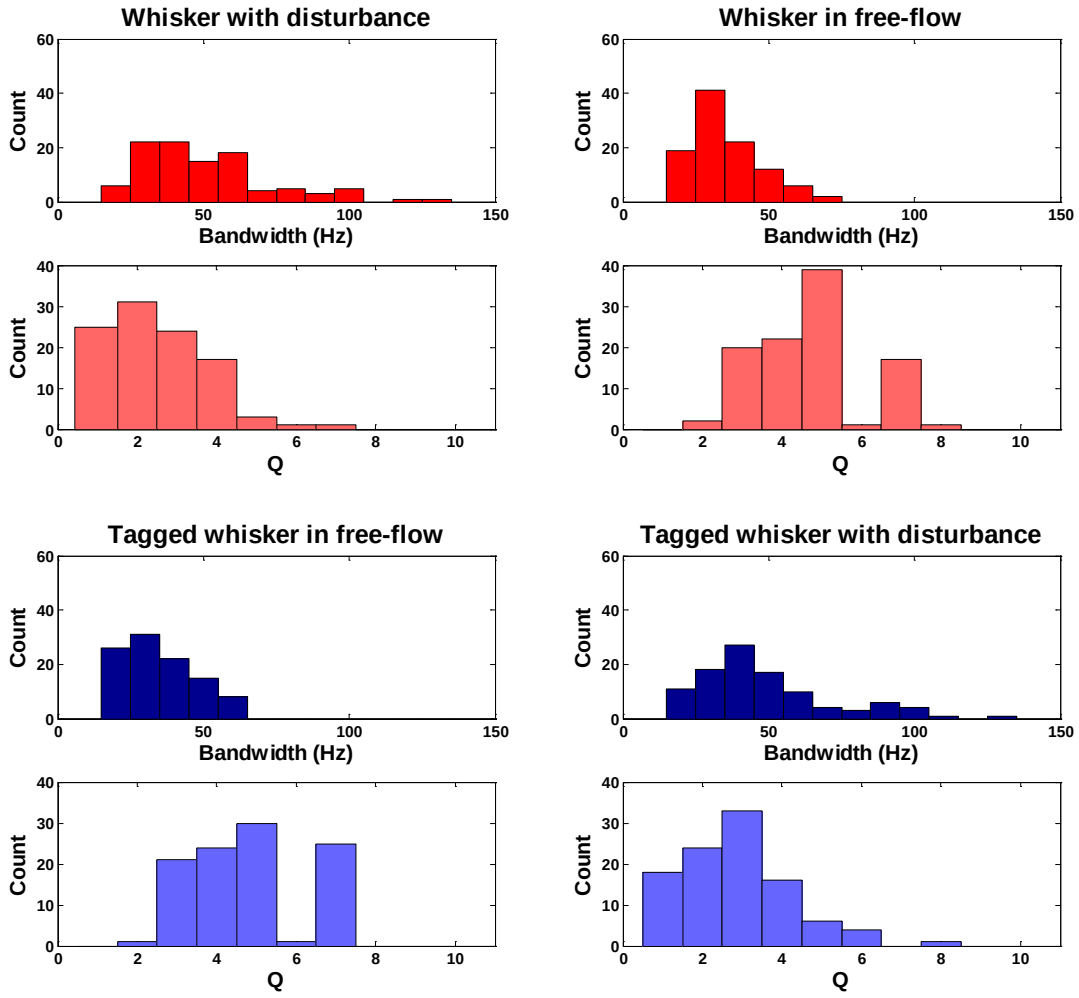

Figure 3.8 Histograms of -6 dB bandwidth and Q values for the four laser vibrometer recordings presented in Figure 3.7. Recordings are from an excised whisker (*Whisker*) (top row: red histograms) and the same whisker fitted with the tag (*Tagged whisker*) (bottom row: blue histograms). The top histogram in each pair (dark shading) shows the distribution of the -6 dB bandwidths (Hz) of the largest peak based on a series of FFTs with 8 Hz frequency resolution. The bottom histogram in each pair (light shading) shows the distribution of Q-values calculated from the same dataset.

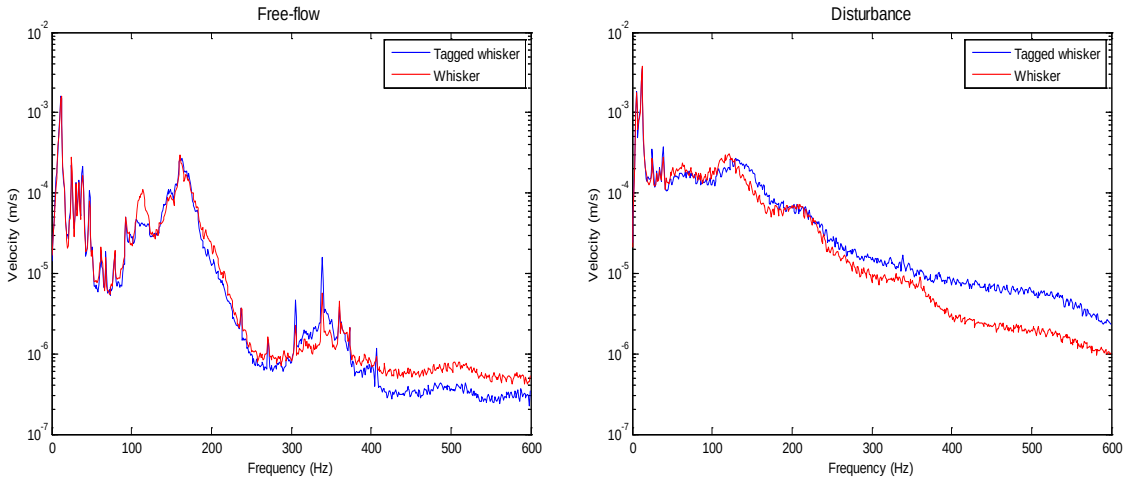

Figure 3.9 Overlaid power spectra for an excised vibrissa with and without the accelerometer in the *free-flow* and *disturbance* conditions. Within each condition, the is minimal difference in the vibration of the untagged *whisker* as compared to the *tagged whisker*. This indicates that the attachment of the accelerometer to the whisker had little effect on its vibration.

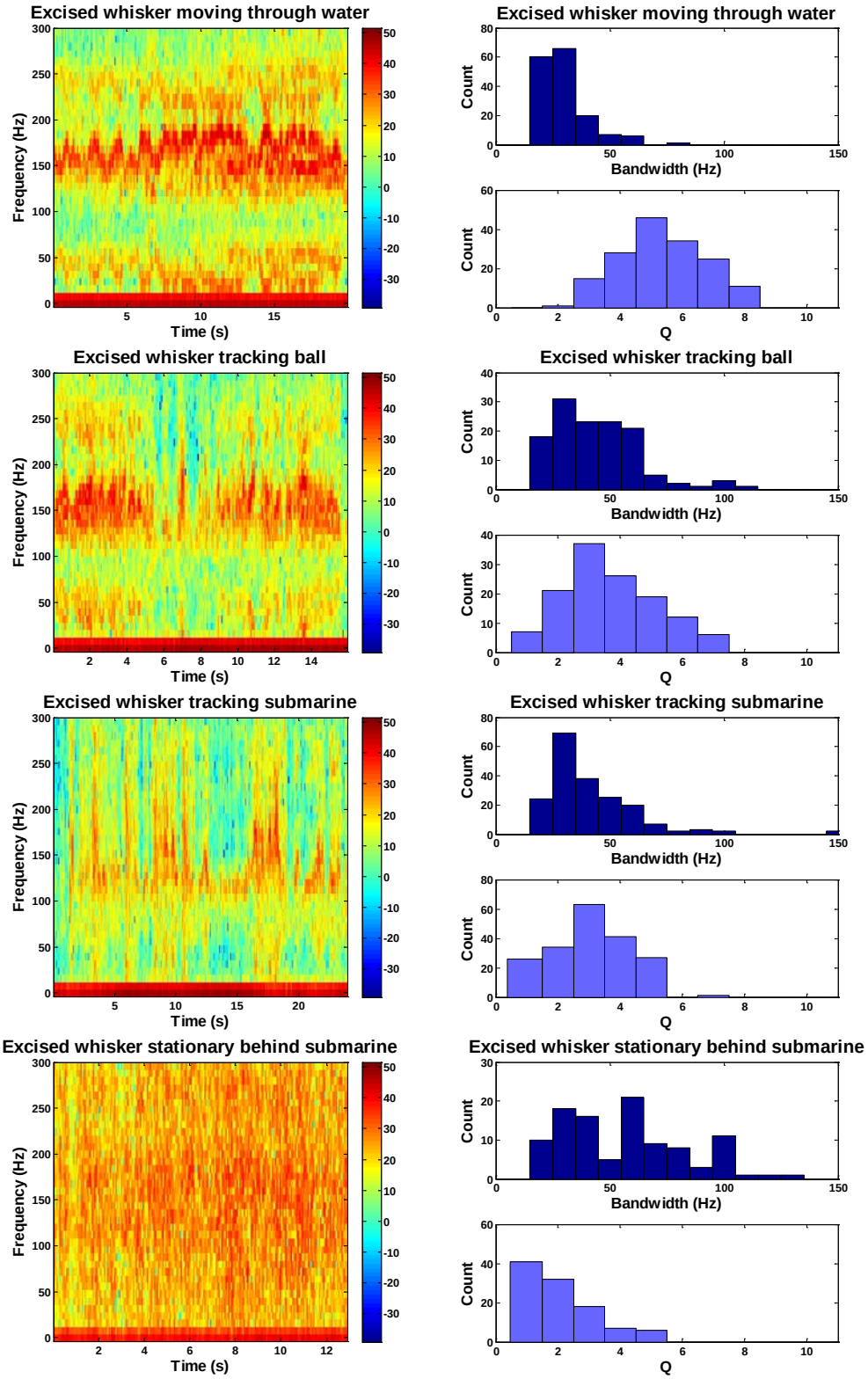

Figure 3.10 Example tag recordings from excised whisker pool testing under different hydrodynamic conditions. Spectrograms (left column) of whisker vibrations and corresponding histograms (right column) of 6 dB bandwidth and Q values for accelerometer recordings from an excised vibrissa exposed to different flow conditions.

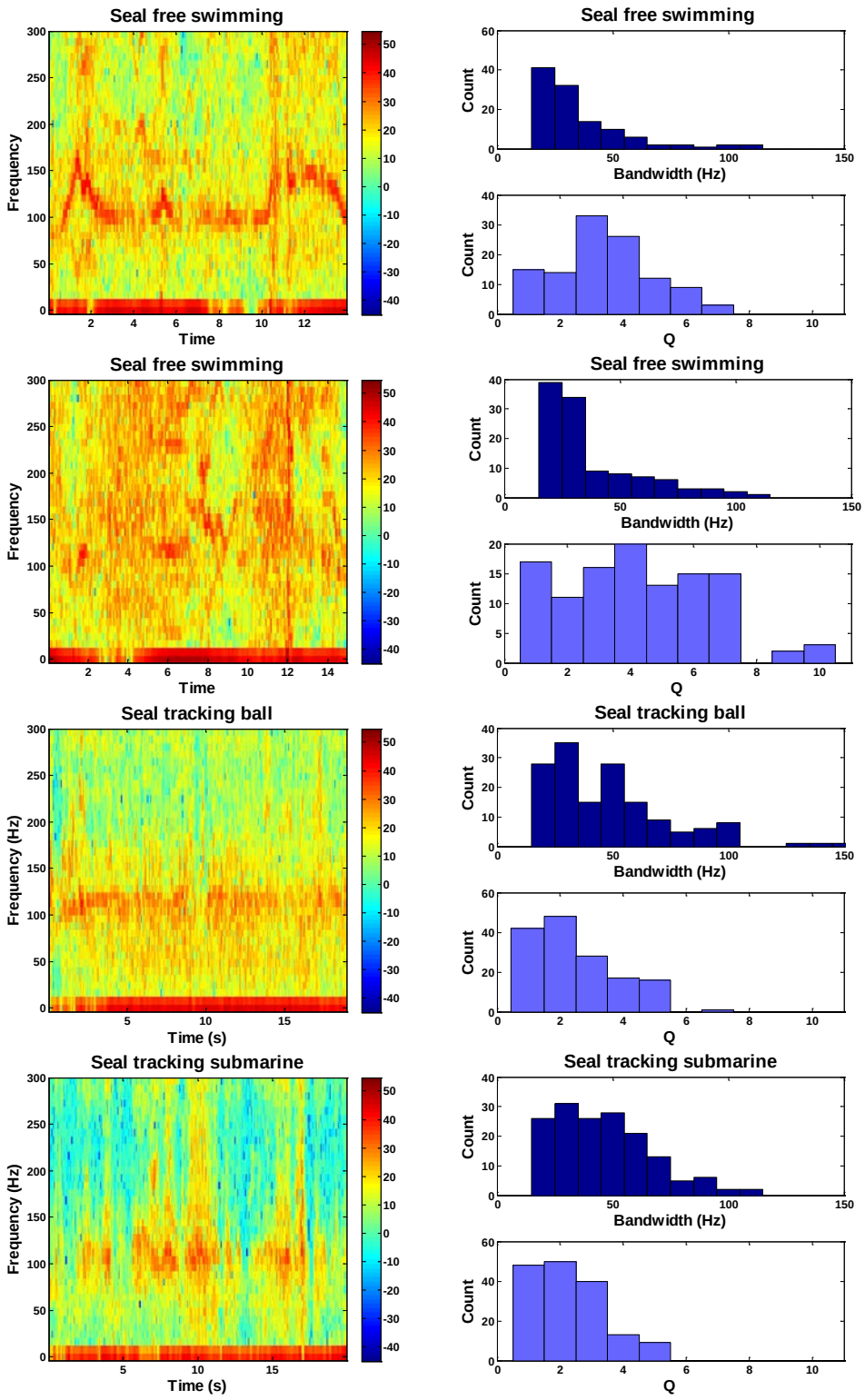

Figure 3.11 Example tag recordings from live animal tests under different hydrodynamic conditions. Spectrograms (left column) of whisker vibrations and corresponding histograms (right column) of 6 dB bandwidth and Q values for accelerometer recordings from the whisker of an actively swimming seal.

References

Bleckmann, H. (1994) Reception of Hydrodynamic Stimuli in Aquatic and Semiaquatic Animals *Progress in Zoology* 41.

Cooke, S.J., Hinch, S.G., Wikelski, M., Andrews, R.D., Kuchel, L.J., Wolcott, T.G. and Butler, P.J. (2004) Biotelemetry: a mechanistic approach to ecology. *Trends in Ecology & Evolution* 19(6), 334-343.

Dehnhardt, G., Mauck, B. and Bleckmann, H. (1998) Seal whiskers detect water movements. *Nature* 394(6690), 235-236.

Dehnhardt, G., Mauck, B., Hanke, W. and Bleckmann, H. (2001) Hydrodynamic trail-following in harbor seals *(Phoca vitulina*). *Science* 293(5527), 102-104.

Dehnhardt, G. and Mauck, B. (2008) Sensory evolution on the threshold: adaptations in secondarily aquatic vertebrates. Thewissen, J. and Nummela, S. (eds), pp. 295-314, University of California Press, Berkeley.

Engelmann, J., Hanke, W., Mogdans, J. and Bleckmann, H. (2000) Hydrodynamic stimuli and the fish lateral line. *Nature* 408(6808), 51-52.

Hanke, W., Wieskotten, S., Marshall, C. and Dehnhardt, G. (2012) Hydrodynamic perception in true seals (Phocidae) and eared seals (Otariidae). *Journal of Comparative Physiology A*, 1-20.

Hyvärinen, H. (1995) Sensory Systems of Aquatic Mammals Kastelein, R., Thomas, J. and Nachtigall, P. (eds), pp. 429-445, De Spil Publishers, Woerden.

Ladygina, T., Popov, V. and Supin, A.Y. (1985) Topical organization of somatic projections in the fur seal cerebral cortex. *Neurophysiology* 17(3), 246-252.

Marshall, C.D., Amin, H., Kovacs, K.M. and Lydersen, C. (2006) Microstructure and innervation of the mystacial vibrissal follicle-sinus complex in bearded seals, *Erignathus barbatus* (Pinnipedia: Phocidae). *Anat Rec A Discov Mol Cell Evol Biol* 288A(1), 13-25.

Murphy, C.T., Eberhardt, W.C., Calhoun, B.H., Mann, K.A. and D.A. Mann (*in press*) Effect of angle on flow-induced vibrations of pinniped vibrissae. *PloS one*.

Schulte-Pelkum, N., Wieskotten, S., Hanke, W., Dehnhardt, G. and Mauck, B. (2007) Tracking of biogenic hydrodynamic trails in harbour seals (Phoca vitulina). *Journal of experimental biology* 210(5), 781-787.

Stocking, J., Eberhardt, W., Shakhsheer, Y., Calhoun, B., Paulus, J. and Appleby, M. (2010) A capacitance-based whisker-like artificial sensor for fluid motion sensing, pp. 2224-2229, IEEE.

Viviant, M., Trites, A.W., Rosen, D.A., Monestiez, P. and Guinet, C. (2010) Prey capture attempts can be detected in Steller sea lions and other marine predators using accelerometers. *Polar biology* 33(5), 713-719.

Vogel, S. (1994) Life in moving fluids: the physical biology of flow, Princeton University Press.

Watanabe, Y.Y. and Takahashi, A. (2013) Linking animal-borne video to accelerometers reveals prey capture variability. *Proceedings of the National Academy of Sciences* 110(6), 2199-2204.

Wieskotten, S., Dehnhardt, G., Mauck, B., Miersch, L. and Hanke, W. (2010) Hydrodynamic determination of the moving direction of an artificial fin by a harbour seal (Phoca vitulina). *The Journal of experimental biology* 213(13), 2194-2200.

Wieskotten, S., Mauck, B., Miersch, L., Dehnhardt, G. and Hanke, W. (2011) Hydrodynamic discrimination of wakes caused by objects of different size or shape in a harbour seal (Phoca vitulina). *The Journal of experimental biology* 214(11), 1922-1930.

CONCLUSIONS

The present body of research employed several experimental approaches to investigate the structure and function of the vibrissal system of pinnipeds. The aims of this research were to better understand the adaptive significance of vibrissal structure, the sensitivity of the vibrissal system, and the signals received by the sensors. In order to approach these objectives in a comprehensive manner, laser vibrometry, computed tomography (CT) scanning, behavioral testing and animal borne-tagging methods were utilized.

Laser vibrometer recordings in a water flume revealed that whiskers vibrated with a distinct fundamental frequency when exposed to water flow. Comparative tests investigated the effect that vibrissal surface structure and angle of orientation had on these flow-induced vibrations. When the vibrational signal from the whiskers of harbor seals (*Phoca vitulina*), elephant seals (*Mirounga angustirostris*) and California sea lions (*Zalophus californianus*) were compared, no significant effect of species, and consequently vibrissal surface structure, was observed. However, when vibrissae oriented at different angles to the direction of water flow were compared, a significant effect of angle of orientation was revealed. The velocity of flow-induced vibrations was lowest and frequency of vibrations was highest when the flattened edge of the vibrissa was oriented into the water flow. Furthermore, using vortex shedding calculations, vibration frequency at a given angle of orientation could be accurately predicted by the diameter of the vibrissa facing into the flow alone. This implies that the cross-sectional flattening of

the vibrissae, rather than the surface structure, may explain most of the trend observed in measured vibration frequency at the flow speed tested. CT scanning and digital cross-sectioning of the vibrissae confirmed that both undulated and smooth vibrissae are cross-sectionally flattened. I hypothesize that this shared characteristic between the vibrissal types is responsible for trends observed in flow-induced vibrations and may play a key role in the specialized aquatic functioning of the vibrissal system.

The sensitivity of the vibrissal system was investigated using behavioral measures with a trained harbor seal. Absolute thresholds for directly coupled stimuli were measured and demonstrated that the vibrissal system of the seal was sensitive to vibrations across a range of frequencies from at least 10 to 1000 Hz. Interestingly, the thresholds collected for the seal were similar to the absolute sensitivity measures obtained in the same set-up for the human thumb. The similarities in the performance of a seal using its vibrissae and humans using their thumb demonstrates good tactile sensitivity for these structurally different mechanoreceptive systems.

This study reports better sensitivity for the vibrissal system of the harbor seal than previous in-air measures (Mills and Renouf, 1986;Renouf, 1979) and agrees more closely with measures of underwater sensitivity for this species (Dehnhardt et al., 1998). The present study identifies a frequency of best vibrotactile sensitivity of 80 Hz. This frequency is much lower than that reported in the prior in-air studies and is within the natural frequency range of hydrodynamic stimuli to which the vibrissae are most likely specialized (Bleckmann, 1994). Furthermore, the range of frequencies to which the trained seal was highly sensitive overlap with the frequencies of flow-induced vibrations of vibrissae measured in the first portion of this study.

In the final component of this research, an animal-borne tag was developed and used to investigate the vibrational signals that are received by the vibrissae during active swimming and hydrodynamic detection. This study introduced a novel tagging device, wLogger, that utilized an accelerometer fixed to the base of a whisker to collect *in situ* measurements of whisker vibration. Prototype testing of this system demonstrated the feasibility of this approach. Laboratory experiments with excised vibrissae in a water flume demonstrated that the tag unit could effectively record vibrations without hampering the natural movement of the whisker. In addition, the wLogger tag successfully measured vibrations from the supraorbital vibrissae of a harbor seal during active swimming and hydrodynamic detection. Live animal testing, along with recordings from excised vibrissae, revealed that interaction with hydrodynamic disturbances disrupted the vibrational signal received by the whisker. When exposed to a hydrodynamic signal, whisker vibrations increased in bandwidth, spreading energy across a wider range of frequencies. This finding suggests that modulation of the vibrational signal may play a key role in the detection of hydrodynamic stimuli by the seal.

The results of this dissertation research provide insight into the functioning of the vibrissal system of harbor seals and other pinnipeds. By investigating the vibrissal system from the focal points of structure, sensitivity, and received signals, we begin to develop a more comprehensive understanding this sensory modality. The present research demonstrated that seal whiskers vibrate when moved through the water, and that the vibrational signal on the whisker is complex. In addition, the characteristics of this vibrational signal are influenced both by the structure of the vibrissa itself and by interactions with stimuli in the environment. The data demonstrate that seals can detect

vibrations. Furthermore, the natural vibrations of the whiskers are within the detectable range of the seal. Integrating these findings begins to bridge the gap in understanding of what is received by the sensors and what is perceived by the seal. In addition, it provides insights into how the morphology of the vibrissal system in pinnipeds may be adapted for aquatic functioning in these amphibious animals.

This research provides groundwork for future avenues of investigation. The tag instrumentation designed for this research will facilitate continued exploration of the vibrissal system under more complex and biologically relevant stimulus conditions. This instrumentation will allow for field measurements on free swimming animals in order to characterize the whisker signal across the vibrissal array in naturally occurring hydrodynamic flow fields. Continued data collection in this area can aid in the characterization of the vibrissal system and enhance understanding the underlying functioning of these advanced biological sensors.

References

Bleckmann, H. (1994) Reception of Hydrodynamic Stimuli in Aquatic and Semiaquatic Animals *Progress in Zoology* 41.

Dehnhardt, G., Mauck, B. and Bleckmann, H. (1998) Seal whiskers detect water movements. *Nature* 394(6690), 235-236.

Mills, F.H. and Renouf, D. (1986) Determination of the vibration sensitivity of harbour seal *Phoca vitulina* vibrissae. *Journal of experimental marine biology and ecology* 100(1), 3-9.

Renouf, D. (1979) Preliminary measurements of the sensitivity of the vibrissae of harbour seals (Phoca vitulina) to low frequency vibrations. *Journal of Zoology* 188(4), 443-450.

APPENDICES

Appendix A: Use of animal and human subjects

Animal research was authorized under National Marine Fisheries Service permit 14535 and conducted with the approval of the Institutional Animal Care and Use Committee at UCSC. The use of marine mammal samples was authorized under the National Marine Fisheries Service, letter of authorization to C. Murphy. Research with human subjects was conducted under a Category 2 exemption by the UCSC Internal Review Board.